

DEVELOPMENT OF A NEW IMMOBILIZATION PROCEDURE FOR DETECTION OF
STAPHYLOCOCCAL ENTEROTOXIN B (SEB) AND *CANDIDA ALBICANS*

A THESIS SUBMITTED TO
THE GRADUATE SCHOOL OF NATURAL AND APPLIED SCIENCES
OF
MIDDLE EAST TECHNICAL UNIVERSITY

BY

DENİZ ERTÜRKAN

IN PARTIAL FULFILLMENT OF THE REQUIREMENTS
FOR
THE DEGREE OF MASTER OF SCIENCE
IN
CHEMICAL ENGINEERING

JUNE 2012

Approval of the thesis:

**DEVELOPMENT OF A NEW IMMOBILIZATION PROCEDURE
FOR DETECTION OF
STAPHYLOCOCCAL ENTEROTOXIN B (SEB) AND CANDIDA ALBICANS**

submitted by **DENİZ ERTÜRKAN** in partial fulfillment of the requirements for the degree of Master of Science in **Chemical Engineering Department, Middle East Technical University** by,

Prof. Dr. Canan ÖZGEN
Dean, Graduate School of **Natural and Applied Sciences**

Prof. Dr. Deniz ÜNER
Head of Department, **Chemical Engineering**

Prof. Dr. Canan ÖZGEN
Supervisor, **Chemical Engineering Dept., METU**

Assoc. Prof. Dr. Haluk KÜLAH
Co-Supervisor, **Electrical and Electronics Engineering Dept., METU**

Examining Committee Members:

Prof. Dr. Hayrettin Yücel
Chemical Engineering Dept., METU

Prof. Dr. Canan ÖZGEN
Chemical Engineering Dept., METU

Assoc. Prof. Dr. Haluk KÜLAH
Electrical and Electronics Engineering Dept., METU

Prof. Dr. Ufuk BAKIR
Chemical Engineering Dept., METU

Assoc. Prof. Dr. Uğur TAMER
Analytical Chemistry Dept., Gazi University

Date: **11.06.2012**

I hereby declare that all information in this document has been obtained and presented in accordance with academic rules and ethical conduct. I also declare that, as required by these rules and conduct, I have fully cited and referenced all material and results that are not original to this work.

Name, Last Name: Deniz ERTÜRKAN

Signature : 

ABSTRACT

DEVELOPMENT OF A NEW IMMOBILIZATION PROCEDURE FOR DETECTION OF STAPHYLOCOCCAL ENTEROTOXIN B (SEB) AND *CANDIDA ALBICANS*

ERTÜRKAN, Deniz

M.Sc., Department of Chemical Engineering

Supervisor: Prof. Dr. Canan Özgen

Co-Supervisor: Assoc. Prof. Dr. Haluk Külah

June 2012, 92 pages

Fast and accurate detection of pathogens such as bacteria, their toxins and viruses at low concentrations is very important. The conventional techniques are time consuming where expensive equipment is required with a consumption of excess amount of blood from patients. Recently, immunosensors are used for the detection of pathogens because they are miniature, sensitive, biocompatible and require low power.

According to the Centers for Disease Control and Prevention (CDCP), 76 million people become ill due to food poisoning and 5,000 of them die each year in United States. In addition, SEB causing food poisoning has listed as a bioterrorism agent by CDCP. Thus, accurate and selective detection in short time is very important for SEB detection.

Candida albicans (*C. albicans*) is a yeast-like fungus and causes anxiety, insomnia, constipation, hiatal hernia, panic attacks, denture-induced stomatitis, angular cheilitis, gingivitis and prosthetic implant infections. In addition, it can cause death if the immune system of patient is under failure due to cancer, chemotherapy and AIDS.

In this study, a new procedure was developed. A simple and highly selective homogeneous sandwich immunoassay was obtained for ultrasensitive detection of Staphylococcal Enterotoxin B (SEB) using Atomic Force Microscopy (AFM) and Surface Enhanced Raman Scattering (SERS) probe. In the developed procedure, thiolated antibodies were produced and SEB was immobilized on the biosensor surface using these antibodies. In addition, theory of SEB adsorption on a gold surface was studied and the reaction rate constant between SEB and its toxin was calculated. Moreover, *C. albicans* was detected using the developed procedure by a microscope. Thus, it is proved that, the developed procedure can be used for detection of different pathogens. Furthermore, nonspecific interaction between SEB antibody and BSA was determined in this study. Also, the developed procedure and a procedure found from literature were compared. In the procedure used in the literature (second procedure), self-assembled monolayer (SAM) was formed and antibodies were immobilized on SAM. After formation of sandwich structure, the roughness of gold surface and the minimum concentration of SEB detected were determined by AFM and SERS, respectively.

Keywords: SEB, *Candida albicans*, SERS, thiolated antibody, biosensor

ÖZ

STAPHYLOCOCCAL ENTEROTOKSİN B (SEB) VE *CANDIDA ALBICANS*
SAPTAMASI İÇİN YENİ TUTUNDURMA PROSEDÜRÜ GELİŞTİRİLMESİ

ERTÜRKAN, Deniz

Yüksek Lisans, Kimya Mühendisliği Bölümü

Tez Yöneticisi: Prof. Dr. Canan Özgen

Ortak Tez Yöneticisi: Doç. Dr. Haluk Külah

Haziran 2012, 92 sayfa

Patojenlerin (bakteri, bakteri toksinleri ve virüsler) kısa zamanda ve düşük derişimlerde dahi hızlı ve doğru saptanması çok önemlidir. Geleneksel yöntemler zaman alan, pahalı aletlere ihtiyaç duyulan ve hastalardan fazla miktarda kan alınması gereken yöntemlerdir. Son zamanlarda, patojenlerin saptanması için minyatür, duyarlı, biyo-uyumlu, az enerji gereksinimi olmaları nedeni ile immünosensörler kullanılmaktadır.

Birleşmiş Milletler Hastalık Kontrol ve Korunma Merkezine göre besin zehirlenmesi sebebi ile her yıl Amerikada 76 milyon insan hasta olmakta ve bu hastaların 5000'i hayatını kaybetmektedir. Ayrıca, besin zehirlenmesine sebep olan Staphylococcal Enterotoksin B (SEB) Birleşmiş Milletler Hastalık Kontrol ve Korunma Merkezince biyolojik silah olarak listelenmiştir. Böylece, kısa sürede doğru ve seçici SEB toksini saptaması çok önemlidir.

Candida albicans (*C. albicans*) maya benzeri mantardır ve endişe, uykusuzluk, kabızlık, fitik, panik atak, ayrıca, ağız, dudak, diş eti ve protez implantasyon iltihabına sebep olur. Ayrıca, eğer hastanın bağıışıklık sistemi kanserden, kemoterapiden ve AİDS'den zarar görmüş ise *C. albicans* ölüm nedeni olabilmektedir.

Bu çalışmada, atomik kuvvet mikroskobu (AFM) ve yüzeye kuvvetlendirilmiş Raman saçılması (SERS) kullanılarak SEB toksininin ultra duyarlı saptanması için yeni bir prosedür geliştirilerek, basit ve oldukça seçici homojen sandviç tutunma deneyi ile gerçekleştirılmıştır. Geliştirilen prosedürde, tiyoller bulunan antikorlar üretilerek, SEB toksini antikorlar yardımıyla sensor yüzeyine tutundurulmuştur. Ayrıca, SEB toksininin altın yüzeyine bağlanması teorisi ile toksin ve onun antikoru arasındaki reaksiyon hız sabiti hesaplanmıştır. Ayrıca, geliştirilen prosedür kullanılarak *C. albicans* mayası mikroskop ile saptanmıştır. Böylece, geliştirilen prosedürün farklı patojenleri saptamada da kullanılabileceği kanıtlanmıştır. Bunun yanında, bu çalışmada SEB toksininin antikoru ile BSA proteini arasında non spesifik olmayan etkileşim belirlenmiştir. Diğer taraftan, geliştirilen prosedür ile literatürde kullanılan farklı bir prosedür karşılaştırılmıştır. İkinci prosedürde, kendinden birleşen tek tabakalı yapılar oluşturularak, antikorlar bu yapılara tutundurulmuştur. Sandviç yapılar ikinci prosedür kullanılarak oluşturulduktan sonra, altın yüzeyin pürüzlülüğü ve saptanabilen en az SEB konsantrasyonu sırasıyla AFM ve SERS ile saptanmıştır.

Anahtar Kelimeler: SEB, *Candida albicans*, SERS, tiyoller bulunan antikor, biyosensör

To my mother, sister, brother and love

ACKNOWLEDGEMENTS

First of all, I would like to thank my supervisor Prof. Dr. Canan Özgen and co-supervisor Assoc. Prof. Dr. Haluk Külah for their support, guidance throughout this study and for their kindly attitude. I wish to thank also to Assoc. Prof. Dr. Uğur Tamer for his allowance for using his laboratory for some experiments.

I would like to acknowledge TÜBİTAK for the scholarship given to me throughout my second and third year of my master of science study.

I would like to thank Ms Hatice Ceylan Koydemir for her guidance in my studies for answering my unending questions, for sharing her experience and knowledge and also for supplying me with the gold surfaces produced by her. I also would like to express my thanks to Dr. Yekbun Adıgüzel for her helps throughout the thesis studies. I would also like to thank Dr. Ender Yıldırım and Mr. Aziz Koyuncuoğlu for their support and help during the fabrication of biosensors.

I would also like to show my appreciation to Mr. Caner Hocaoğlu for his help, encouragement and endless patience.

Finally, I would like to present last but not the least thanks to my family for their love and support throughout my education and life.

TABLE OF CONTENTS

	<u>Page No</u>
ABSTRACT	iv
ÖZ	vi
ACKNOWLEDGEMENTS	ix
TABLE OF CONTENTS	x
LIST OF TABLES	xii
LIST OF FIGURES	xiii
NOMENCLATURE.....	xvii
INTRODUCTION	1
LITERATURE SURVEY	3
2.1 Microorganisms	3
2.1.1 Bacteria	3
2.1.1.1 Classification of Bacteria According to Shape	4
2.1.1.2 Classification of Bacteria According to Nucleus	5
2.1.1.3 Clasification of Bacteria According to Gram Stain	6
2.1.1.4 Bacteria Causing Food Poisoning	7
2.1.1.4.1 <i>Staphylococcus aureus</i>	9
2.1.1.4.2 Staphylococcal Enterotoxin B (SEB).....	10
2.1.2 Fungi	11
2.1.2.1 <i>Candida albicans</i> (<i>C. albicans</i>).....	11
2.1.2.2 Detection of Pathogens	14
2.1.2.2.1 Antibody.....	15
2.1.2.2.2 Physical Adsorption of Antibody on Biosensor Surface.....	16
2.1.2.2.3 Chemical Adsorption of Antibody on Biosensor Surface	18
2.1.2.2.4 Microelectromechanical Systems (MEMS) Based Biosensors...	20
2.1.2.2.5 Detection Methods for Pathogens.....	22
2.1.2.2.5.1 Mechanical Detection Method	22
2.1.2.2.5.2 Optical Detection Method	24
2.1.2.2.5.3 Magnetic Detection Method.....	25
2.1.2.2.5.4 Electrochemical Detection Method.....	26

2.1.2.2.5.5 Spectroscopy Techniques for Detecting Pathogens.....	29
THEORETICAL STUDIES.....	32
3.1 Self-Assembled Monolayer (SAM)	32
3.2 Antibody- Antigen Reaction	34
3.3 Adsorption.....	36
EXPERIMENTAL STUDIES.....	38
4.1 Method I.....	38
4.1.1 Chemicals used in the experiment.....	39
4.1.2 Experimental Procedure for Method I.....	40
4.2 Method II.....	43
4.2.1 Chemicals used in the experiments	43
4.2.2 Formation of Sandwich Structure using SAM	44
4.3 Equipments used during experiment.....	46
4.3 Fabrication of Biosensor Surface	48
4.4 Fabrication of Biosensor with Channel.....	49
RESULT AND DISCUSSION	51
5.1 Results with Method I	51
5.1.1 Bare Gold Surface Characterization with AFM.....	52
5.1.2 Toxin Modified Gold Surface Characterization with AFM	53
5.1.3 Toxin Modified Gold Surface Characterization with SERS	57
5.1.4 <i>C. albicans</i> Immobilized Gold Biosensor Surface Characterization with Microscope.....	61
5.2 Results with Method II.....	68
5.2.1 Toxin Modified Gold Surface Characterization with AFM.....	68
5.2.2 Toxin Modified Gold Surface Characterization with SERS	70
CONCLUSIONS AND RECOMMENDATIONS	72
REFERENCES.....	74
APPENDIX A	86
DATA FOR METHOD I FOR THE DETECTION OF <i>C. albicans</i>	
BY MICROSCOPE.....	86

LIST OF TABLES

TABLES

	<u>Page No</u>
Table 2.1 Principal Differences Between Prokaryotic and Eukaryotic Bacteria	5
Table 2.2 Pathogens causing foodborne illnesses, hospitalizations and deaths annually.....	8
Table 2.3 Proteins and toxins produced by <i>Staphylococcus aureus</i>	10
Table 2.4 Detection limit of <i>Candida</i> species using by AB-ELISA	14
Table 2.5 Immobilization Methods for Antibodies	14
Table 5.1 Average roughness (Ra) and maximum height (Rt) of different analyzed areas on the same gold surface measured by AFM.....	53
Table 5.2 AFM roughness values for gold surface after each step of the sandwich immunoassay.....	68

LIST OF FIGURES

FIGURES

	<u>Page No</u>
Figure 2.1 a) Coccii, b) rod c) spirilla bacteria	4
Figure 2.2 Gram stain reaction of a) gram-positive bacteria and b) gram-negative bacteria.....	7
Figure 2.3 Amount of detection of pathogenic bacteria in different areas according to literature survey	7
Figure 2.4 Structure of Staphylococcal Enterotoxin B	11
Figure 2.5 Oval and hyphal forms of <i>C. albicans</i>	12
Figure 2.6 SEM images of CNTFET device after immobilization of antibody and <i>Candida albicans</i>	13
Figure 2.8 Vroman effect	16
Figure 2.9 Displacement of LMW to HMW protein.....	17
Figure 2.10 Detection of thyroglobulin (Tg) by using the principle of Vroman Effect	17
Figure 2.11 Schemes of different immobilization methods	18
Figure 2.12 Immobilization of antibody on polystyrene surface	20
Figure 2.13 Biosensors	21
Figure 2.14 Principal working of cantilever	23
Figure 2.15 a) Sketch of the experimental set up of cantilever b) Cantilever deflection versus time (Glucose concentrations: (1) 0, (2) 0.2, (3) 0.5, (4) 1, (5) 2, (6) 5, (7) 10, and (8) 20 mM).....	23
Figure 2.16 Working principle of AFM	25
Figure 2.17 Schematic illustration of separation of <i>E.coli</i> onto magnetic glyco- nanoparticles	25
Figure 2.18 Schematic drawing of the microfluidic chip.....	26
Figure 2.19 Schematic drawing of SEB detection	28

Figure 2.20 a) Schematic illustration of self-assembled monolayer (SAM)	
b) Redox reaction between enzyme and its substrate c) Drawing of	
amperometric immunosensor	29
Figure 2.21 Detection of SEB with using different SAM structures and different	
antibody fragments.....	31
Figure 2.22 Detection of SEB with using neutravidin conjugated gold	
nanoparticles	31
Figure 3.1 Schematic drawing showing layers of SAM	32
Figure 3.2 Schematic view of thiol molecule orientation (α , β and γ)	
on a gold surface	33
Figure 3.3 Schematic drawing of an antibody.....	34
Figure 3.4 Schematic diagram of antibody-antigen interaction	35
Figure 4.1 Molecular structure of sulfo-LC-SPDP.	39
Figure 4.2 Schematic procedure of toxin immobilization using thiolated	
antibody.....	41
Figure 4.3 Schematic procedure of antibody conjugated gold particle.....	42
Figure 4.4 SERS-based sandwich immunoassay for SEB using thiolated	
antibody.....	43
Figure 4.5 Molecular structure of a) 3-MPA and b) 11-MUA.....	44
Figure 4.6 Schematic drawing of toxin immobilization using 11-MUA and	
3-MPA for SAM.	45
Figure 4.7 Schematic Procedure of SERS-based sandwich immunoassay using	
11-MUA and 3-MPA for SAM.	46
Figure 4.8 AFM, Vecoo MultiMode V	47
Figure 4.9 Delta Nu Raman microscope.	47
Figure 4.10 Karl Suss PM5 Analytical Wafer Prober.....	48
Figure 4.11 Fabrication steps of the biosensor.....	50
Figure 4.12 Schematic illustration of biosensor.....	50
Figure 5.1 a) 2-D profile b) 3-D profile c) Cross section of first analyzed	
area ($1 \times 1 \mu\text{m}^2$).....	52
Figure 5.2 Surface I a) 2-D profile b) 3-D profile c) Cross section after sandwich	

immunoassay.....	54
Figure 5.3 Surface II a) 2-D profile b) 3-D profile c) Cross section after sandwich immunoassay.....	55
Figure 5.4 Surface III a) 2-D profile b) 3-D profile c) Cross section after sandwich immunoassay.....	55
Figure 5.5 Surface IV a) 2-D profile b) 3-D profile c) Cross section after sandwich immunoassay.....	56
Figure 5.6 Optimum time for antibody immobilization using 10^{-3} mg/ml of SEB.	57
Figure 5.7 Surface Coverage as a function of Concentration of SEB	58
Figure 5.9 Raman intensity of different concentrations of toxin immobilization using thiolated antibody.....	59
Figure 5.10 Calibration curve for toxin immobilization using thiolated antibody....	60
Figure 5.11 Comparison of Raman intensity between 10^{-1} mg/ml and 10^{-3} mg/ml of SEB and BSA using thiolated antibody.....	61
Figure 5.12 Immobilization of <i>C. albicans</i> using thiolated antibody.....	62
Figure 5.13 Immobilization of 1 mg/ml <i>C. albicans</i> on gold surface.....	63
Figure 5.14 Immobilization of 250 pg/ml <i>C. albicans</i> on gold biosensor surface....	64
Figure 5.15 Immobilization of a) 100 μ g/ml and b) 1 ng/ml <i>C. albicans</i> on gold biosensor surface stored at -20 $^{\circ}$ C for one week.....	65
Figure 5.16 Immobilization of a) 500 μ g/ml b) 1 ng/ml and c) 250 pg/ml <i>C. albicans</i> inside the biosensor channel	66
Figure 5.17 Immobilization of are 250 pg/ml <i>C. albicans</i> inside the biosensor channel	67
Figure 5.18 Immobilization of 1 μ g/ml <i>C. albicans</i> on gold surface of biosensor in the channel stored at -20 $^{\circ}$ C for one week.....	67
Figure 5.19 2D (a) and phase images (b) of AFM topography of A) bare gold surface; B) SAM+ antibody; C) SAM, + antibody+SEB+ antibody + gold nanorods.....	69
Figure 5.20 Raman intensity for different concentrations of toxin immobilization using SAM	70
Figure 5.21 Calibration curve for toxin immobilization using SAM	71

Figure 5.22 Comparison of Raman intensity between 10^{-1} mg/ml and 10^{-3} mg/ml of SEB and BSA using SAM	71
Figure A.1 Characterization of 500 $\mu\text{g}/\text{ml}$ <i>C. albicans</i> on gold biosensor surface.	86
Figure A.2 Characterization of 100 $\mu\text{g}/\text{ml}$ <i>C. albicans</i> on gold surface	87
Figure A.3 Characterization of 50 $\mu\text{g}/\text{ml}$ <i>C. albicans</i> on gold surface	87
Figure A.4 Characterization of 10 $\mu\text{g}/\text{ml}$ <i>C. albicans</i> on gold surface	88
Figure A.5 Characterization of 1 $\mu\text{g}/\text{ml}$ <i>C. albicans</i> on gold surface	88
Figure A.6 Characterization of 50 ng/ml <i>C. albicans</i> on gold surface.....	89
Figure A.7 Characterization of 1 ng/ml <i>C. albicans</i> on gold surface.....	89
Figure A.8 Characterization of 800 pg/ml <i>C. albicans</i> on gold surface.....	90
Figure A.9 Characterization of 500 pg/ml <i>C. albicans</i> on gold surface.....	90
Figure A.10 Characterization of 10 $\mu\text{g}/\text{ml}$ <i>C. albicans</i> on gold surface stored at -20 $^{\circ}\text{C}$ for one week.....	91
Figure A.11 Characterization of 1 $\mu\text{g}/\text{ml}$ <i>C. albicans</i> on gold surface stored at -20 $^{\circ}\text{C}$ for one week.....	91
Figure A.12 Characterization of 1 ng/ml <i>C. albicans</i> on gold surface stored at -20 $^{\circ}\text{C}$ for one week.....	92

NOMENCLATURE

k_i Association constant

k_{-i} Disassociation constant

K Reaction rate constant

R_a Rate of adsorption

R_d Rate of desorption

Abbreviations

<i>S. aureus</i>	<i>Staphylococcus aureus</i>
<i>C. albicans</i>	<i>Candida albicans</i>
SEB	Staphylococcal Enterotoxin B
SERS	Surface Enhanced Raman Scattering
AFM	Atomic Force Microscope
CDCP	Center for Disease Control and Prevention
SAM	Self-Assembled Monolayer
MEMS	Micro-Electromechanical System
ELISA	Enzyme Linked Immunosorbent Assay

CHAPTER 1

INTRODUCTION

Pathogens such as bacteria, viruses and toxins causes different diseases in different industries. Thus, accurate, sensitive, inexpensive and rapid detection of pathogens at low concentrations is very important. The conventional techniques such as culture and colony counting methods and polymerase chain reaction based methods have time-consuming enrichment steps. They require expensive equipment and consume excess amount of blood from patients. Recently, biosensors such as immunosensors are started to be used for detection of pathogens because of their miniature, sensitive, biocompatible and low power.

For immobilization and detection of pathogens and their toxins, antibodies are generally used as molecular recognition units because of their affinity and specificity. Each antibody has a unique region for a specific antigen and an antibody can bind to only its specific antigen. Thus, antibody-antigen interaction is very strong due to electrostatic forces such as Van der Waals forces, hydrophobic interactions, ionic bonds and hydrogen bonds. In different surface enhanced Raman scattering (SERS) immunoassays, pathogens and their toxins are detected using their antibodies (de Freitas et al., 2010). SERS-based immunoassay has a high sensitivity in the range of picomole to femtomole (Montville et al., 2008). Femtomolar amounts of biomolecules (small molecules, nucleic acids, proteins, toxins and cells etc.) can be detected by SERS in dry or wet conditions.

According to World Health Organization (WHO), up to 30 % of the population of industrialized countries suffers from food-poisoning in each year. *Staphylococcus*

aureus (*S. aureus*) is among the food-poisoning bacteria with the highest incidence. Approximately 100-200 ng of *S. aureus* is enough to cause food poisoning (Zourob et al., 2008). Staphylococcal Enterotoxin B (SEB) is a heat resistant toxin of *S. aureus* and even small amount (~1 ng/ml) of SEB causes intoxication. It can be used as a biological weapon and hence it has been listed as a bioterrorism agent by the Centers for Disease Control and Prevention (CDCP).

In this study, a new procedure and a simple and highly selective homogeneous sandwich immunoassay was designed and developed for ultrasensitive detection of SEB using atomic force microscopy (AFM) and SERS probe. In the developed procedure, thiolated antibodies were produced and using these antibodies, SEB was immobilized on a gold biosensor surface. In addition, theory of SEB adsorption on a gold surface was studied and the reaction rate constant between SEB and its antibody was calculated. In addition, sandwich immunoassay was obtained after SEB immobilization and the toxin was detected by AFM and SERS. Additionally, another pathogen, a yeast-like fungus causing diseases in digestive systems named as *Candida albicans* (*C. albicans*), was detected by microscope using the developed procedure. Thus, it is proved that the developed procedure can be used for detection of different pathogens.

Lastly, the developed procedure and a procedure found from the literature were compared. By using the procedure found from literature, self-assembled monolayer (SAM) was formed and antibodies were immobilized on SAM. After formation of sandwich structure, SEB was also detected by AFM and SERS using this procedure. Thus, the procedures developed in this study and the one found in the literature are compared and the limits of detection of the procedures are compared.

CHAPTER 2

LITERATURE SURVEY

In this chapter, literature information about microorganisms, bacteria and their classification according to shape and nucleus with bacteria causing food poisoning will be given. Also, *Staphylococcus aureus*, Staphylococcal Enterotoxin B (SEB), fungi, *Candida albicans*, detection of pathogens, antibodies, physical and chemical adsorption of antibody on biosensor surface will be explained. Lastly, microelectromechanical systems (MEMS) based biosensors, detection methods for pathogens (mechanical, optical, magnetic, electrochemical) and spectroscopy techniques will be outlined.

2.1 Microorganisms

Microorganisms are microscopic organisms which can not be seen by the naked eye. They live in all parts of the biosphere, i.e. in air, land and water environments. Some microorganisms are critical for nutrient recycling in ecosystems and they are also a vital part of the nitrogen cycle. On the other hand, some of microorganisms called pathogens can be harmful and cause diseases. Detection of them in a short time and accurately is very important. Microorganisms are divided into four types which are bacteria, fungi, viruses and protozoa (Alouf, 2006; Hogg, 2005; Lazcka, 2007).

2.1.1 Bacteria

Bacteria are a large domain of microorganisms. There are approximately five nonillion (5×10^{30}) bacteria on the earth (Whitman, 1998). Bacteria can be classified on the basis of

- shape
- nucleus
- ability to form spores
- method of energy production
- nutritional requirements
- reaction to the gram stain

Also, bacteria causing food poisoning is another classification. Some characteristics of bacteria such as shape, nucleus, reaction to the gram stain and ability to cause food poisoning are important for the detection of bacteria by biosensors. Therefore, only these characteristics will be explained in the following sections.

2.1.1.1 Classification of Bacteria According to Shape

Bacteria have many sizes and several shapes. Their diameter and length range are between 0.2 to 2.0 μm and 2 to 8 μm , respectively (Hogg, 2005). They have three basic shapes which are spherical coccus, rod-shaped bacillus and spiral as shown in **Figure 2.1** (Glauert, 1962; Hogg, 2005). Therefore, different bacteria can be detected by microscope easily by their size and shape.

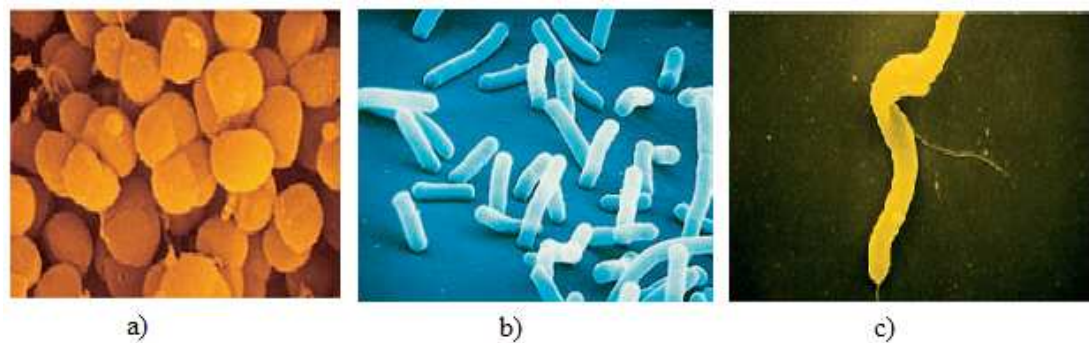


Figure 2.1 a) Coccis, b) Rod, c) Spirilla Bacteria (Glauert, 1962).

2.1.1.2 Classification of Bacteria According to Nucleus

According to nucleus of bacteria, there are two types which are prokaryotes and eukaryotes. The main difference between prokaryotic and eukaryotic bacteria is that prokaryotic bacteria do not have a nucleus, but eukaryotic bacteria have a nucleus. Other differences between prokaryotic and eukaryotic bacteria are shown in **Table 2.1.**

Table 2.1 Principal Differences Between Prokaryotic and Eukaryotic Bacteria
(Tortora et al., 2010).

	Prokaryote Bacteria	Eukaryotic Bacteria
Size of Cell	0.2–2.0 mm in diameter	10–100 μm in diameter
Nucleus	Absent	Present
Membrane-Enclosed Organelles	Absent	Present
Flagella	Consist of two protein building blocks	Consist of multiple microtubules
Cell Wall	Chemically complex (typical bacterial cell wall includes peptidoglycan)	Chemically simple (includes cellulose and chitin)
Cytoplasm	No cytoskeleton	Cytoskeleton
Ribosomes	Smaller size	Larger size
Chromosome (DNA)	Single circular chromosome	Multiple linear chromosomes with histones
Cell Division	Binary fission	Mitosis

2.1.1.3 Classification of Bacteria According to Gram Stain

Bacteria are divided into two groups according to reaction to the gram stain which are gram-positive and gram-negative bacteria. The outer membrane of cell-wall of gram-negative bacteria covers thin layer of peptidoglycan and it is made of lipopolysaccharide. Moreover, the cell-wall contains porins and a lipoprotein exists in the cell-wall structure linked to the peptidoglycan layer. Gram-negative bacteria have a cytoplasmic membrane (Glauert, 1962; Hogg, 2005). There is a space between cytoplasmic and outer membrane. This space is called the periplasmic space which contains a loose network of peptidoglycan chains. In a gram stain test, gram-negative bacteria do not retain crystal violet dye and it is colored with a red or pink color due to the counterstain. Some examples of the gram-negative bacteria are named as *Acinetobacter*, *Actinobacillus*, *Bordetella*, *Brucella*, *Campylobacter*, *Cyanobacteria*, *Enterobacter*, *Erwinia*, *Escherichia coli*, *Francisella*, *Helicobacter*, *Hemophilus*, *Klebsiella*, *Legionella*, *Moraxella*, *Neisseria*, *Pasteurella*, *Proteus*, *Pseudomonas*, *Salmonella*, *Serratia*, *Shigella*, *Treponema*, *Vibrio* and *Yersinia* (Koch, 2006).

Some gram-positive bacteria contain teichoic acid linked to the muramic acid of the peptidoglycan layer. Moreover, some bacteria have capsule polysaccharides (Koch, 2006; Books, 2011). In comparison to gram-negative bacteria, the cell wall of gram-positive bacteria is thick and approximately 80 percent of the cell wall is made of peptidoglycan (Koch, 2006). A gram stain test is a common technique for differentiation bacteria based on their different cell wall constituents and gram-positive bacteria retain the crystal violet stain due to the high amount of peptidoglycan in the cell wall. This explained feature results in different colors for gram-positive and gram-negative bacteria as is shown in **Figure 2.2** (Biswas et al., 1970).

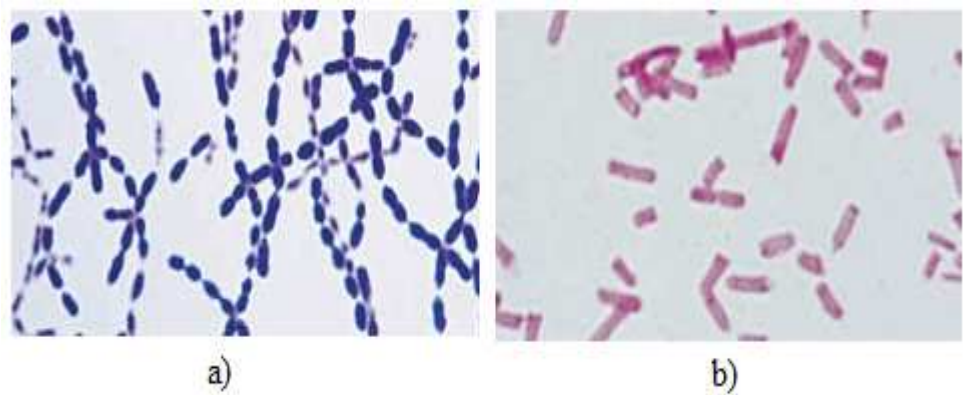


Figure 2.2 Gram stain reaction of a) gram-positive bacteria and b) gram-negative bacteria (Biswas et al., 1970).

2.1.1.4 Bacteria Causing Food Poisoning

Pathogens such as virus, bacterium, prion or fungus cause different diseases in different mediums. According to 2500 articles about pathogenic bacteria detection over the last two decades, food industry is the area where pathogenic bacteria were detected at most (38%) as is shown in **Figure 2.3** (Lazcka et al., 2007).

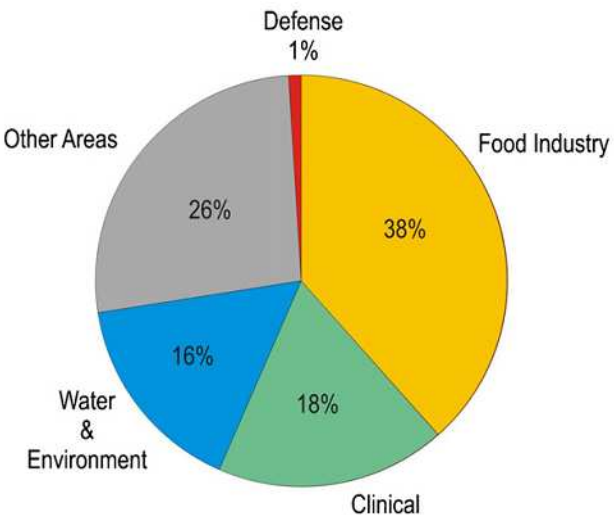


Figure 2.3 Amount of detection of pathogenic bacteria in different areas according to literature survey (Lazcka et al., 2007).

According to the Centers for Disease Control and Prevention (CDCP) in United States, 76 million people become ill due to food poisoning and 5,000 of them die each year (Nedelkov et al., 2003; Labib et al., 2009; Natesan et al., 2009). In addition, according to CDCP 31 pathogens are known which cause foodborne illness. Some of pathogens causing food-related death are *Salmonella*, *Listeria*, *Toxoplasma*, Norwalk-like viruses, *Campylobacter*, *E. coli* O157:H7 and others (5%) (Velusamy et al., 2010). According to CDCP, the top five pathogens causing domestically acquired foodborne illnesses and their annual number of illnesses in 2011 are listed in **Table 2.2** (Group USCSW, 2010).

Table 2.2 Top five pathogens causing domestically acquired foodborne illnesses
(Group USCSW, 2010)

Bacteria	Estimated annual number of illnesses	90% Credible Interval
Norovirus	5,461,731	3,227,078–8,309,480
<i>Salmonella</i>	1,027,561	644,786–1,679,667
<i>Clostridium perfringens</i>	965,958	192,316–2,483,309
<i>Campylobacter spp.</i>	845,024	337,031–1,611,083
<i>Staphylococcus aureus</i>	241,148	72,341–529,417

As mentioned above, different types of bacteria can cause food poisoning. In this study, a toxin of *Staphylococcus aureus* named as SEB, causing food poisoning and also *C. albicans* used as an example of pathogens due to their extensive impacts on cases detected. Therefore, detailed literature survey was done on *Staphylococcus aureus*, its toxin (SEB) and *C. albicans* and some important information about them will be introduced in the following sections.

2.1.1.4.1 *Staphylococcus aureus*

Among the food-poisoning bacteria, *Staphylococcus aureus* (*S. aureus*) is one of them which causes large infection cases **Table 2.2**. According to the U.S. Food and Drug Administration (FDA) more than 10^5 cells/g of *S. aureus* cause food poisoning (Montville et al., 2008). Whereas, the minimum concentration causing food poisoning is around 100-200 cells/g (Alouf et al., 2006). The symptoms appear within approximately 4.5 hours after eating the *S. aureus* bearing food (Montville et al., 2008). *S. aureus* is a gram-positive bacterium having 0.5-1.5 μm diameter. The cell wall of *S. aureus* contains three main components which are the peptidoglycan comprising repeating units of N-acetyl glucosamine β -1,4 linked to N-acetyl muramic acid, a ribitol teichoic acid bound via N-acetyl mannosaminyl- β -1,4-N-acetyl glucosamine to a muramyl-6-phosphate and Protein A (Koch, 2006). *S. aureus* produces adhesion proteins, enterotoxins, superantigens, pore-forming hemolysins, and ADP-ribosylating toxins which are listed in **Table 2.3**.

S. aureus produces 17 different toxins which are called Staphylococcal enterotoxins (SEs) (SEA-SER except SEF) (Alouf et al., 2006). The molecular weights of SEs are approximately 26-35 kD. SEs are heat resistant and they can be damaged only if they are heated at 100 $^{\circ}\text{C}$ for more than two hours. *S. aureus* and its toxins cause nausea, acute vomiting, abdominal pain, diarrhea, headache, cramping and anaphylactic shock (Books, 2011). The food poisoning which is caused by a toxin of *S. aureus* named as Staphylococcal Enterotoxin B (SEB) is known as ‘intoxication’ or ‘poisoning’ due to the fact that bacteria itself do not have to grow in the patient (Montville et al., 2008). This toxin is one of the harmful toxins which needs to be detected in an early stage. Thus, the detection of SEB was aimed in this study.

Table 2.3 Proteins and toxins produced by *S. aureus* (Hiramatsu et al., 2004).

Virulence Factors produced by <i>S. aureus</i>	Receptors produced by <i>S. aureus</i>
Adhesion Proteins Spa (protein A) Bap (biofilm-associated proteins) Fbp (fibronectin-binding protein) ClfA (fibrinogen-binding protein) Can (collagen adhesion) IsdA, IsdB, IsdC, IsdH (iron-regulated surface proteins) Pls (plasmin-sensitive cell wall protein) Atl (autolysin amidase)-bacteriolytic action Enolase Teichoic acid	Fc part of IgG Fibronectin, fibrinogen, elastin Fibrinogen Collagen Hemoglobin, transferring, hemin Cellular lipid ganglioside GM Fibronectin, fibrinogen, vitronectin Laminin Unknown-binds epithelial cells
Enterotoxin (SEs) (17 in number) Staphylococcal enterotoxin SEA-SER, except SEF	Glycosphingolipid
Pore-forming hemolysins Hemolysins α , β , γ , δ	Cholesterol
Superantigens TSST (toxic shock syndrome toxin) Enterotoxins Exfoliative toxins (A, B)	MHC class II Glycosphingolipid
ADP-ribosylating toxins Leukocidin Pyrogenic exotoxin	

2.1.1.4.2 Staphylococcal Enterotoxin B (SEB)

Staphylococcal Enterotoxin B (SEB) is one of the 17 enterotoxins of *S. aureus* (SEs) and a heat resistant toxin. SEB consists of 239 amino acid residues and its molecular weight is 31.4 kDa. As shown in **Figure 2.4**, the shape of SEB is like an ellipsoid with dimensions of 50 Å×45 Å×34 Å (Papageorgiou et al., 1998). The incubation period of SEB in the human body is 3-12 h and it causes headache, chills, myalgias, non-productive cough and a high fever up to 41.1 °C. The symptoms are generally observed within six hours. Antibiotics can not treat acute gastrointestinal illness and

are also not effective on SEB (Emmeluth et al., 2011). Thus, SEB can be used as a biological weapon. Moreover, the Center for Disease Control and Prevention (CDCP) has listed SEB as a bioterrorism agent (Tortora et al., 2009). Small amount (~1 ng/ml) of SEB causes intoxication (Banada et al., 2008).

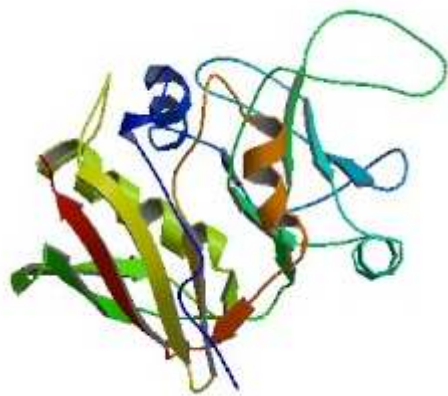


Figure 2.4 Structure of Staphylococcal Enterotoxin B (Swaminathan et al., 1992).

2.1.2 Fungi

Fungi are eukaryotic and heterotrophic organisms. They are different from plants, animals, and bacteria. They have a cell wall made of chitin but they have no chlorophyll. They have fundamental roles in nutrient cycling and they can be used as a source of food like mushrooms. In addition fungi have been used for the production of antibiotics since 1940s. Fungi have approximately 300 000 different species and about 200 of them are potential parasites (Hogg, 2005). Some fungal diseases such as skin infections or chronic infection of deep tissues are typically caused by *Candida* species (Alouf, 2006; Hogg, 2005).

2.1.2.1 *Candida albicans* (*C. albicans*)

Candida albicans (*C. albicans*) is a yeast-like fungus which lives on the skin and in mucous membranes like the vagina, mouth or rectum. *C. albicans* lives in our body and it is inactivated by friendly and protective bacteria called *Acidophilus* and

Bifidus. If the number of these bacteria decreases in the body *C. albicans* multiplies out of control.

C. albicans causes different diseases in digestive systems. It spreads to the other parts of the body and causes negative yeast infections. The fourth most common cause of the nosocomial blood stream infections is the *Candida* infections (Gudlaugsson et al., 2003; Pfaller et al., 2007; Forrest et al., 2010). Also, different factors such as antibiotics, birth control pills, stress, constipation, hormonal imbalance and alcohol can lead to *candida* infections (Jenkinson et al., 2002). In the last decades, *Candida* infections have increased due to immunosuppressive treatments, use of the broad-spectrum antibiotics and long-term catheterization (Molero et al., 1998). *C. albicans* causes anxiety, insomnia, constipation, hiatal hernia, panic attacks, denture-induced stomatitis, angular cheilitis, gingivitis, prosthetic implant infections. If the immune system of an individual is under failure due to cancer, chemotherapy hospitalization or AIDS, the infection of *C. albicans* can be lethal (Hall et al., 2010). In addition, *C. albicans* can transfer from one person to another person sexually. *C. albicans* has two morphologic forms as oval and hyphal forms (**Figure 2.5**). Its yeast form is 10-12 μm in diameter (Han et al., 2011).

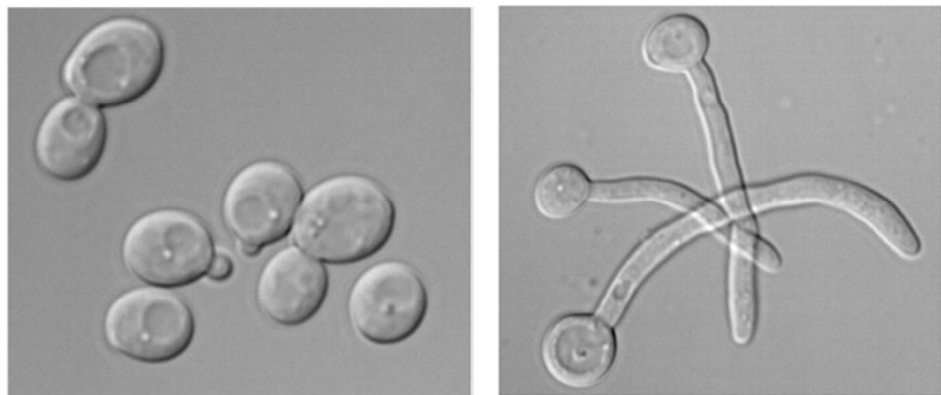


Figure 2.5 Oval and hyphal forms of *C. albicans* (Gutierrez-Escribano et al., 2011).

C. albicans or its antibody can be detected with different methods. In the study of (Kumar et al., 2007), anti-*Candida* antibodies were determined in the blood or in the serum of immunocompromised (HIV or cancer) patients by using ELISA tests. 41.43% of HIV and 5% of cancer patients who did not possess candidemia, had greater than 12 U/ml anti-*Candida* antibodies. As studied by Kumar et al. (2007), candidemia was determined among patients who had not anti-Candida antibodies. Takaki et al. (1996) developed the detection method for *Candida* antigen and antibody from the serum of patients with candidasis by using three different detection assays which were Cand-tee, counterimmunoelectrophoresis assay (CIE), and a passive hemagglutination assay (PHA)

Villamiza et al. (2009) used carbon nanotube field-effect transistor to detect *C. albicans*. After immobilization of anti-*Candida*, 50 cfu/ml of *C. albicans* bound to antibody. The carbon nanotube field-effect transistor (CNTFET) was incubated in antibody solution. After immobilization of antibody, CNTFET was immersed in *C. albicans* solution. SEM images were taken after antibody and *C. albicans* immobilization (**Figure 2.6**)

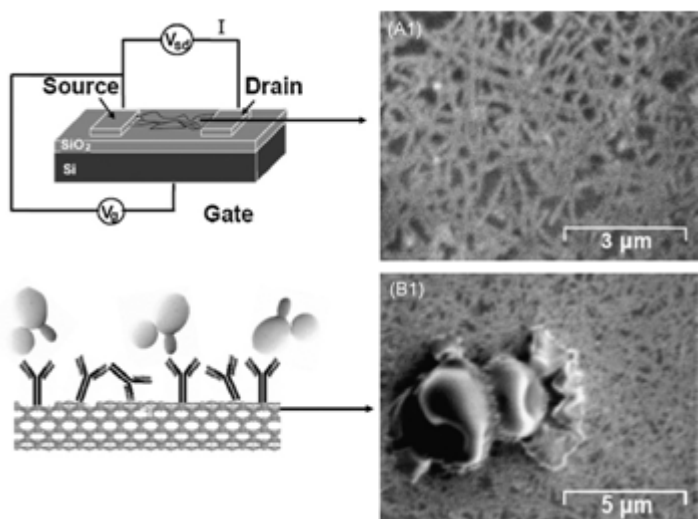


Figure 2.6 SEM images of CNTFET device after immobilization of antibody and *Candida albicans* (Villamizar et al., 2009).

In the study of Takaki et al. (1996), 610 to 15 *C. albicans* cells were detected in 100 ml of whole blood by polymerase chain reaction (PCR) technique (Vandeventer et al., 1995). In addition, Takaki et al. (1996) developed an avidin-biotin-amplified enzyme-linked immunosorbent assay (AB-ELISA) for detection of *Candida* species such as *C. albicans* (serotypes A and B), *C.tropicalis*, *C. parapsilosis*, *C. guilliermondii*, *C. glabrata*, and *C. krusei*. The detection limits of *Candida* species are listed in **Table 2.4** (Takaki et al., 1996).

Table 2.4 Detection limit of *Candida* species using by AB-ELISA (Takaki et al., 1996).

Species	Detection Limit (ng/ml)
<i>C. albicans</i> (serotypes A)	1
<i>C. albicans</i> (serotypes B)	2
<i>C.tropicalis</i>	1.4
<i>C. parapsilosis</i>	2.8
<i>C. guilliermondii</i>	6.7
<i>C. glabrata</i>	20
<i>C. krusei</i> .	>50

2.1.2.2 Detection of Pathogens

The conventional methods for the detection of pathogens (bacteria, their toxins and fungi) are time consuming techniques and they generally require expensive equipments and excess amount of blood from patients. In recent years, immunoassays are used for the detection of pathogens using biosensors which are robust and fast due to their accuracy, sensitivity, specificity. In the next section, antibody, which is used in the immunoassays, is introduced and immobilization techniques for antibodies will be given.

2.1.2.2.1 Antibody

Antibody is a protein which is produced by the body to neutralize and to detect foreign objects such as pathogens and their toxins etc. The molecular weight of an antibody is approximately 150 kDa. There are three types of antibodies, as monoclonal, polyclonal and recombinant antibodies (Byrne et al., 2009). In **Figure 2.7** the structure of an antibody is shown. An antibody consists of two light and two heavy chains. Heavy chain has three constant domains (C_{H1-3}) and a variable domain (V_H). Antibodies which have the same isotype have identical constant domains (Nelson et al., 2004). There are two disulfide bonds between heavy chains. Heavy chain is composed of about 220 amino acid residues. In addition, light chain has one constant domain (C_L) and variable domain (V_L). On the other hand, light chain is composed of about 440-550 amino acid residues. There is disulfide bond between the heavy and light chains (Zourob et al., 2008; Zourob, 2010). The dimensions of an antibody are approximately 15 x 7 x 3.5 nm and that of the smallest antibody is approximately 4 x 3.5 x 2.5 nm (Saerens et al., 2008).

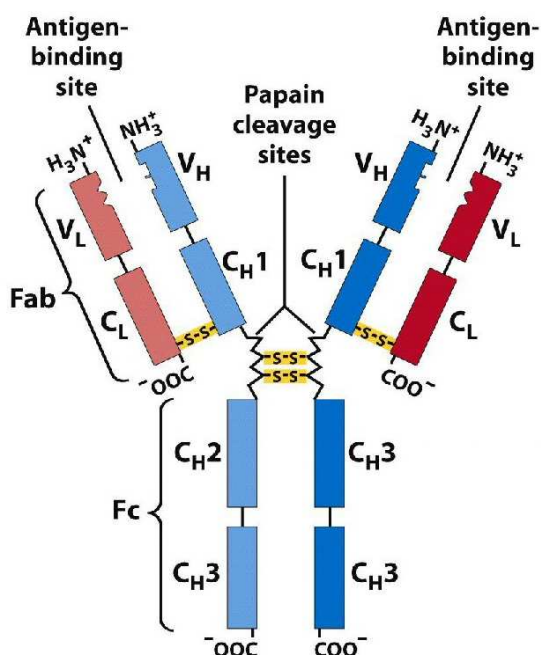


Figure 2.7 Structure of an antibody (Nelson et al., 2004).

Each antibody has two antigen-binding sites as shown in **Figure 2.7** and these sites of a antibody are specific for only one antigen. Thus, antibodies can be used to detect pathogens on biosensor surfaces. In the next section, this phenomenon will be explained considering biosensors.

2.1.2.2 Physical Adsorption of Antibody on Biosensor Surface

Antibody-antigen interaction is generally used to detect pathogens with the help of biosensors. Antibodies can be adsorbed physically or chemically on a biosensor surface. Proteins, molecules or cross-linkers are not required in physical adsorption which is the simplest technique. Antibodies bind onto surface randomly as a result of hydrophobic interaction between the antibody and the sensor surface.

Physical adsorption is affected by Vroman Effect. According to Vroman Effect, the proteins that have highest mobility or low molecular weight (LMW) in the blood move and adsorb on the surface earlier (Choi et al., 2010). However, less mobile proteins or high molecular weight (HMW) proteins displace the highest mobility proteins or LMW proteins. **Figure 2.8** shows the Vroman Effect on protein adsorption.

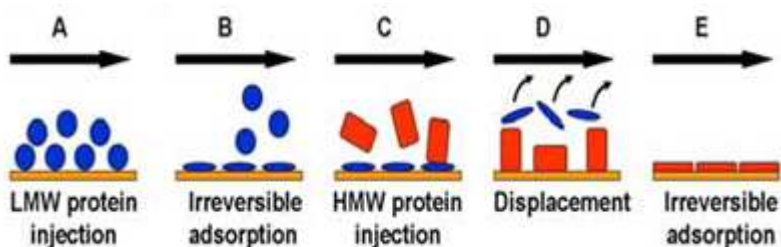


Figure 2.8 Vroman effect (Choi et al., 2010).

Seokheun Choi et al. (2010) investigated physical adsorption and Vroman Effect on three different proteins which are albumin (Alb, 67 kDa), immunoglobulin (IgG, 150 kDa) and fibrinogen (Fib, 340 kDa) (Choi et al., 2010). Displacement was detected

by resonant frequency changes as illustrated in **Figure 2.9** (Choi et al., 2010). Fib with HMW replaced others (Alb, IgG) with LMW in 340 seconds.

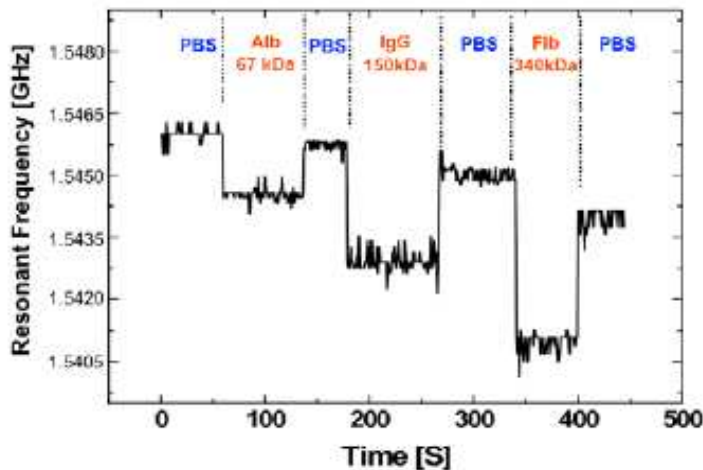


Figure 2.9 Displacement of LMW to HMW protein (Choi et al., 2010).

Seokheun Choi et al. (2010) used the principle of Vroman Effect for detection of thyroglobulin (Tg) which is a biomarker for thyroid. Tg (660 kDa) having HMW was detected by surface plasmon resonance (SPR) angle in a mixture of three different proteins which are albumin (Alb, 66 kDa), haptoglobin (Hp, 86 kDa) and immunoglobulin G (IgG, 150 kDa) all of which can be considered as LMW as shown in **Figure 2.10**.

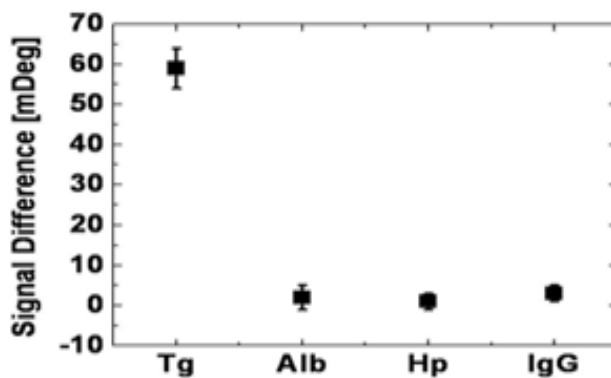


Figure 2.10 Detection of thyroglobulin (Tg) by using the principal of Vroman Effect (Choi et al., 2010).

2.1.2.2.3 Chemical Adsorption of Antibody on Biosensor Surface

Biosensor designs are majorly based on interaction between antibody and antigen. Antigens in the sample bind to antibody after immobilization of antibody chemically on the surface. Then, antigen which binds to the antibody on the surface can be detected. K. Nakanishi et al. (2008) summarized different immobilization methods for antibodies as shown in **Figure 2.11** and given in **Table 2.4**. Immobilization of antibodies was achieved after the formation of self-assembled monolayer (SAM) by streptavidin-biotin interaction or by binding proteins such as Protein A, Protein G or by carboxymethyl dextran (CM5) crosslinking (Subramanian et al., 2006).

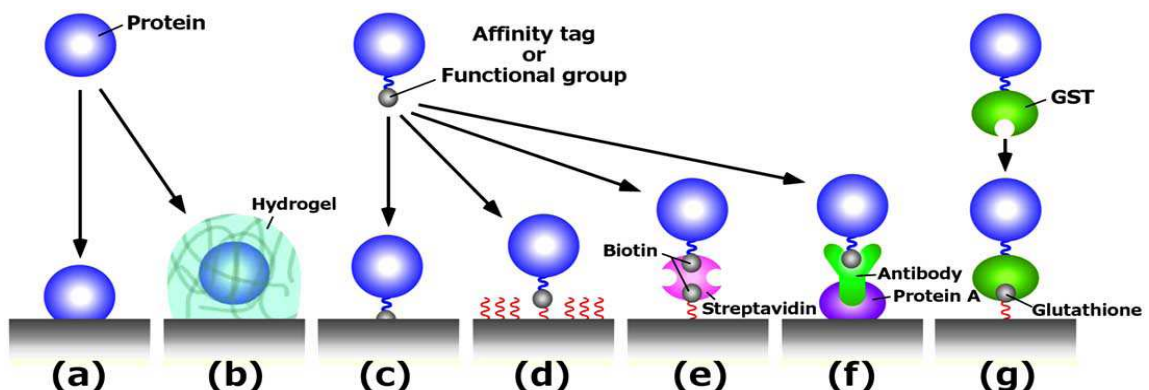


Figure 2.11 Schemes of different immobilization methods (Nakanishi et al., 2008).

Table 2.5 Immobilization Methods for Antibodies (Nakanishi et al., 2008).

Immobilization method	Surface for immobilization	Protein modification	Capturing mechanism	Figure
Physical adsorption	Polystyrene, Nitrocellulose, Glass coated with poly-Lys	Wild proteins	Physical adsorption	2.11 a
Immobilization using hydrogel	Glass plate	Wild proteins	Entrapment in gels	2.11 b
Hisx6-tag-mediated immobilization	Nickel-coated glass, Ni-NTA functionalized surface	Proteins fused with Hisx6	Affinity between Hisx6 and Ni ²⁺	2.11 c
Immobilization using coiled coil interaction	OTS coated surface covalently bound with Artificial polypeptide containing Leu zipper	Proteins fused with Leu zipper	Coiled coil association of a Heterodimeric Leu zipper pair	2.11 d
Immobilization on Au surface	Au surface	Wild proteins containing Cys residues or recombinant ones with Cys introduced	Chemisorption of SH-groups on Au	2.11 c
Silane coupling method	Glass modified with bifunctional silane coupling reagents containing aldehyde	Wild proteins	Schiff's base linkage between aldehyde and amino groups	2.11 d
Transglutaminase-mediated immobilization	Casein-grafted polyacrylic surface	Proteins fused with TGase specific peptide substrate	Acyl transfer reaction of TGase	2.11 d
Streptavidin-mediated immobilization	Polystyrene or glass coated with streptavidin, or biotynylated BSA	Biotinylated protein	Affinity between Streptavidin- biotin	2.11 e
FLAG-tag-mediated immobilization	Polystyrene coated with protein A and conjugated with anti-FLAG monoclonal antibody	Proteins fused with FLAG	Affinity between FLAG and anti-FLAG antibody	2.11 f
Glutathione /GSTmediated immobilization	Polystyrene coated with protein followed by covalently coupling with glutathione	Protein fused with GST	Affinity between glutathione and GST	2.11 g

SAM can be obtained on different surfaces such as silicon, polystyrene and gold. F. Darain et al. (2009) developed the protocol for SAM structure formation on polystyrene surface. As shown in **Figure 2.12**, first gold was sputtered on a polystyrene surface (**Figure 2.12 a and b**) and SAM was then obtained by 16-mercapto-hexadeconic acid (16-MHA) (**Figure 2.12c**). In order to change the terminal carboxylic group of 16-MHA to N-Hydroxysuccinimide (NHS) ester, the mixture of 1-Ethyl-3-(3-dimethylaminopropyl)carbodiimide (EDC) was used (**Figure 2.12d**). Finally, antibody was bound to the SAM structure due to NHS ester (**Figure 2.12e**) (Darain et al., 2009).

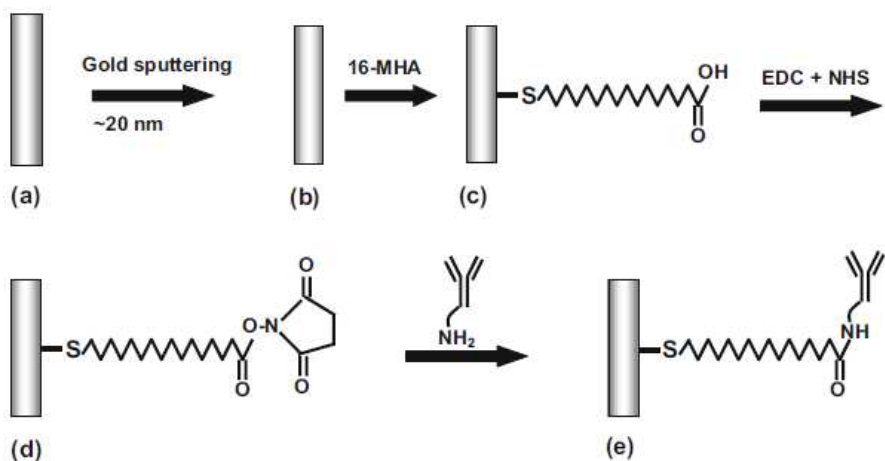


Figure 2.12 Immobilization of antibody on polystyrene surface (Darain et al., 2009).

2.1.2.2.4 Microelectromechanical Systems (MEMS) Based Biosensors

The detection of pathogens can be done by different conventional methods such as conventional culture method, polymerase chain reaction (PCR) method and immunology-based method (Bhattacharya et al., 2007). The culture method is the most reliable method. However, it is a time consuming method due to the fact that it takes 7–10 days for the detection of pathogens (Banada et al., 2008). PCR is the most commonly used method due to its sensitivity. However, this method requires expensive devices. Immunology-based methods are enzyme immunoassay (EIA)

(Borck et al., 2002), enzyme linked immunosorbent assay (ELISA) (Mattingly et al., 1988), enzyme-linked fluorescent assay (ELFA), bioluminescent enzyme immunoassay (BEIA) and western blot test. All are based on antibody-antigen interaction. These techniques take long time and require medical devices (Subramanian et al., 2006; Baldrich et al., 2008).

In recent years, the use of micro-electromechanical systems (MEMS) based biosensors is increased. These are the analytical devices which are used for detection of the biological agents. They are miniature in size, sensitive, robust and biocompatible. Moreover, they require low power and small amount of blood from the patients. They are cheap and have short time of operation with high performance (Carrascosa et al., 2006; Subramanian et al., 2006). As seen in the **Figure 2.13**, biosensors are combination of bioreceptors and transducers (Byrne et al., 2009; Velusamy et al., 2010). In biosensors, different detection methods are used to detect biological molecules (Carrascosa et al., 2006; Velusamy et al., 2010). In the following section, these methods will be explained.

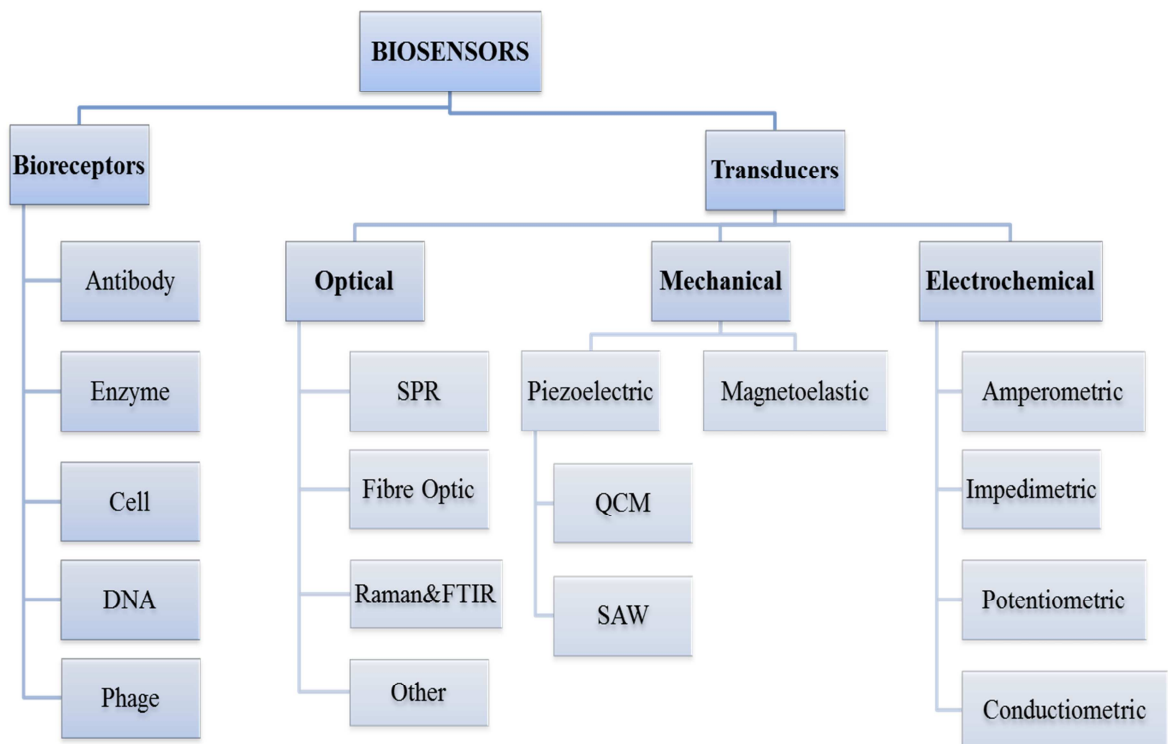


Figure 2.13 Biosensors (Velusamy et al., 2010).

2.1.2.2.5 Detection Methods for Pathogens

There are mainly four different methods for MEMS for the detection of pathogens which are mechanical, optical, magnetoresistive and electrochemical methods.

2.1.2.2.5.1 Mechanical Detection Method

Microfabricated cantilevers are mechanical devices that are used most widely in mechanical detection. Mechanical label-free detection is a sensitive method using cantilever which is a clamped, suspended beam shown in **Figure 2.14**. Sensors with the working principle of mechanical detection have two different sensing modes which are based on the determination of surface stress changes and mass changes. In the stress detection mode, the stress difference is determined related to biomolecule binding before and after the immobilization of biomolecules on the cantilever surface. In the mass detection mode, the frequency of cantilever is obtained which varies as a function of molecular adsorption due to mass difference (Carrascosa et al., 2006; Liu et al., 2011). The frequency change of cantilever can be determined by different techniques such as optical, piezo-resistive and piezo-electric methods. In order to detect bending of cantilever, external devices are required in optical methods. However, piezo-resistive cantilevers do not require any external devices (Bhattacharya et al., 2007). Cantilevers can be fabricated in arrays consisting of one to thousands of cantilevers. Thus, thousands of biomolecules can be detected at the same time without any labeling. When pathogen is detected in liquid by cantilever, the frequency of cantilever is affected by liquid media (Fritz et al., 2000). Thus, obtaining accurate results in liquid media is problematic in case of mechanical detection.

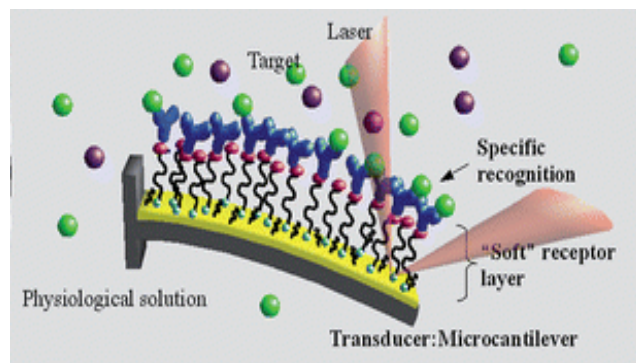


Figure 2.14 Principal working of cantilever (Alvarez et al., 2010).

Different biomolecules can be detected by mechanical detection. N. S. Kale and V. R. Rao (2006) developed a polymeric microcantilever with embedded piezoresistors. In another study, biomolecules such as DNA, protein and polymers were detected by cantilever as a label-free detection (Liu et al., 2011). On the other hand, G. Wu et al. (2001) developed a microcantilever for the detection of prostate specific antigen (PSA) which is a marker of prostate cancer (Wu et al., 2001; Wee et al., 2005) reported a piezo-resistive microcantilever for the detection of PSA and C-reactive proteins (CRP) (Wee et al., 2005).

The bending change of the cantilever was measured due to the reaction of glucose oxidase (GO_x) which is an enzyme and reacts with glucose. During reaction, hydrogen peroxide (H_2O_2) was produced and the bending of cantilever was proportional to the concentration of glucose (**Figure 2.15**) (Pei et al., 2004).

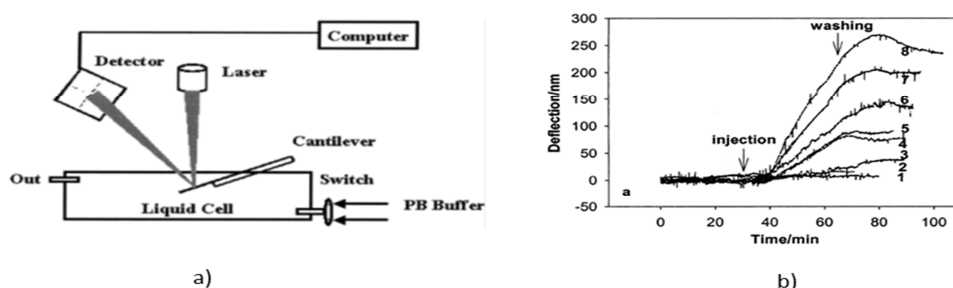


Figure 2.15 a) Sketch of the experimental set up of cantilever b) Cantilever deflection versus time (Glucose concentrations: (1) 0, (2) 0.2, (3) 0.5, (4) 1, (5) 2, (6) 5, (7) 10, and (8) 20 mM) (Pei et al., 2004).

2.1.2.2.5.2 Optical Detection Method

Optical detection method can be done by labeling or label free. Fluorescent dye, quantum-dot labels, metal colloid labels can be used as label molecules. The principle of label detection is monitoring the excitation of label molecules by optic devices such as microscope, fiber optic sensors etc. In DNA detection process, dsDNA is dyed with fluorescence dye. On the other hand, in the bacteria detection the nucleus of bacteria is dyed. Imaging surface plasmon resonance (SPR) and imaging ellipsometry are commonly used in label free optical detection. However, fluorescence detection has not been widely used because it is expensive and time consuming and requires sophisticated instruments for scanning. C. A. Rowe et al. (2003) developed a fluorescence-based immunosensor for detection of multiple samples. Biotin conjugated antibody was immobilized on the biosensor surface and captured antigen. In the study of El-Boubou et al. (2005) cancer cells were detected by secondary antibody conjugated with Rhodamine RedTM flow rate of which was 15 $\mu\text{L}/\text{min}$. The capturing efficiency of tumor cells was greater than 30%.

In label free optical detection, atomic force microscopy (AFM) is widely used to detect single biomolecule such as protein, nucleic acid, antibody or antigen. AFM has a nanometer-scale tip which is attached to a flexible cantilever. As can be seen in **Figure 2.16**, the working principal of AFM is monitoring of the interaction forces between a microscope probe and molecules immobilized a surface using a laser (Braga and Ricci, 1998). There are two types of AFM as contact and tapping mode AFM. Contact mode AFM can deform biomolecules immobilized on a surface. However, tapping mode AFM does not distort the molecules because it does not contact the molecules. The lateral and vertical resolutions of AFM are 2 nm and 1 nm, respectively (Huff et al., 2004).

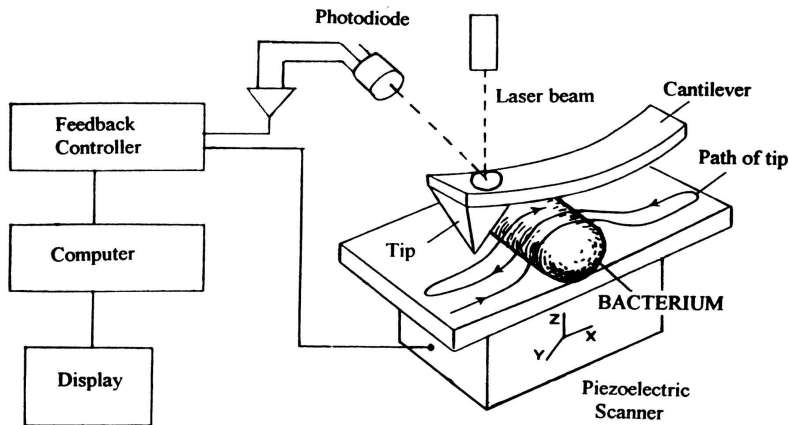


Figure 2.16 Working principle of AFM (Braga and Ricci, 1998).

2.1.2.2.5.3 Magnetic Detection Method

The principal of magnetic detection method is based on conjugation of magnetic particles to biological agents. The magnetic particles can be produced easily by different methods. However, the drawback of this method is its low sensitivity and that, its results may not be reproducible (Palecek et al., 2007).

K. El- Boubou et al. (2007) developed magnetic glyco-nanoparticles to detect *Escherichia coli* (*E. coli*). Nanoparticles offered more surface area for capturing the bacteria. *E.coli* was bound to magnetic particles by using concanavalin A (Con A). Then, bacteria modified particles were separated by using a magnet, as shown in **Figure 2.17**.

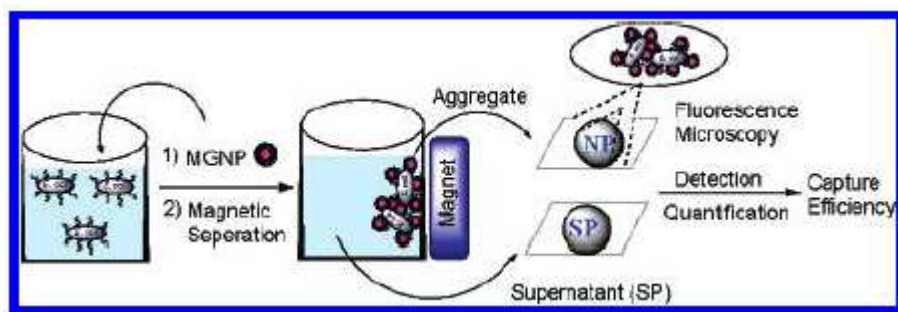


Figure 2.17 Schematic illustration of separation of *E. coli* onto magnetic glyco-nanoparticles (El-Boubou et al., 2007).

S. Y. Yang et al. (2008) presented a bead-based immunoassay for detection of a virus. As seen in **Figure 2.18**, firstly specific antibodies of virus were immobilized onto magnetic beads. Then, viruses bound to their specific antibody. In order to detect immobilized viruses by optical detection, dye labeled antibodies were bound to viruses. Virus conjugated beads were collected by magnet. Optical detection occurred with photo-multiplier tube. Limit of detection (LOD) was 10^3 PFU/ml and detection took 40 minutes.

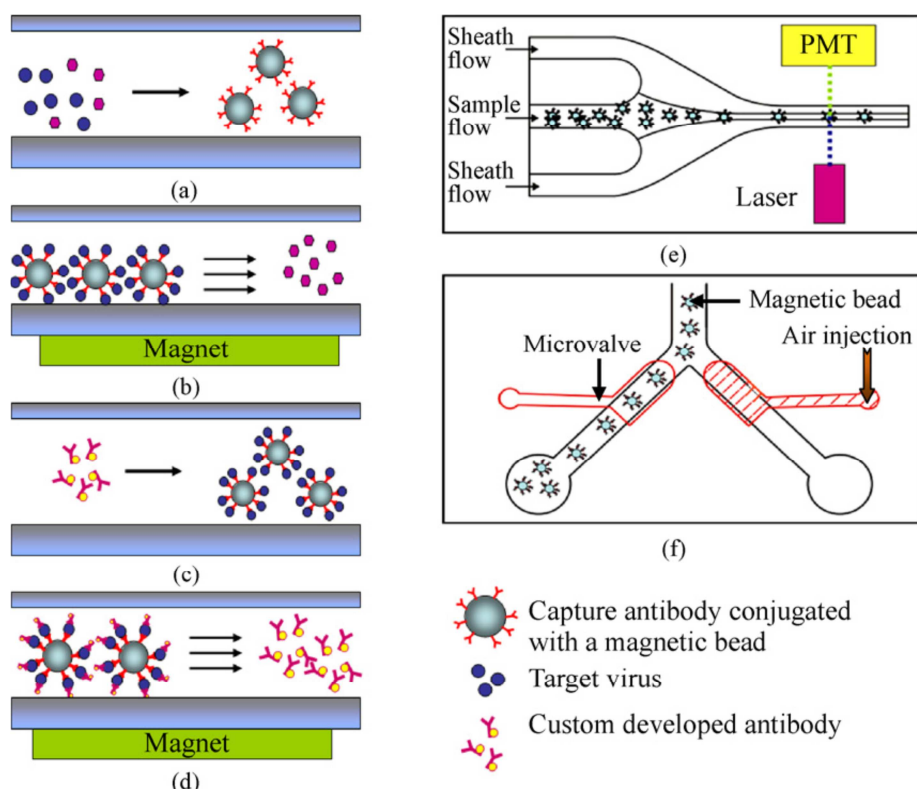


Figure 2.18 Schematic drawing of the microfluidic chip (Yang et al., 2008).

2.1.2.2.5.4 Electrochemical Detection Method

Electrochemical detection can be done by three different methods, named as amperometric, potentiometric and conductometric. In the amperometric detection, a current difference is measured after the redox reaction. Electric potential difference

resulting due to ion difference is measured after redox reaction. In conductometric detection, conductance change is measured by sensors (Bhattacharya et al., 2007).

In the study of K. Riebeseel et al. (2006) Troponin I was detected by biosensor electrochemically by using a marker. Firstly, primary antibody was immobilized on a resist layer. Then, troponin I was bounded to specific antibody. In order to detect antigen, an enzyme was conjugated to antibody. The current difference between the enzyme and its substrate was obtained by the auxiliary, working and reference electrodes made of platinum, gold and silver, respectively.

Popovtzer et al. (2006) investigated measurement of the intrinsic catalase activity of *Escherichia coli* (*E. coli*) for the detection of *E. coli* on a platinum (Pt) wire electrode which was modified with H₂O₂-selective organic/inorganic-hybrid sol-gel film.

In the study of Quiel et al. (2010), SEB was detected with eMicroLISA device of AJ eBiochip GmbH. Firstly, the EZ-Link® Sulfo-NHS-LC Biotinylation Kit was used to get the biotin conjugated primary antibody. Then, antibodies were immobilized on the gold surface after a duration of 2 h. Afterwards, 5% trehalose solution was added on the surface and incubated for 1-2 h in a humidity chamber. By this way, the surface could be stored at room chamber for a few days or at 4 °C for 3 months. After immobilization of primary antibody, SEB and the streptavidin-β-galactosidase conjugated secondary antibody were adsorbed. This took only 23 min. Then, p-aminophenyl-β-D-galactopyranoside was added as substrate and the product of redox reaction, p-aminophenol, was obtained (**Figure 2.19**). The limiting concentration of detection of this study was 1 ng/ml.

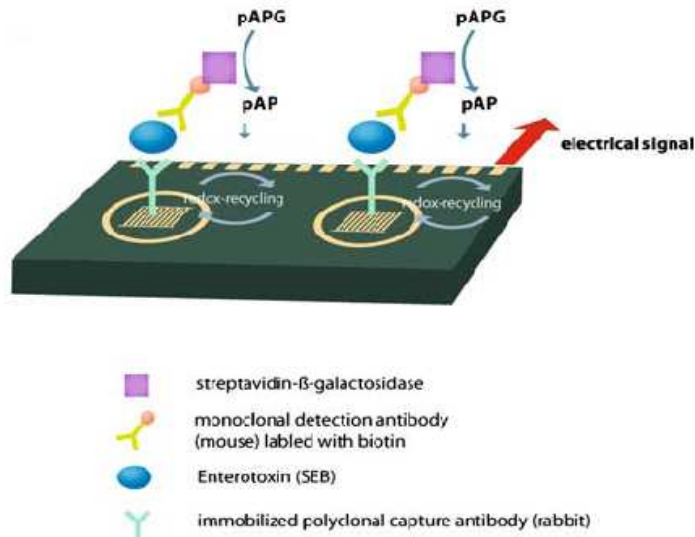


Figure 2.19 Schematic drawing of SEB detection (Quiel et al., 2010).

In the study of M. Odijk (2009), bone mineral density (BMD) testing, optical and electrochemical testing were compared for the detection of osteoporosis. It is found that electrochemical testing has the highest sensitivity in detection methods.

Y. Xu et al. (2006) developed an amperometric immunosensor having three electrodes as working, reference and counter electrodes. Self-assembled monolayer (SAM) was obtained by binding 1,6-hexanedithiol to gold surface. In order to increase the surface area, gold particles were immobilized on SAM. Then, protein A was attached physically to gold particles. Thus, self-assembled multi-monolayer was obtained (**Figure 2.20**). Primary antibodies of human immunoglobulin (H IgG) were immobilized on protein A. Then, H IgG was bound to antibodies specifically. In order to determine antigen binding, horseradish peroxidase (HRP)-conjugated secondary antibodies were immobilized. Current difference due to the redox reaction between enzyme and substrate was determined by using cyclic voltammetry which is a function of working electrode potential ramped linearly versus time.

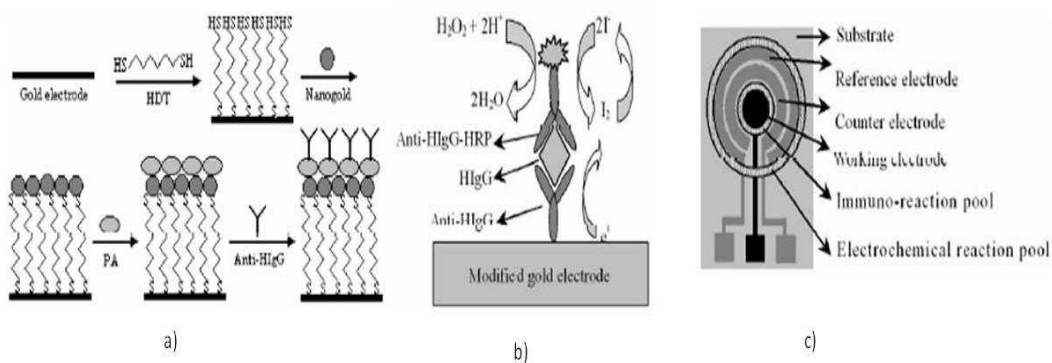


Figure 2.20 a) Schematic illustration of self-assembled monolayer (SAM) b) Redox reaction between enzyme and its substrate c) Drawing of amperometric immunosensor (Xu et al., 2006).

2.1.2.2.5.5 Spectroscopy Techniques for Detecting Pathogens

There are different spectroscopy techniques which can be used to determine structure of the surface and also to determine hybridization of DNA and bacteria. These techniques are subtractively normalized interfacial Fourier-transform infrared spectroscopy (SNIFTIRS), surface-enhanced infrared reflection-absorption spectroscopy with the attenuated total reflection technique (ATR-SEIRAS), surface-enhanced Raman spectroscopy (SERS), surface X-ray scattering (SXS), X-ray photoelectron spectroscopy (XPS) (Darain et al., 2009), scanning tunneling microscopy (STM), surface Plasmon resonance (SPR) (Lin et al., 2007), electrochemical impedance spectrometry (EIS) (Barreiros dos Santos et al., 2009), polarization modulation reflection absorption infrared spectroscopy (PM-RAIRS), Fourier Transform Infrared (FTIR) (Yu et al., 2006), Fourier transform infrared attenuated total reflection (FTIR-ATR) (Liao et al., 2006) quartz crystal microbalance (QCM) (Su et al., 2005) and quartz crystal microbalance with dissipation (QCM-D) (Boujday et al., 2008).

Most of the photons are electrically scattered which is called Rayleigh scattering and they have the same frequency and the wavelength as the incident radiation. This is the common case. However, small amounts of photons are scattered by an excitation

and they have different frequency which is lower than that of the incident photons. This inelastic scattering of light is called Raman scattering (Cochran, 1982).

Raman spectroscopy is a useful method for the identification of biomolecules due to extreme sensitivity. It gives information on rotational and vibrational behavior of molecules with the help of lasers. Surface enhanced Raman spectroscopy (SERS) is 10^{14} fold enhanced form of Raman spectroscopy. Femtomolar amounts of biomolecules (small molecules, nucleic acids, proteins, and cells etc.) can be detected by SERS in dry or wet conditions (Liu et al., 2009; Temur et al., 2010).

W.Tsai and P.Pai (2009) detected SEB with different self-assembled monolayer (SAM) and different antibody fragments. In their study, $F(ab')_2$ fragments of Anti-SEB were obtained using an ImunoPure® $F(ab')_2$ preparation kit. Moreover, $F(ab')_2$ fragments were reduced to $F(ab')$ by using dithiothreitol solution. The study was occurred in a cuvette with gold surface. Firstly, SAM was obtained with different molecules which are 10 Mm 16-MHA/6-MHOH at 1:10. It was waited for one hour to get SAM on the surface. Then, the mixture of 0.4 M EDC and 0.1 M NHS was added to activate carboxylic group. After activation, antibodies which were full in length, $F(ab')$ and $F(ab')_2$ fragments were immobilized on the gold surface for 15 min (**Figure 2.21**). To reduce the blank surface, 0.2 M glycine was placed on the surface for 10 min. Then, SEB was placed on the surface for one hour and at the end, PBS was used to remove unbounded toxin. The immobilization of toxin was detected by SPR. According to the results, the limit of detection was 10 ng/ml toxin and also 50% increase in the antigen binding efficiency was observed in case of the oriented immobilization of $F(ab')$, compared to randomly immobilized covalent $F(ab')$ fragments (Tsai et al., 2009).

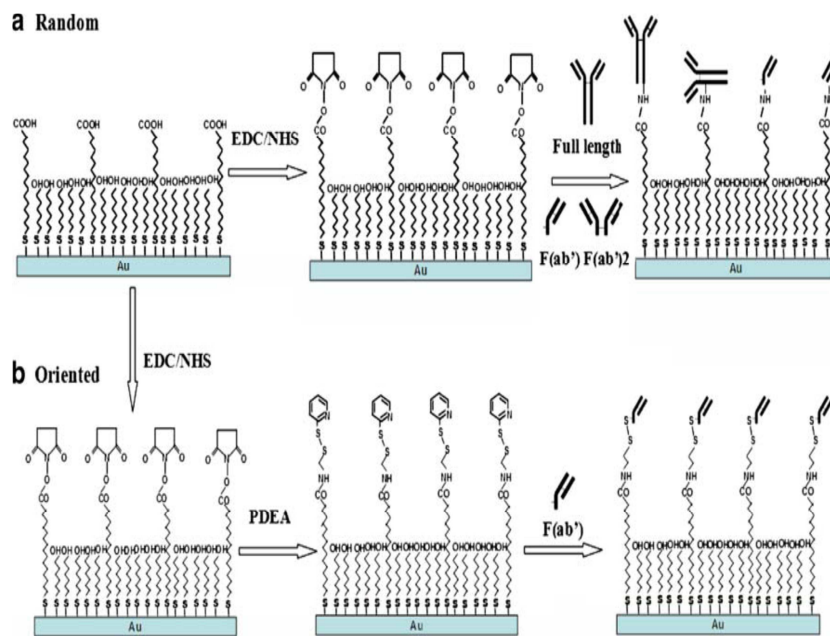


Figure 2.21 Detection of SEB with using different SAM structures and different antibody fragments (Tsai et al., 2009).

Tsai and Pai (2009) detected SEB by Resonant Acoustic Profiling (RAP). Biotin conjugated antibodies were immobilized after immobilization of SEB secondary antibody. Then, neutravidin conjugated gold nanoparticles were bound to the biotin conjugated antibodies (**Figure 2.22**). Therefore, the mass was increased. The limiting concentration for detection was 0.5 ng/ml (Tsai et al., 2009).

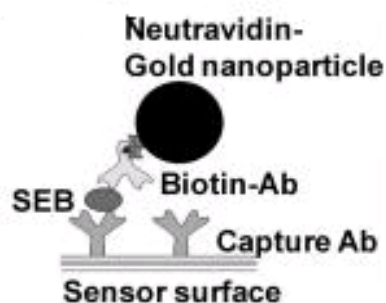


Figure 2.22 Detection of SEB with using neutravidin conjugated gold nanoparticles (Tsai et al., 2009).

CHAPTER 3

THEORETICAL STUDIES

In this chapter, theory related to self-assembled monolayer (SAM) formation, antibody-antigen interaction and adsorption phenomena will be explained.

3.1 Self-Assembled Monolayer (SAM)

Self-assembled monolayer (SAM) is a layer obtained by adsorbing some organic materials on metal surfaces. Generally, three types of organosulfur compounds which are alkanethiols ($\text{HS}(\text{CH}_2)_n\text{X}$), dialkyl disulfides ($\text{X}(\text{CH}_2)_m\text{S-S}(\text{CH}_2)_n\text{X}$) and dialkyl sulfides ($\text{X}(\text{CH}_2)_m\text{S}(\text{CH}_2)_n\text{X}$) (where n and m are the numbers of methylene units and X symbolizes the end group of the alkyl chain (-CH₃, -OH, -COOH)) are used as organic materials for the formation of SAM as shown in **Figure 3.1** (Duong, 1998).

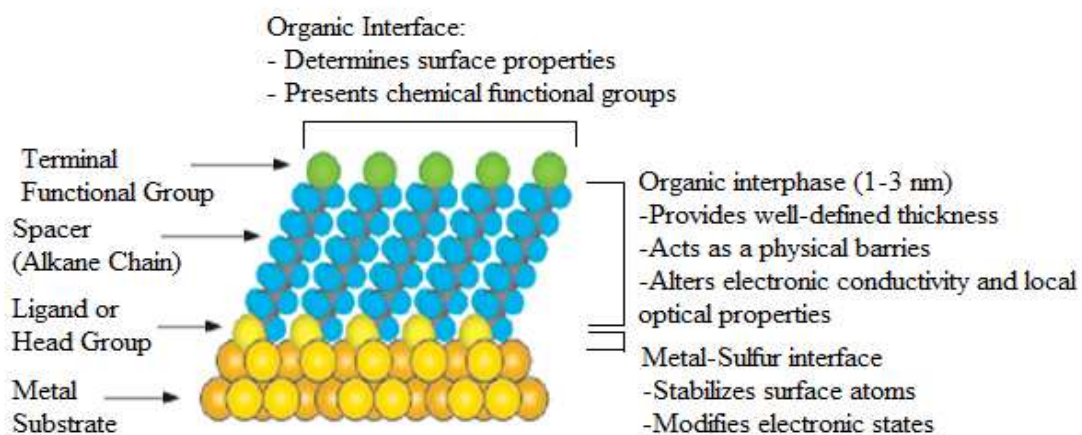


Figure 3.1 Schematic drawing showing layers of SAM (Duong, 1998).

The sulfur atoms of thiol molecules bind to different metals and semiconductor surfaces (Au, Ag, Cu, Pd, Pt, Ni, Si, etc.) as a result of Van der Waals Forces. In general, gold (Au) is used because it's inert, stable and has high electrical conductivity. Also it is not toxic for biological agents and has strong S–Au bonding (Duong, 1998; Vericat et al., 2008). Reaction between the thiol group (-SH) and gold is a reversible reaction as given in Equation 3.1. Besides, Au-S bond is very strong which is approximately 50 kcal/mol (Schreiber, 2000).



C. Vericat et al. (2008) developed thiol molecule orientation on a gold surface (**Figure 3.2**). The angle with respect to the surface normal (α), the hydrocarbon chain twist angle (β) and the precession angle (χ) were determined as 30° , $40-55^\circ$ and 15° , respectively.

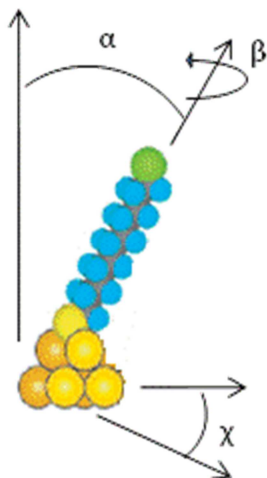


Figure 3.2 Schematic view of thiol molecule orientation (α , β and χ) on a gold surface (Vericat et al., 2008).

3.2 Antibody- Antigen Reaction

Antibody consists of two light and two heavy chains. Heavy chain has three constant domains and a variable domain. There are two disulfide bonds between the heavy chains and there is one disulfide bond between the heavy and light chain (**Figure 3.3**) (Banada et al., 2008; Byrne et al., 2009).

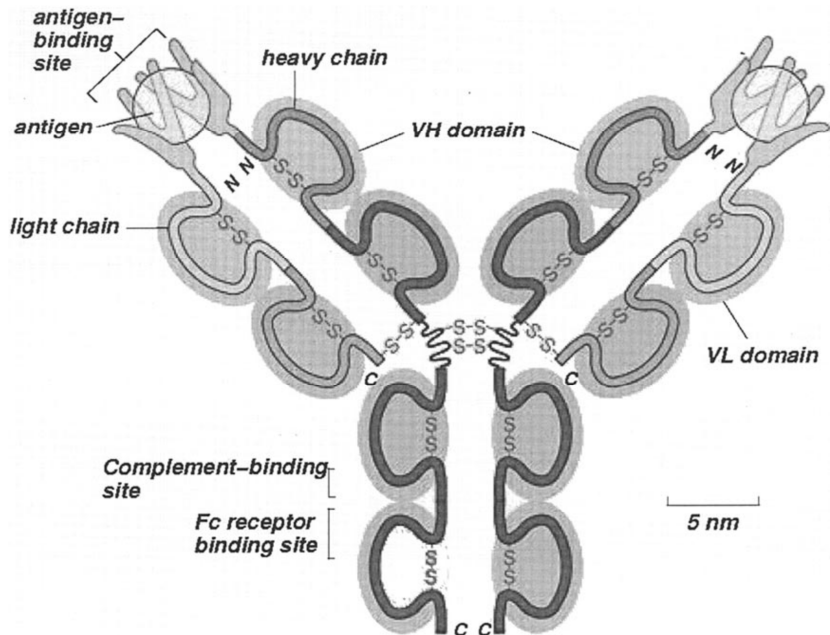


Figure 3.3 Schematic drawing of an antibody (Selvaganapathy et al., 2003).

The light chain of each antibody has unique hypervariable region for a specific antigen. Antibody-antigen interaction is very strong due to electrostatic forces such as ionic bonds, Van der Waals forces, hydrophobic interactions and hydrogen bonds as shown **Figure 3.4** (Duong, 1998; Selvaganapathy et al., 2003).

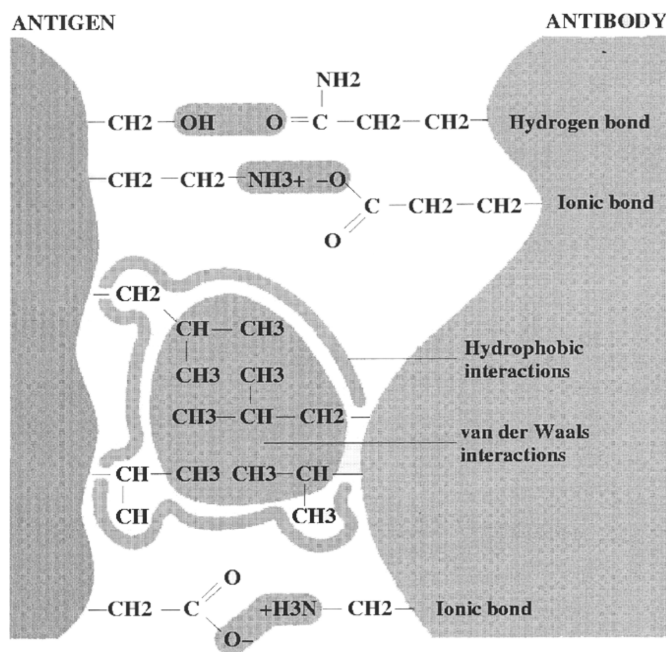


Figure 3.4 Schematic diagram of antibody-antigen interaction (Duong, 1998).

Each antibody binds to a specific antigen and the reaction between an antibody (Ab) and an antigen (Ag) is reversible like an enzymatic reaction as given in Equation 3.2.



where, k_1 =association constant

k_{-1} =disassociation constant

At equilibrium, the rate of adsorption reaction is equal to that of desorption reaction as given in Equation 3.3.

$$k_a[Ag][Ab] = k_d[AgAb] \quad (3.2)$$

The association equilibrium constant (K) is determined as given in Equation 3.4.

$$K = \frac{k_a}{k_d} = \frac{[AgAb]}{[Ag][Ab]} \quad (3.3)$$

Affinity constant (K) for antibody-antigen binding is between 10^6 and 10^9 M^{-1} (Selvaganapathy et al., 2003; Lee et al., 2006).

3.3 Adsorption

The adsorption phenomenon was first studied by Irving Langmuir in 1918. Langmuir theory suggests a monolayer surface adsorption on a flat surface. In Langmuir theory, the major approach is based on the reaction kinetics of molecules. The assumptions for Langmuir theory are:

- All sites of the surface have the same surface energy and are uniform.
- The location of adsorbed particles is definite.
- Each site of adsorption is only for one particle (Duong, 1998; Chevallier et al., 2005).

Langmuir Equation shows a relationship between the number of active sites of the surface undergoing adsorption (i.e. extent of adsorption) and concentration of molecules which are covered. Rate of adsorption and desorption can be written as given in Equations 3.5 and 3.6.

$$\text{Rate of adsorption} = R_a = k_a(1 - \theta)[Ag] \quad (3.4)$$

$$\text{Rate of desorption} = R_d = \theta k_d \quad (3.5)$$

where;

$$\theta = \frac{\text{Number of occupied surface sites}}{\text{Total number of surface sites}}$$

At equilibrium, the rate of adsorption is equal to that of desorption (Equation 3.7). Subtracting Equations 3.5 and 3.6 in 3.7, θ can be obtained as given in Equations 3.9 and 3.10.

$$R_a = R_d \quad (3.6)$$

$$k_a(1 - \theta)[Ag] = k_d\theta \quad (3.8)$$

$$\theta = \frac{k_a[Ag]}{k_d + k_a[Ag]} \quad (3.9)$$

Dividing by k_d , θ can be written as;

$$\theta = \frac{K[Ag]}{1+K[Ag]} \quad (3.7)$$

where K = reaction rate constant= k_a/k_d

Rearranging Equation 3.10;

$$\frac{1}{\theta} = \frac{1}{K} \cdot \frac{1}{[Ag]} + 1 \quad (3.8)$$

Equation 3.8 is the Langmuir Equation and can be used for antigen-antibody reaction. Thus, the reaction rate constant between antigen and antibody is equal to the inverse of the slope of the graph of $1/\theta$ vs. $1/[Ag]$ (Eqn. 3.11).

CHAPTER 4

EXPERIMENTAL STUDIES

The aim of this study is to be able to detect of Staphylococcal enterotoxin B (SEB) in a fast and easy way. In the study two different immobilization methods were utilized. In the first method, thiolated antibody was obtained. In addition, type of adsorption was determined. In the second method, self-assembled monolayer was obtained. Then, toxin was detected by atomic force microscopy (AFM) and surface-enhanced Raman scattering (SERS) using two different procedures.

In this chapter, preparation of gold surface and two different immobilization methods used in this study will be explained. Also, information about the chemicals, the experimental procedures and equipments will be given.

4.1 Method I

The first method (Method I) was used for the detection of pathogens with the help of biosensors. There were five steps followed in Method I as given below:

- a) Formation of thiolated antibody
- b) Immobilization of thiolated antibody on a biosensor surface
- c) Immobilization of toxin SEB
- d) Formation of sandwich structure using antibody conjugated gold particle
- e) Detection of pathogens in sandwich structure by AFM and SERS.

The main difference between this method and other immunoassays found in literature is that there is no SAM formation in this procedure.

4.1.1 Chemicals used in the experiment

In the first method, sulfosuccinimidyl 6-[3'-(2-pyridyldithio)-propionamido] hexanoate (**sulfo-LC-SPDP**) was used as a cross-linker. Sulfo-LC-SPDP is a heterobifunctional cross-linker and its structure is given in **Figure 4.1**. The molecular weight and length of spacer arm of sulfo-LC-SPDP are 527.57 kDa and 1.57 nm, respectively (Carlsson et al., 1978). Sulfo-LC-SPDP was bought from Pierce (Rockford, IL, USA). It was stored at -20 °C. 20 mM sulfo-LC-SPDP in distilled water is used as cross-linker solution.

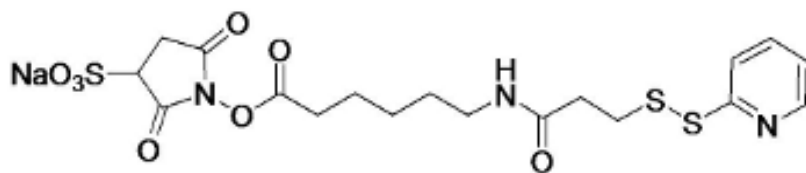


Figure 4.1 Molecular structure of sulfo-LC-SPDP.

As can be seen in Figure 4.1, sulfo-LC-SPDP has a disulfide bond in the spacer arm. Disulfide bond can be reduced by tris(2-Carboxyethyl) phosphine hydrochloride (**TCEP.HCl**), dithiothreitol (DTT) or 2-mercaptoethanol (BME). TCEP.HCl was preferred in this study as a reducing agent due to its advantages of being stable and not containing free thiol groups. Therefore, TCEP.HCl is not needed to be removed from solution after reduction (Dauksaite et al., 2007; Le Brun et al., 2008). TCEP.HCl was purchased from Sigma Aldrich (St. Louis, MO, USA). 150 mM TCEP.HCl solution was prepared in distilled water and stored at room temperature (25 °C).

As stated in Chapter 2, Staphylococcal enterotoxin B (**SEB**) is a toxin of *Staphylococcus aureus*. According to Center for Disease Control and Prevention

(CDC), SEB is a bioterrorism agent. Therefore, after getting permission from the Turkish government, SEB was purchased from Sigma Aldrich (St. Louis, MO, USA). It was stored at -20 °C and SEB solution was obtained with 20 mM PBS (pH 7.4).

Anti-SEB is an antibody of SEB. It was bought from US Biologicals (Massachusetts, USA) and it was stored at -20 °C. The antibody dilution buffer contained 20 mM PBS (pH 7.4) and washing buffer consisted of 100 mM PBS.

Phosphate-buffered saline (**PBS**) was used as washing buffer. It was purchased from Sigma Aldrich (St. Louis, MO, USA) and stored at 25 °C. In addition, the surfaces were cleaned with **piranha solution** (%50 H₂SO₄ + %50 H₂O₂) to remove biological contaminants.

Dithiobis(2-nitrobenzoic acid) (**DTNB**) was bought from Acros (Morris Plains, NJ). 4-(2-hydroxyethyl)-1-piperazineethanesulfonic acid (**HEPES**) was used as a washing buffer. It was purchased from Sigma Aldrich (St. Louis, MO, USA) and it was stored at 25 °C.

4.1.2 Experimental Procedure for Method I

As stated before, the five steps in Method I are formation of thiolated antibody, immobilization of it on a biosensor surface, toxin (SEB) immobilization, formation of sandwich structure using antibody conjugated gold particles and last but not the least detection. The procedures follow in each step will be given below one by one.

- a) For formation of thiolated antibody, 8.4 µl of 0.1 mg/ml anti-SEB and 3 µl of 20 mM sulfo-LC-SPDP were added to 4 µl of 20 mM PBS buffer solution. After one hour for binding the antibody to cross-linker, 7 µl of 150 mM TCEP.HCl solution was added and reduction was done in 30 minutes. Thus, thiolated antibody was obtained and antibody could bind gold surface easily due to thiol group (-SH). During reduction, the gold surface was rinsed with piranha solution (H₂O₂:H₂SO₄ 1:1, v/v).

b and c) The gold surfaces used in the study were fabricated in the METU MEMS Research and Applications Center. After reduction, thiolated antibody solution was incubated on the piranha-cleaned gold surface for about one hour. Then, the gold surface was rinsed with washing buffer three times to remove unbound antibodies.

- d) After cleaning, different concentrations of SEB solution were placed on the antibody immobilized gold surface and it was incubated for one hour. Then, the gold surface was rinsed with washing buffer to remove unbound toxins.
- e) Size of toxin was very small and differences between surface roughness of a sensor surface before and after immobilization of toxin can not be determined by AFM easily. Therefore, a secondary antibody was required to increase the surface roughness. 8.4 μ l of 0.1 mg/ml anti-SEB was placed on the gold surface for one hour. Finally, the surface was washed with washing buffer to remove secondary antibodies. After secondary antibody, the sandwich structure was obtained. **Figure 4.2** shows the schematic procedure for the sandwich immunoassay production using thiolated antibody.

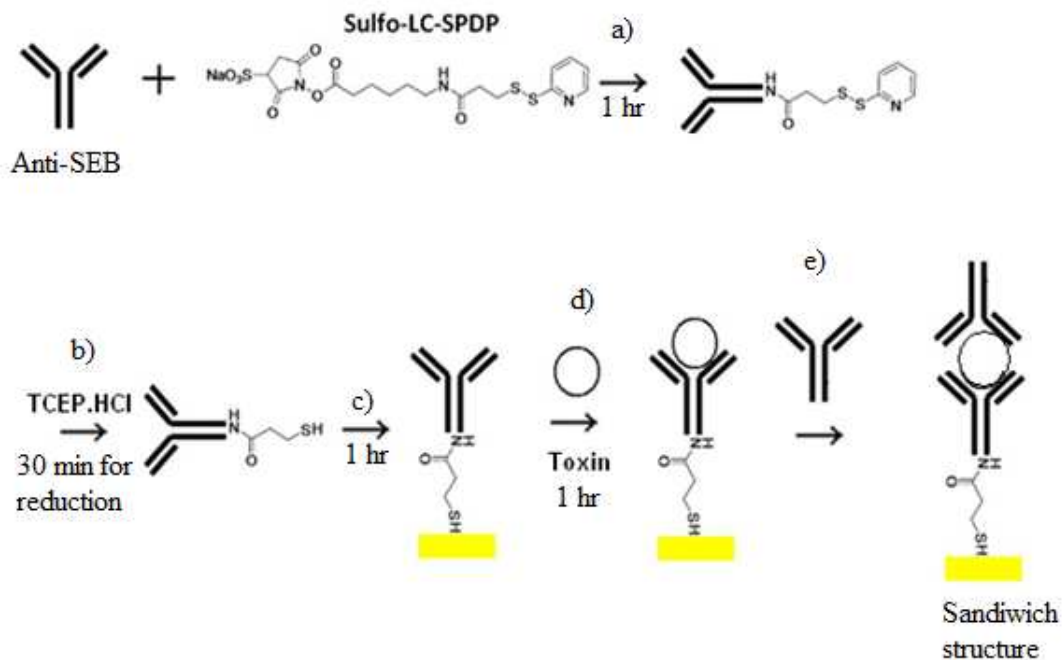


Figure 4.2 Schematic procedure of toxin immobilization using thiolated antibody.

- f) In the detection of toxin using surface-enhanced Raman scattering (SERS), Raman labels were required. Thus, 5,5-dithiobis-(2-nitrobenzoic acid) (DTNB) was used as Raman reporter. The steps for this procedure are shown in **Figure 4.3**. Firstly, 50 mM DTNB solution in ethanol was immersed into gold nanoparticle solution overnight for getting SAM on the gold particles. Then, nanoparticles were rinsed with ethanol and HEPES to remove unbound molecules and collected by centrifugation (1250 rpm, 10 min). After SAM formation on the gold particles, 20 μ l of 0.1 mg/ml anti-SEB was added for one hour.

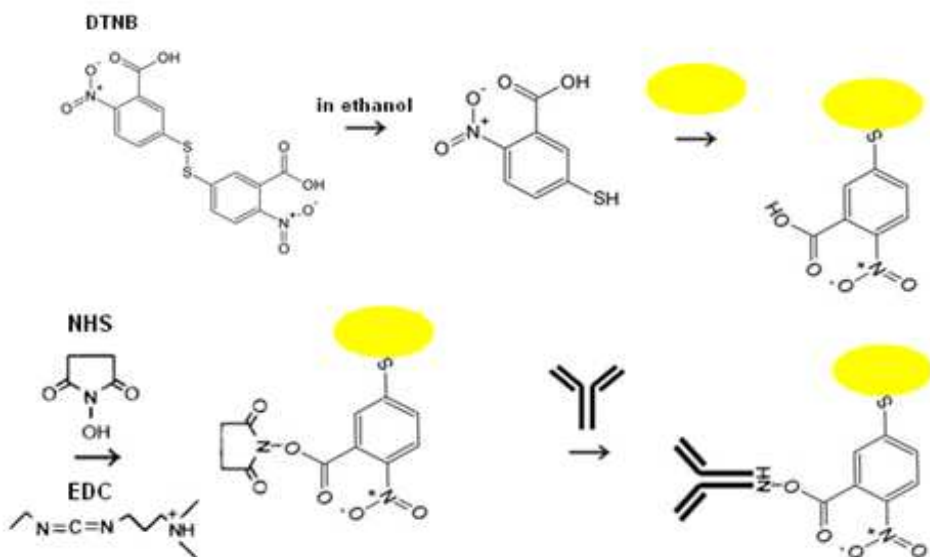


Figure 4.3 Schematic procedure of antibody conjugated gold particle.

To obtain sandwich structure, antibody conjugated gold nanoparticle solution was placed on the toxin conjugated gold surface and incubated for one hour. To remove unbound secondary antibodies, the surface was rinsed with HEPES solution ($\text{pH}=7$). SERS-based sandwich structure obtained can be seen in **Figure 4.4**.

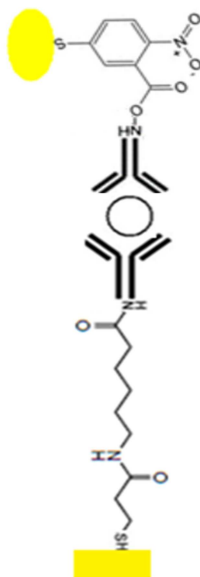


Figure 4.4 SERS-based sandwich immunoassay for SEB using thiolated antibody.

4.2 Method II

In this section Method II results will be compared with the results obtained with the procedure used in the study of F. Darain et al. (2009). Also, the selectivity and limit of detection of Method I and II will be also compared.

Method II like Method I had five steps as:

- Formation of thiolated antibody
- Immobilization of thiolated antibody on a biosensor surface
- Immobilization of toxin (SEB)
- Formation of sandwich structure using antibody conjugated gold particle
- Detection of sandwich structure by AFM and SERS.

Method II differentiates from Method I by the chemicals used and by self-assembled monolayer (SAM) utilization.

4.2.1 Chemicals used in the experiments

In Method II, two different cross-linkers, 3-mercaptopropanoic acid (**3-MPA**) and 11-mercaptoundecanoic acid (**11-MUA**), were used for the formation of self-

assembled monolayer (SAM). As can be seen from **Figure 4.5**, 3-MPA and 11-MUA both have thiol (-SH) and carboxyl (-COOH) groups. Thus, these molecules bind gold surface easily due to thiol group (-SH). 3-MPA and 11-MUA were purchased from Sigma Aldrich (St. Louis, MO, USA). 20 mM 3-MPA and 20 mM 11-MUA solution were prepared using HEPES solution.

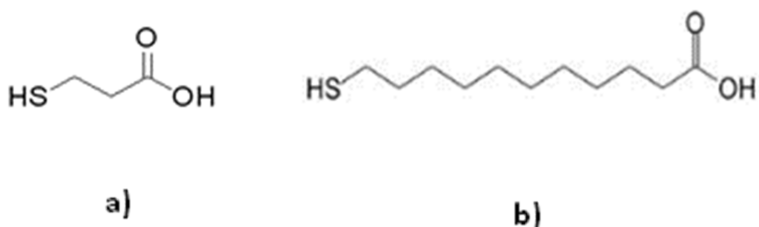


Figure 4.5 Molecular structure of a) 3-MPA and b) 11-MUA.

1-Ethyl-3-(3-dimethylaminopropyl)carbodiimide (**EDC**) and N-Hydroxysuccinimide (**NHS**) were used for activating carboxylate groups of 3-MPA and 11-MUA. They were bought from Pierce (Rockford, IL, USA). EDC was stored at -20 °C and NHS was stored at room temperature (25 °C). Moreover, SEB, anti-SEB, DTNB and HEPES were the used chemicals for Method II similar to the Method I.

4.2.2 Formation of Sandwich Structure using SAM

In the Method II, SAM formation was achieved using by 3-MPAand 11-MUA solutions (**Figure 4.6**).

- a) Firstly, the gold surface was immersed in 20 mM 11-MUA with ethanol incubated overnight.
- b) To block the free regions on the surface, the surface was immersed in 20 mM 3-MPA with ethanol overnight.

- c) Then, to activate carboxylate groups, 0.2 M EDC and 0.05 M NHS solutions were placed on the gold surface for 30 minutes. In order to remove unbound molecules, the surface was rinsed with HEPES buffer three times.
- d) After surface activation, 0.1 mg/ml anti-SEB was added onto the surface and incubated for one hour. Then, the gold surface was washed with HEPES buffer three times. For reducing active groups, 0.5 M ethanolamine was placed onto the surface for 30 minutes.
- e) After removing unbound molecules, different concentrations of SEB solution were added on different antibody conjugated gold surfaces for one hour and the surface was rinsed with HEPES buffer to remove unbound toxins.

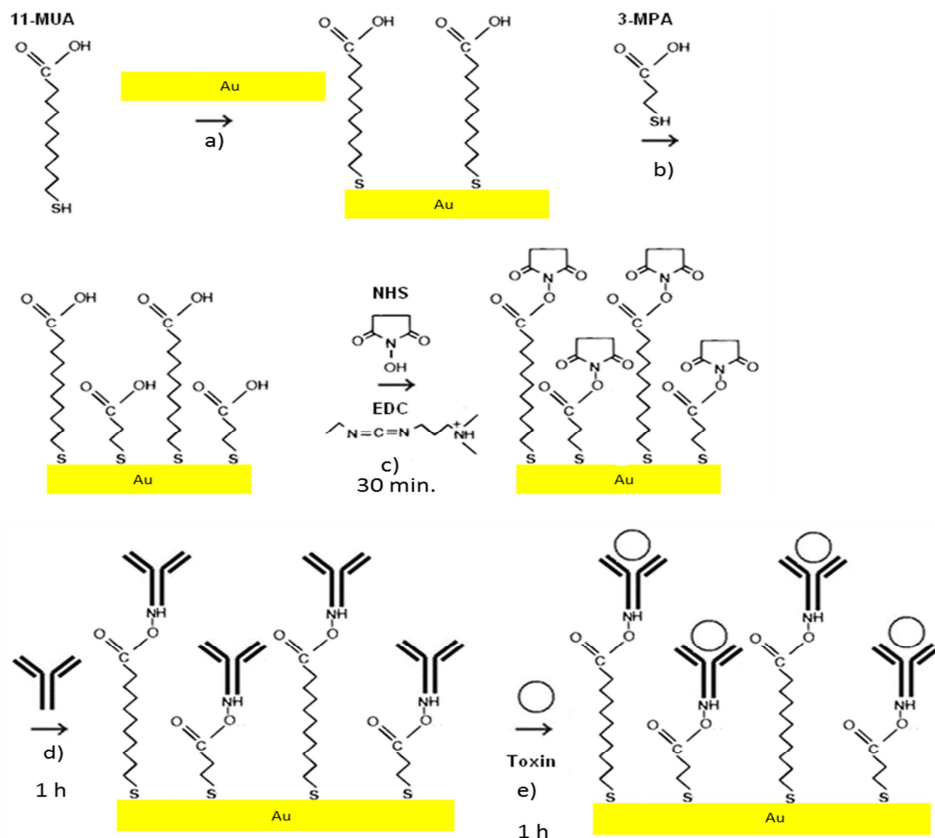


Figure 4.6 Schematic drawing of toxin immobilization using 11-MUA and 3-MPA for SAM.

The detection of toxin using surface-enhanced Raman scattering (SERS) was done by obtaining antibody conjugated gold particles similar to Method I (**Figure 4.3**). Then, antibody conjugated gold particle solution was placed on the gold surface for one hour and sandwich structure was obtained. The SERS- based sandwich immunoassay using SAM is shown in **Figure 4.7**.

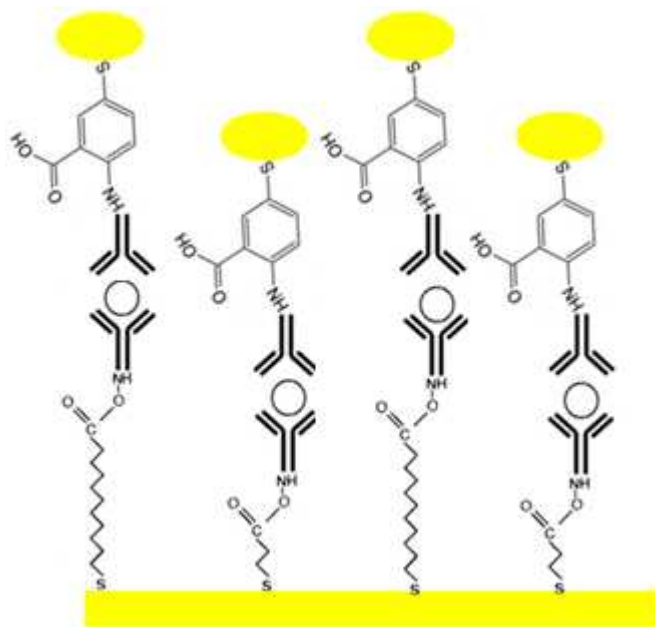


Figure 4.7 SERS-based sandwich immunoassay using 11-MUA and 3-MPA for SAM.

4.3 Equipments used during experiment

In this study, AFM and surface-enhanced Raman scattering (SERS) were used for detection of SEB and *C. albicans*.

AFM was used in the central laboratory in METU. The model of AFM is Vecoo MultiMode V, AS-12 ("E") in PSI mode. The instrument was operated in tapping mode and all measurements were obtained in stable and dry condition. The scan size and vertical range of AFM are 10µm x 10µm and 2.5µm, respectively (**Figure 4.8**).



Figure 4.8 AFM, Vecoo MultiMode V

DeltaNu Examiner Raman microscope (Deltanu Inc., Laramie, WY) which was located at the laboratory in Faculty of Pharmacy Gazi University with a 785-nm laser source, a motorized microscope stage sample holder, and a CCD detector was used for detection of SEB (**Figure 4.9**). The parameters for Raman were 20X objective, 30- μm laser spot size, 100-mW laser power, and 30s acquisition time and baseline correction was performed for all of the measurements. $125 \times 125 \mu\text{m}^2$ and 5 μm are scan size and vertical range, respectively.



Figure 4.9 Delta Nu Raman Microscope.

C. albicans was detected by a microscope of a probe station. The mark of probe station is Karl Suss PM5 Analytical Wafer Prober (**Figure 4.10**). It has four objectives which are Mutitoyo M Plan Apo 5X, 20X, SL50X and SL100X. The depths of focus of these objectives are 14 microns, 3.5 mm, 1.6 mm and 0.9 mm, respectively. During experiment, each objective was used.



Figure 4.10 Karl Suss PM5 Analytical Wafer Prober.

4.3 Fabrication of Biosensor Surface

In this study, it was aimed to detect SEB by two different immobilization procedures on biosensor surfaces. However, biosensors can not be used for the detection using AFM and SERS because SEB were immobilized on the sensor surface inside the channel and could not be detected by AFM and SERS. On the other hand, *C. albicans* was immobilized on the biosensor surface and it was able to detect it by a microscope due to its bigger size unlike SEB.

The biosensor surfaces used in the experiments for, *C. albicans* were produced in METU-MEMS Center. Firstly, ~200 nm Ti/Au layer was sputtered on a silicon wafer. The shape of gold surfaces was shaped by masks (Koydemir et al., 2012). The surfaces have different size of gold and silicon areas. Availability of both gold and the silicon regions on the same surface provided the possibility of the comparison of binding pathogen on the same surfaces under exactly the same experimental conditions.

4.4 Fabrication of Biosensor with Channel

C. albicans has bigger size than SEB. Thus, it can be easily detected by microscope. Also, *C. albicans* which is immobilized inside the channel of biosensor can be detected by a microscope. Thus, a biosensor was fabricated for the detection of *C. albicans* (Yıldırım et al., 2010). **Figure 4.11** shows the process steps of the fabrication of biosensors. Glass wafer was used as base for easy inspection under light microscope (**Figure 4.11a**).

- Firstly, parylene-C was coated on the glass wafer by using PDS 2010 Lab with 10 g dimer to get 5 μ m thickness (**Figure 4.11b**).
- Then, titanium (~25nm) and gold (~200nm) were sputtered, patterned by using positive photoresist, and the photoresist was stripped by using acetone (**Figure 4.11c**). Ti is used to enhance adhesion between parylene and Au layer.
- The diameter of gold surface approximately is 600 μ m. Then, another lithography step was performed to form channels. The height of resist which was 25 μ m was equal to the height of channel (**Figure 4.11d**).
- Then, parylene was coated on the resist (**Figure 4.11e**). Then, another lithography step was performed to form opening on parylene layer for parylene etch. Parylene etch was done by using RIE.
- Lastly, wafers were diced and the devices were immersed into acetone for the removal of photoresist (**Figure 4.11f**). Parylene is a transparent material and the inside of the channel can be easily seen by light microscopy.

biosensors were fabricated only using one wafer. Thus, the price of one biosensor was very low.

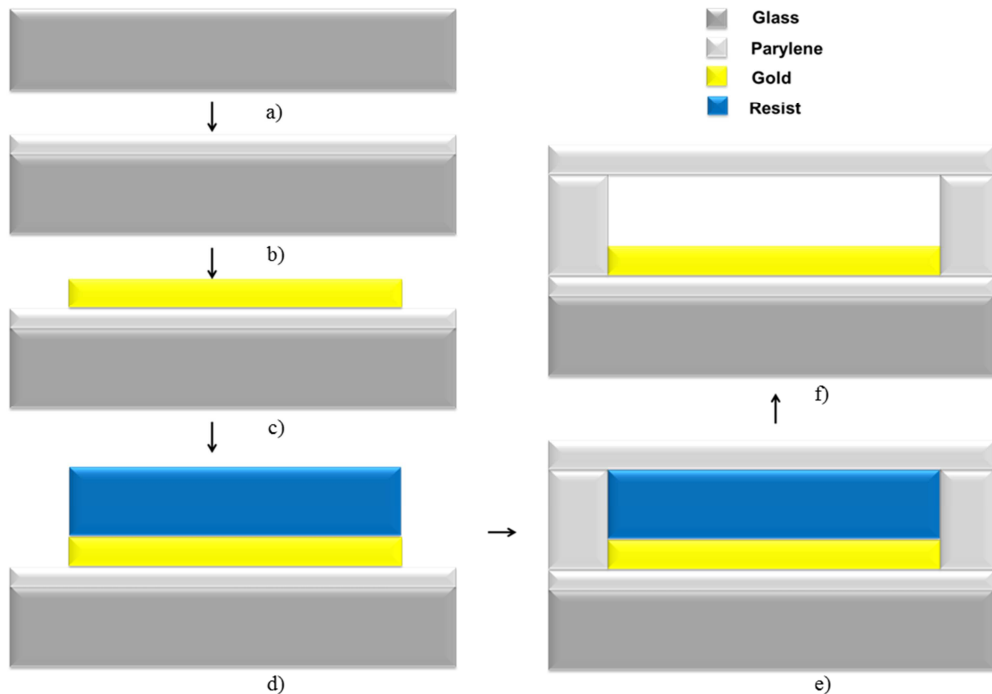


Figure 4.10 Fabrication steps of the biosensor (Yıldırım et al., 2010).

The biosensor had two reservoirs whose diameters were 6 mm. The width, height and length of channel were 100 μm , 25 μm and 1 cm, respectively as shown in **Figure 4.12**.

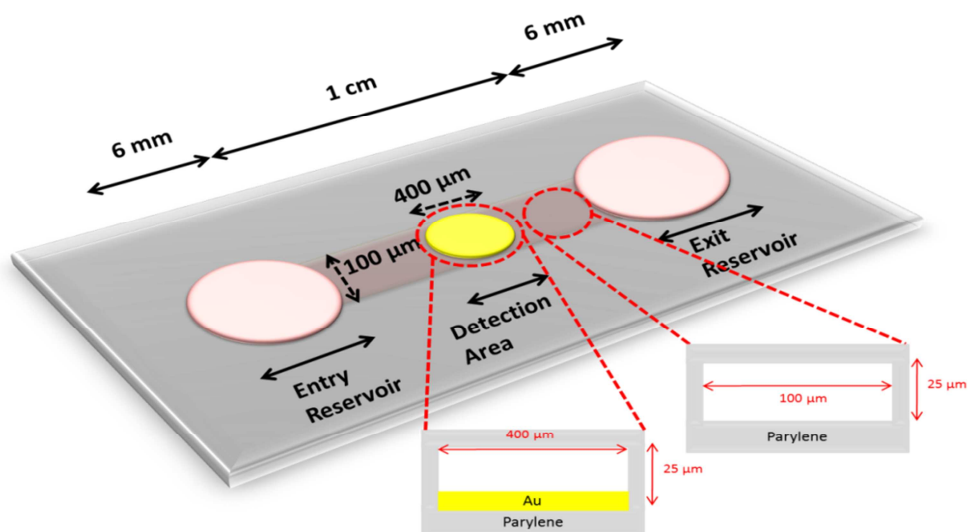


Figure 4.11 Schematic illustration of biosensor (Yıldırım et al., 2010).

CHAPTER 5

RESULT AND DISCUSSION

In this study, two different immunoassays were designed. In the first assay, thiolated antibody was obtained and a new procedure was developed for the detection of pathogens. Finally, SEB was detected by AFM and SERS with the developed procedure. Also, a fungus, *C. albicans*, detection was done using Method I where the last step detection on a biosensor was achieved using a microscope. In Method II, SAM was formed and SEB was detected by AFM and SERS.

5.1 Results with Method I

The experimental steps involved in Method I was given in Chapter 3. Each experiment was repeated at least three times for accurate results. In addition, the conditions (i.e. temperature, pressure) of each experiment were kept constant. The results obtained for the characterization of the toxin modified gold surface will be shown below.

5.1.1 Bare Gold Surface Characterization with AFM

Before the immobilization of toxin on the gold surface, characterization of different analyzed areas on the same gold surface was determined by AFM. The cross sections of three areas that were analyzed on the same gold surface were $1 \times 1 \mu\text{m}^2$. **Figure 5.1a-b** show 2-D and 3-D profiles of first analyzed area on the gold surface, respectively. Average roughness (R_a) and maximum height (R_t) of first analyzed surface were determined as 0.953 nm and 8.92 nm, respectively. In addition, the height of a maximum rise on the surface was obtained as 3.768 nm (**Figure 5.1c**).

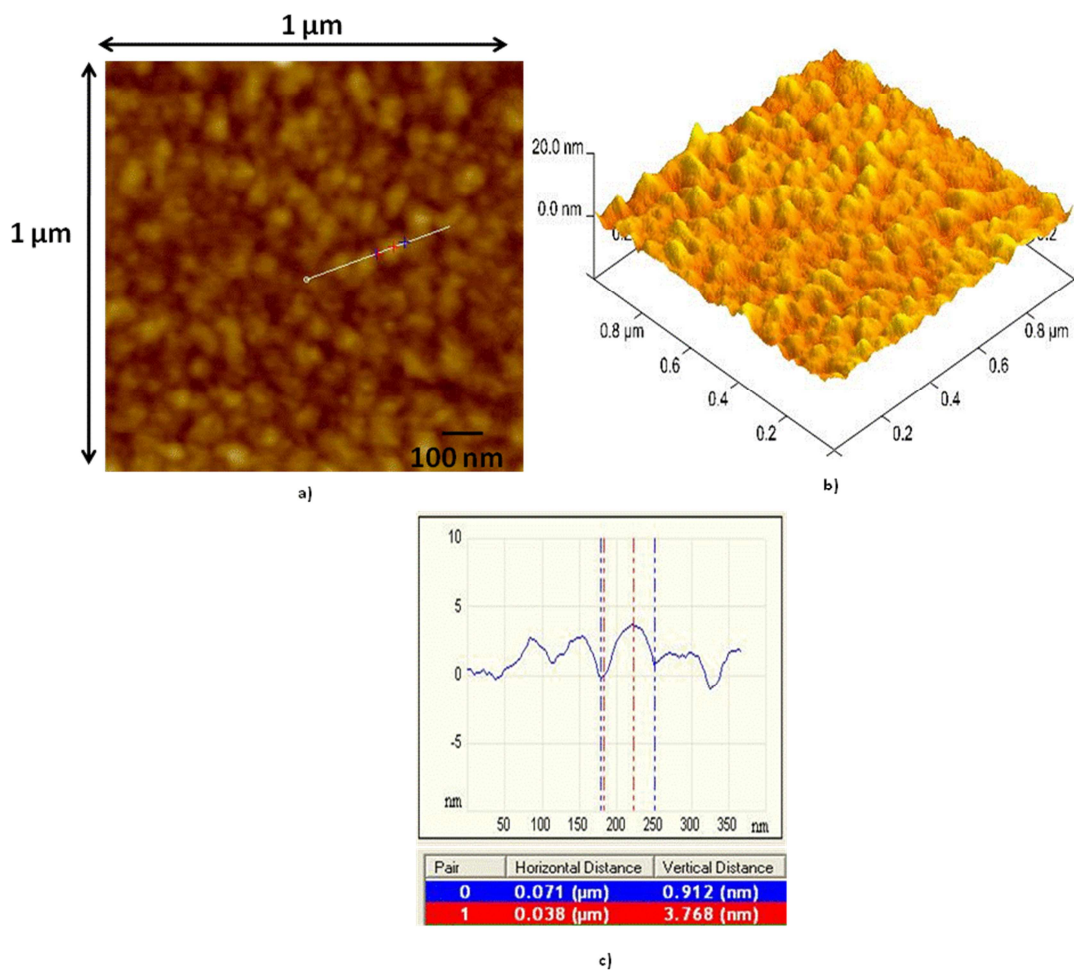


Figure 5.1 a) 2-D profile b) 3-D profile c) Cross section of first analyzed area ($1 \times 1 \mu\text{m}^2$).

Average roughness (R_a) and maximum height (R_t) of three different analyzed areas on the same surface were given in **Table 5.1**. The average roughness and maximum height average of three analyzed areas were calculated as 1.071 and 9.870 nm, respectively.

Table 5.1 Average roughness (R_a) and maximum height (R_t) of different analyzed areas on the same gold surface measured by AFM.

Analyzed Surface (1x1 μm^2)	Average Roughness (R_a) (nm)	Maximum Height (R_t) (nm)
I	0.953	8.92
II	1.10	10.1
III	1.16	10.6
Average	1.07	9.87

5.1.2 Toxin Modified Gold Surface Characterization with AFM

As explained in Chapter 3 sandwich structures were obtained without gold particles. After sandwich immunoassay, the characterization of gold surface was determined by AFM. The concentration of primary antibody was 0.1 mg/ml whereas that of toxin was 20 ng/ml. Thus, toxins immobilized on different analyzed surfaces were rare (**Figure 5.2**). The heights of the sandwich structures on the different analyzed surfaces were more than 30 nm. According to results, the height of sandwich structure ($15+4.54+15+1.57 \approx 36.11$) was more than 30 nm explaining that SEB bound primary antibody (height ≈ 15) and, also, a secondary antibody (height ≈ 15) was immobilized on the surface.

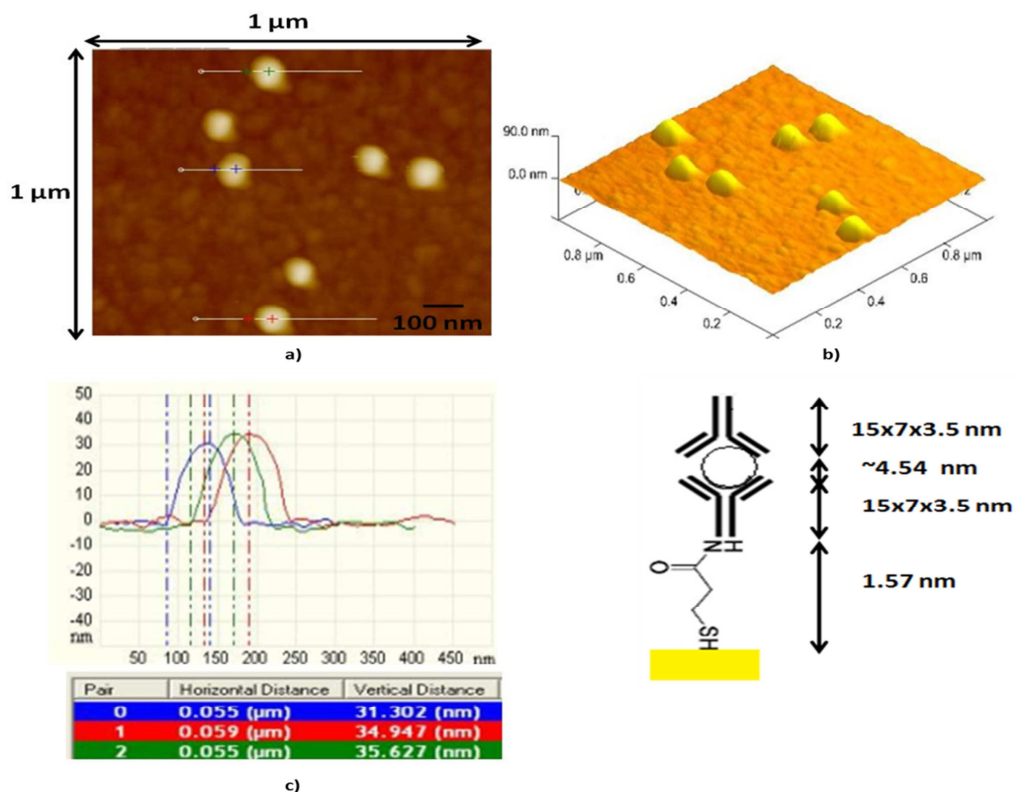


Figure 5.2 Surface I a) 2-D profile b) 3-D profile c) Cross section after sandwich immunoassay.

As can be seen from **Figure 5.3 and 5.4**, the same sandwich structures were obtained on the second and third analyzed surfaces, respectively. The heights of the sandwich structures were more than 30 nm. The heights of sandwich structure were approximately 45 nm in one site for Surface II. This might be due to unbound antibodies which were not removed completely.

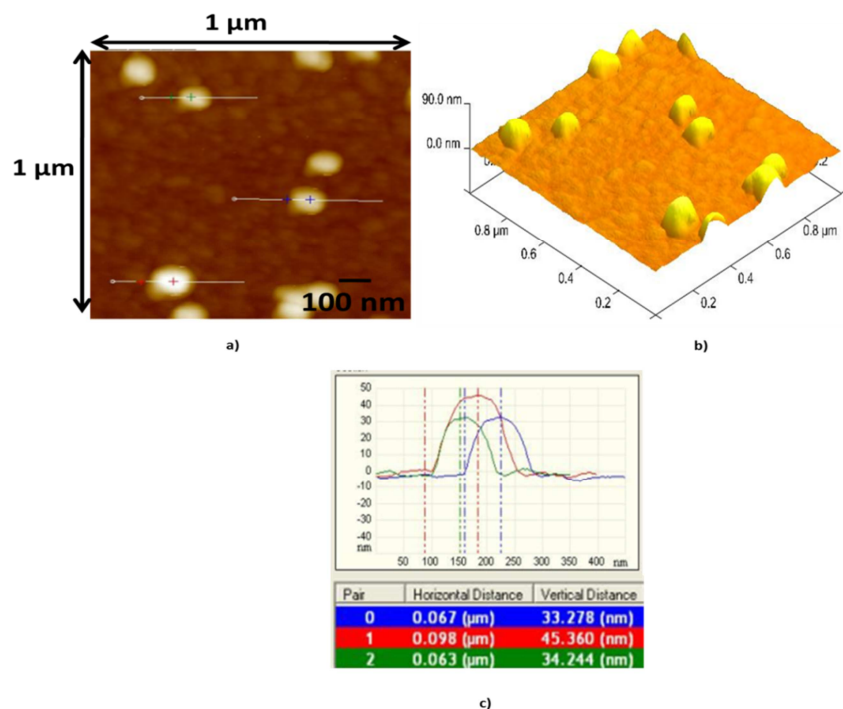


Figure 5.3 Surface II a) 2-D profile b) 3-D profile c) Cross section after sandwich immunoassay.

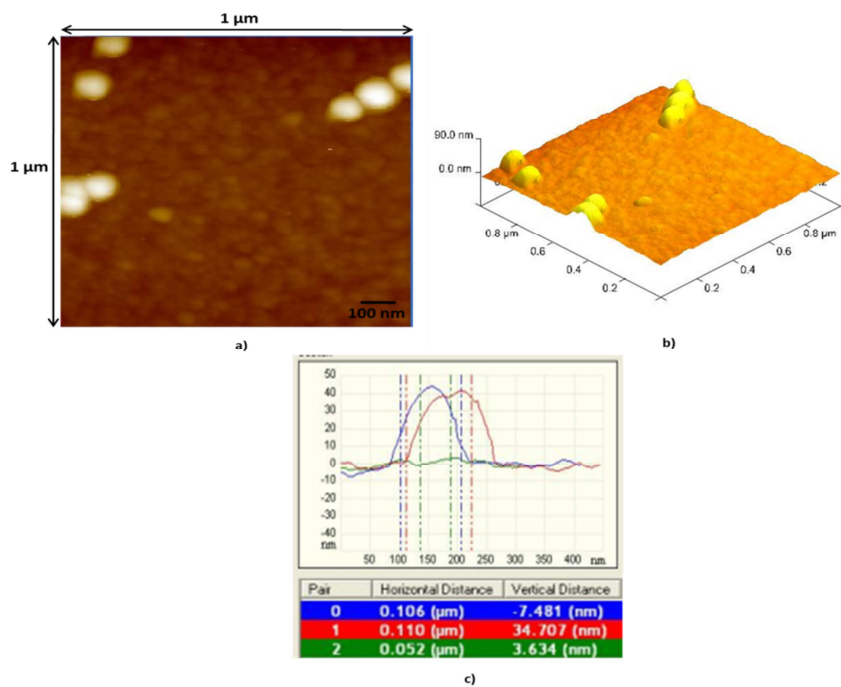


Figure 5.4 Surface III a) 2-D profile b) 3-D profile c) Cross section after sandwich immunoassay.

In order to see the reproducibility of data the same experiment was done a different surface numbered as III. On Surface III the height of rise on some parts of analyzed surface was less than 15 nm meaning that only primary antibodies were immobilized (7+1.57~8.57) (**Figure 5.5**). This might be due to the concentration of toxin which was less than that of primary antibody. Thus, all primary antibodies could not be able to bind toxins.

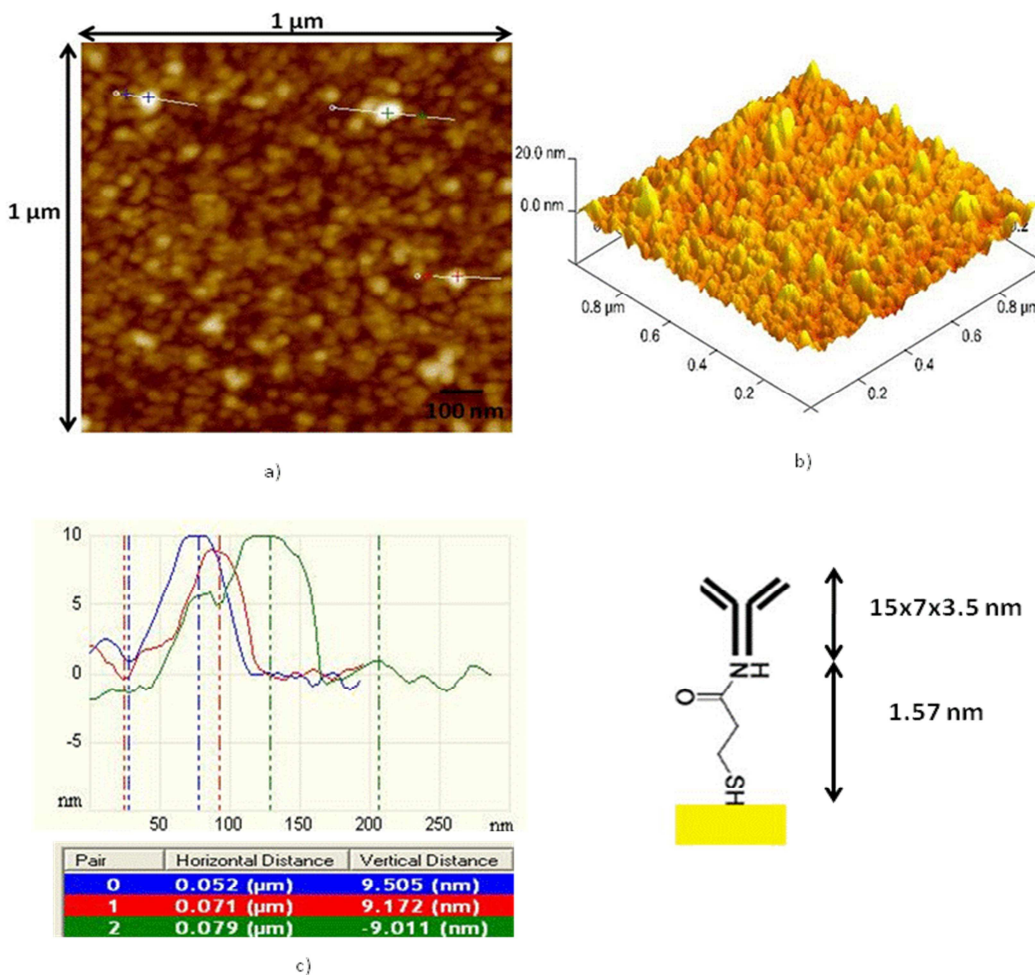


Figure 5.5 Surface IV a) 2-D profile b) 3-D profile c) Cross section after sandwich immunoassay.

5.1.3 Toxin Modified Gold Surface Characterization with SERS

In the first method, firstly thiolated antibodies were obtained by using sulfo-LC-SPDP. Then, antibodies were immobilized on the gold surface. SEB bound antibodies using different concentrations of SEB solution. Finally, antibody conjugated gold particles bound toxins for detection of toxin by SERS.

To find optimal time for antibody immobilization, SEB concentration was taken constant as 10^{-3} mg/ml while immobilization time was changed. Raman signal increased when antibody immobilization time increased. The concentration of immobilized antibody was proportional to time up to one hour. After one hour, immobilized antibody concentration did not change. Thus, the optimum time for antibody immobilization was found as one hour as shown in **Figure 5.6**.

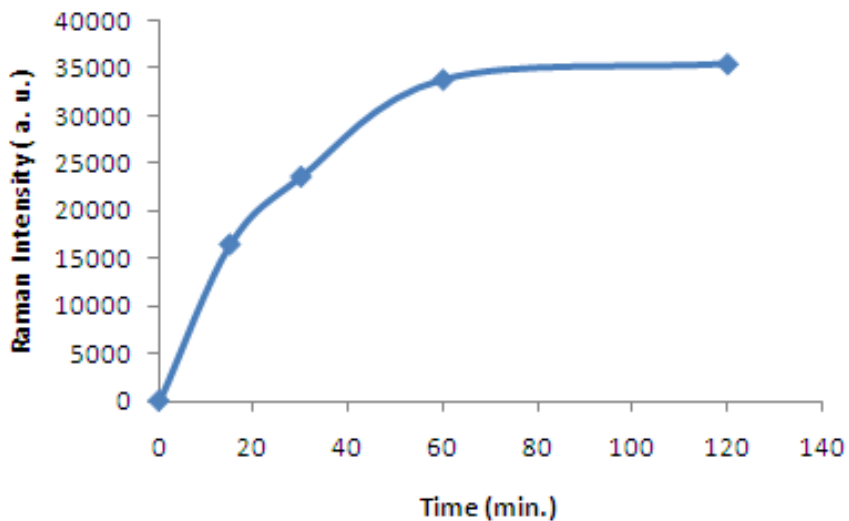


Figure 5.6 Optimum time for antibody immobilization using 10^{-3} mg/ml of SEB.

In **Figure 5.7** surface coverage with respect to concentration of toxin (the time of antibody immobilization was taken as 1 hour) is shown. Surface coverage

(θ =Number of occupied surface sites/Total number of surface sites) increases when concentration of SEB increases. As can be seen in **Figure 5.8**, surface coverage reaches a constant value of $\theta=1.0$ after a concentration of $3 \times 10^{-6} M$ of SEB.

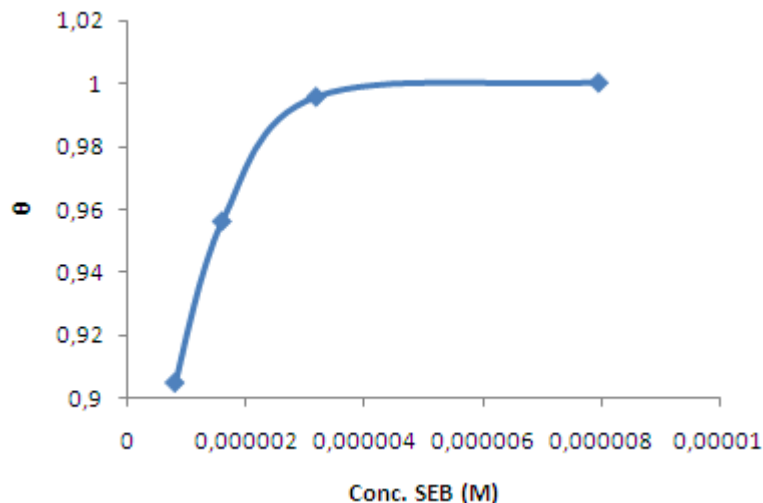


Figure 5.7 Surface Coverage as a function of Concentration of SEB

The reaction rate constant between antigen and antibody can be calculated using the slope of graph of $1/\theta$ vs. $1/[Ag]$ (**Figure 5.8**). The slope of Graph of $1/C$ vs. $1/\theta$ is 1×10^{-7} . The slope is equal to $1/K$. Thus, the reaction rate constant between SEB and its antibody is determined as $10^7 M^{-1}$. In the literature, the reaction rate constant has been reported as $1.6 \times 10^7 M^{-1}$ which is a very close value (Moises, 2010).

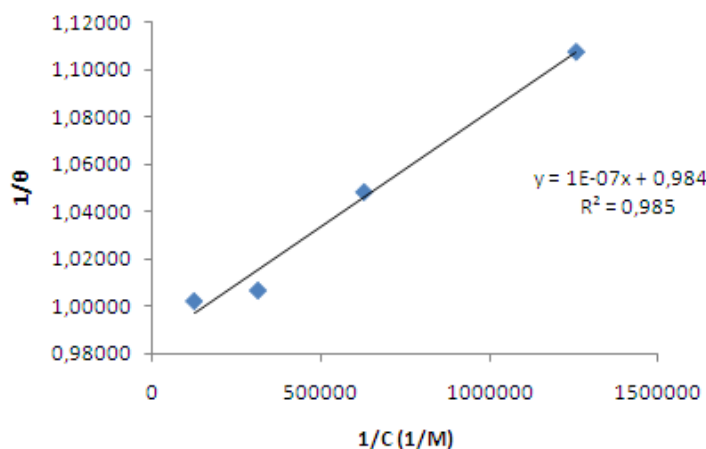


Figure 5.8 Change of $1/\theta$ with $1/C$.

After finding the optimized time for antibody immobilization, different concentrations (10^{-1} - 10^{-15} mg/ml) of SEB was used for the detection by SERS. Raman intensities measured by SERS are given in **Figure 5.9**. The minimum concentration of SEB detected by SERS was 10^{-13} mg/ml (1 attogram (ag)/ml). This result was better than that of conventional methods such as cell counting, spectroscopy techniques, ELISA and electrochemical measurements (Nelson et al., 2001; Lin et al., 2007; Hasebe et al., 2009; Sapsford et al., 2009).

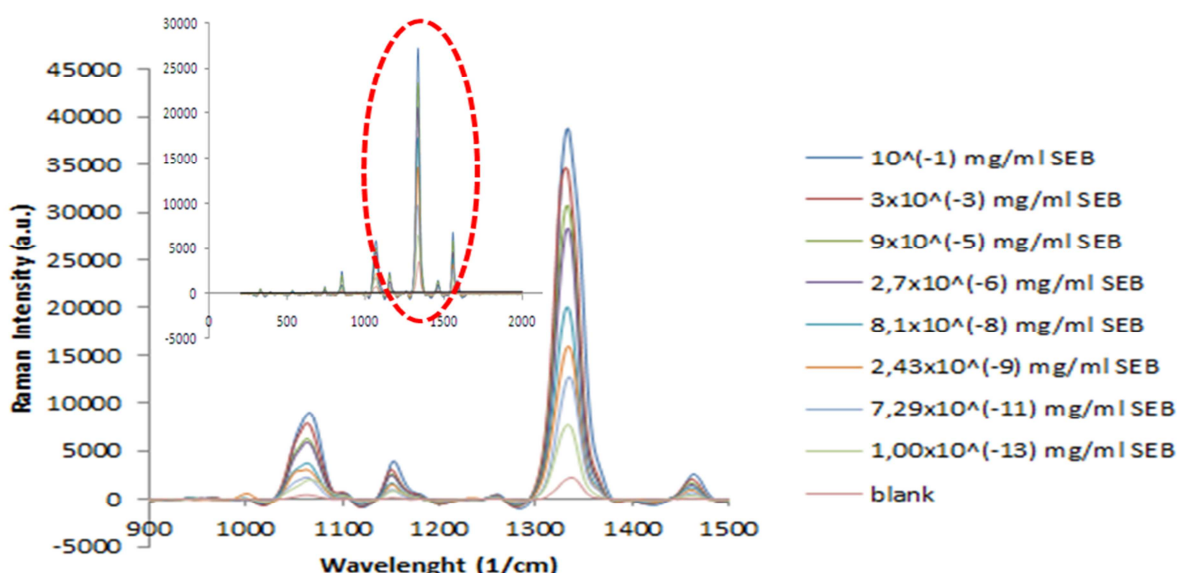


Figure 5.9 Raman intensity of different concentrations of toxin immobilization using thiolated antibody.

The linearity was obtained by using relation between SEB concentration (from 10^{-1} to 10^{-15} mg/ml) and Raman intensity at 1326 cm^{-1} . The calibration curve was obtained for the changes of the peak intensities of DTNB vs. the different concentrations of SEB as shown in **Figure 5.10**. A good linear correlation ($R^2=0.9954$) between Raman intensity and log concentration of SEB was obtained within the working range of SEB concentration.

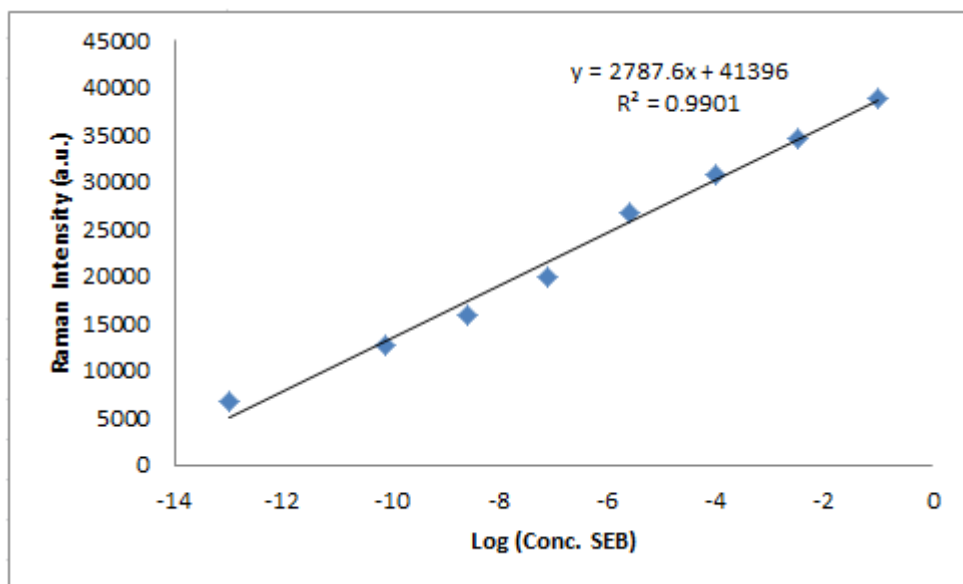


Figure 5.10 Calibration curve for toxin immobilization using thiolated antibody.

In order to confirm and verify the selectivity of the capture surface, bovine serum albumin (BSA) with two different concentrations (10^{-1} and 10^{-3} mg/ml) was used to prove specific and nonspecific interaction between protein and SEB antibody. BSA solution was diluted and adjusted in the same way described above according to SEB concentration which was used in SERS measurement. There was no difference in terms of the SERS tag (gold particle) used in the experiments. Raman intensities at 1338 cm^{-1} for 10^{-1} and 10^{-3} mg/ml of BSA were obtained and is shown in **Figure 5.11** together with the blank one. Results showed that, the intensity was not proportional to concentration of BSA indicating there is no specific interaction between antibody and BSA. However, Raman intensities were greater when

compared with than that for blank. This means that there was a nonspecific interaction between BSA and SEB antibody which was very low.

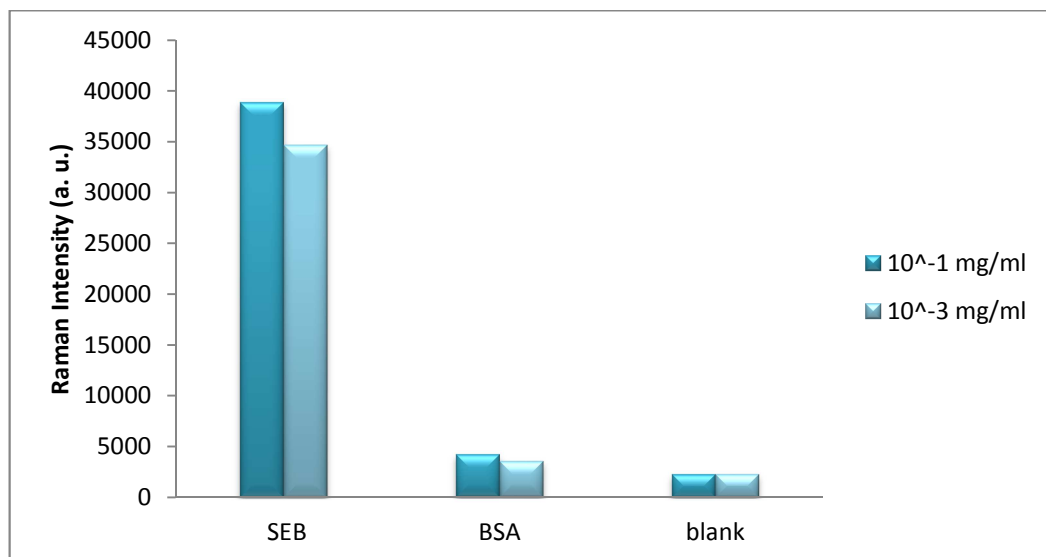


Figure 5.11 Comparison of Raman intensity between 10^{-1} mg/ml and 10^{-3} mg/ml of SEB and BSA using thiolated antibody.

5.1.4 *C. albicans* Immobilized Gold Biosensor Surface Characterization with Microscope

Method I which was used for the immobilization of SEB was also used for the detection of *C. albicans* by microscope. The aim of this assay is to see whether the developed procedure can be used for the detection of different pathogens such as bacterium, virus, fungus and toxin.

- In the experiment, firstly 8.4 μ l of 1 mg/ml anti-*C. albicans* and 2 μ l of sulfo-LC-SPDP were added to 3.6 μ l of 20 mM PBS buffer solution. It took about one hour to bind antibody and cross-linker.
- Then, 7 μ l of 150 mM TCEP.HCl solution was added and reduction period took 30 minutes. During reduction, the gold surface was rinsed with piranha

solution (H_2O_2 : H_2SO_4 , 1:1 v/v). Reduction product had thiol (-SH) group. Thus, reduction product could bind to gold surface easily due to thiol group (-SH).

- c) After reduction, the reduction product was incubated on the gold surface for about one hour. Then, the gold surface was rinsed with distilled water three times to remove unbound antibodies.
- d) Different concentrations of *C. albicans* solution were placed on the antibody immobilized gold surfaces and it was incubated for one hour. Then, the gold biosensor surface was rinsed with distilled water to remove unbound toxins. The size of *C. albicans* was large enough to visualize the cells under the light microscope, without the need of a secondary antibody (Han et al., 2011). **Figure 5.12** shows the steps of the immobilization procedure of *C. albicans* on a gold biosensor surface.

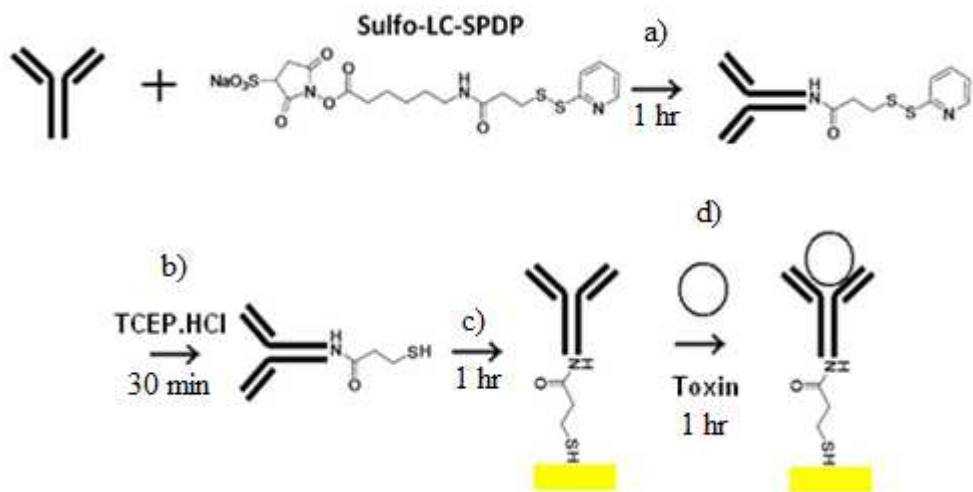


Figure 5.12 Immobilization of *C. albicans* using thiolated antibody.

The determination of the immobilization of *C. albicans* was visualized by optical detection using a microscope due to big size of the yeast. The concentration of anti-

C. albicans solution was constant at 1 mg/ml. However, different concentrations of *C. albicans* solution were used to determine the limits of detection. As an example, in **Figure 5.13**, 1 mg/ml *C. albicans* binding to the gold (Au) surface instead of silicon (Si) surface is shown.

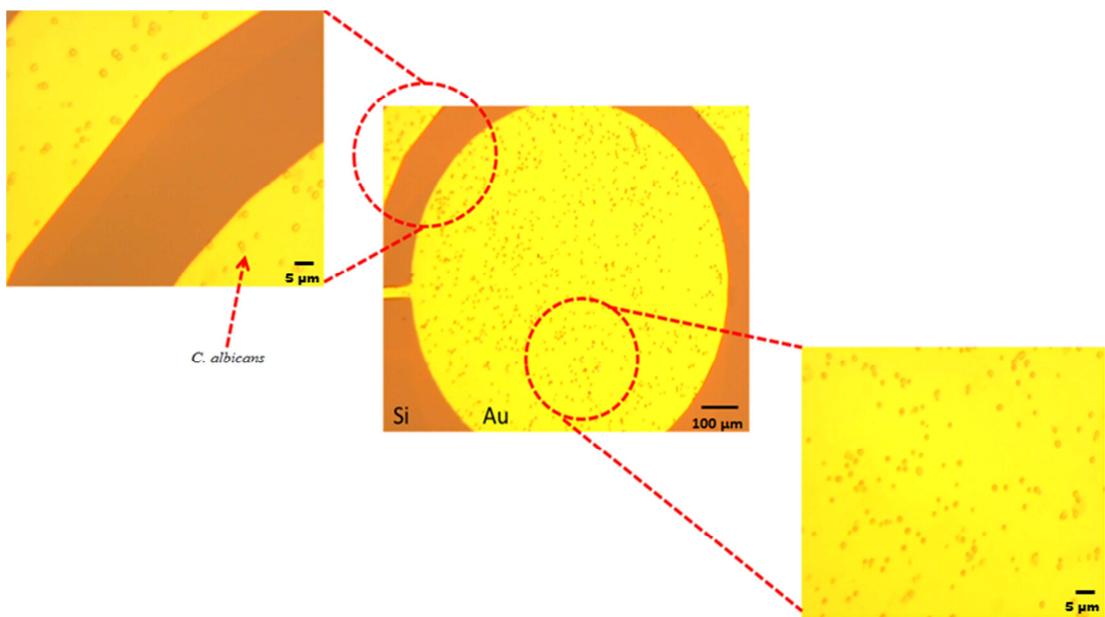


Figure 5.13 Immobilization of 1 mg/ml *C. albicans* on gold surface.

It was also found that 500, 100, 50, 10, 1 $\mu\text{g}/\text{ml}$, 1 and 50 ng/ml and 800, 500 pg/ml of *C. albicans* were detected and the results were shown in Appendix A. The minimum concentration of *C. albicans* detected by microscope was 250 pg/ml (**Figure 5.14**).

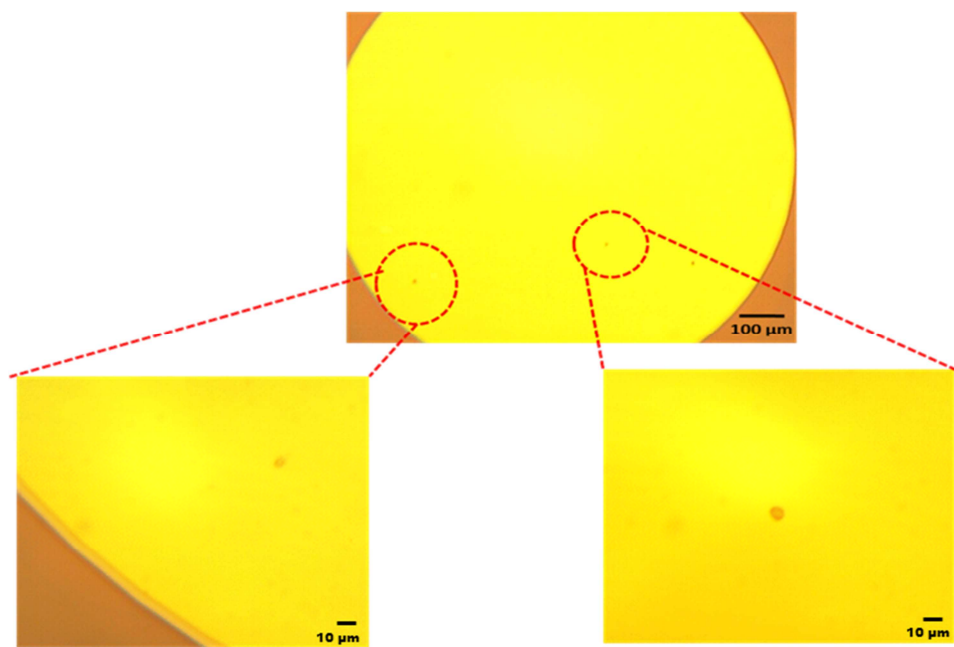


Figure 5.14 Immobilization of 250 pg/ml *C. albicans* on gold biosensor surface.

After determination of concentration limit, antibody conjugated gold surfaces were stored at -20 °C for one week. After one week, different concentrations (100, 10, 1 $\mu\text{g}/\text{ml}$ and 1 ng/ml) of *C. albicans* were again detected by the light microscopy. This proved that, antibody conjugated gold surfaces can be easily carried at -20 °C and patients in different places can use biosensor easily. Immobilization of 100 $\mu\text{g}/\text{ml}$ and 1 ng/ml *C. albicans* on gold surface stored at -20 °C for one week are shown in **Figure 5.15 a-b** and the results of 10 and 1 $\mu\text{g}/\text{ml}$ of *C. albicans* are shown in Appendix A.

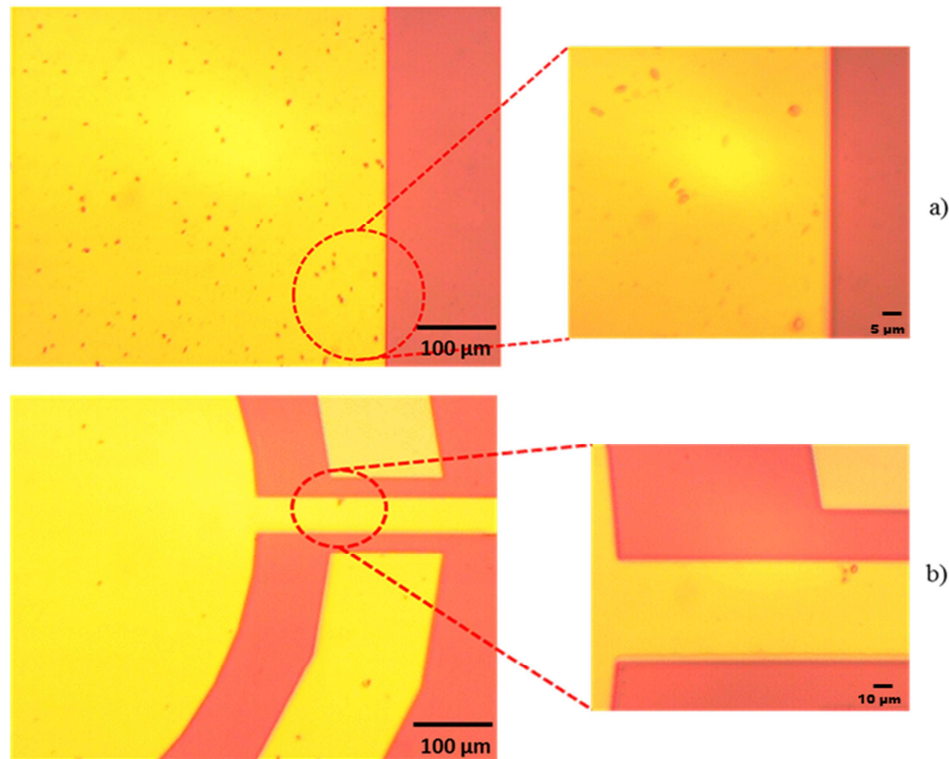


Figure 5.15 Immobilization of a) 100 µg/ml and b) 1 ng/ml *C. albicans* on gold biosensor surface stored at -20 °C for one week.

After detection of *C. albicans* on gold biosensor surface, the same experiments were repeated by using a designed biosensor with a channel (Yıldırım et al., 2010) and different concentration of *C. albicans* (500 µg/ml, 1 ng/ml, 250 pg/ml). As can be seen in **Figure 5.16a-c**, immobilized *C. albicans* on biosensor surface inside the channel decreased with decreasing concentration from 500 µg/ml to 250 pg/ml. Thus, the minimum concentration of *C. albicans* detected by biosensor was 250 pg/ml as seen from **Figure 5.16 c**.

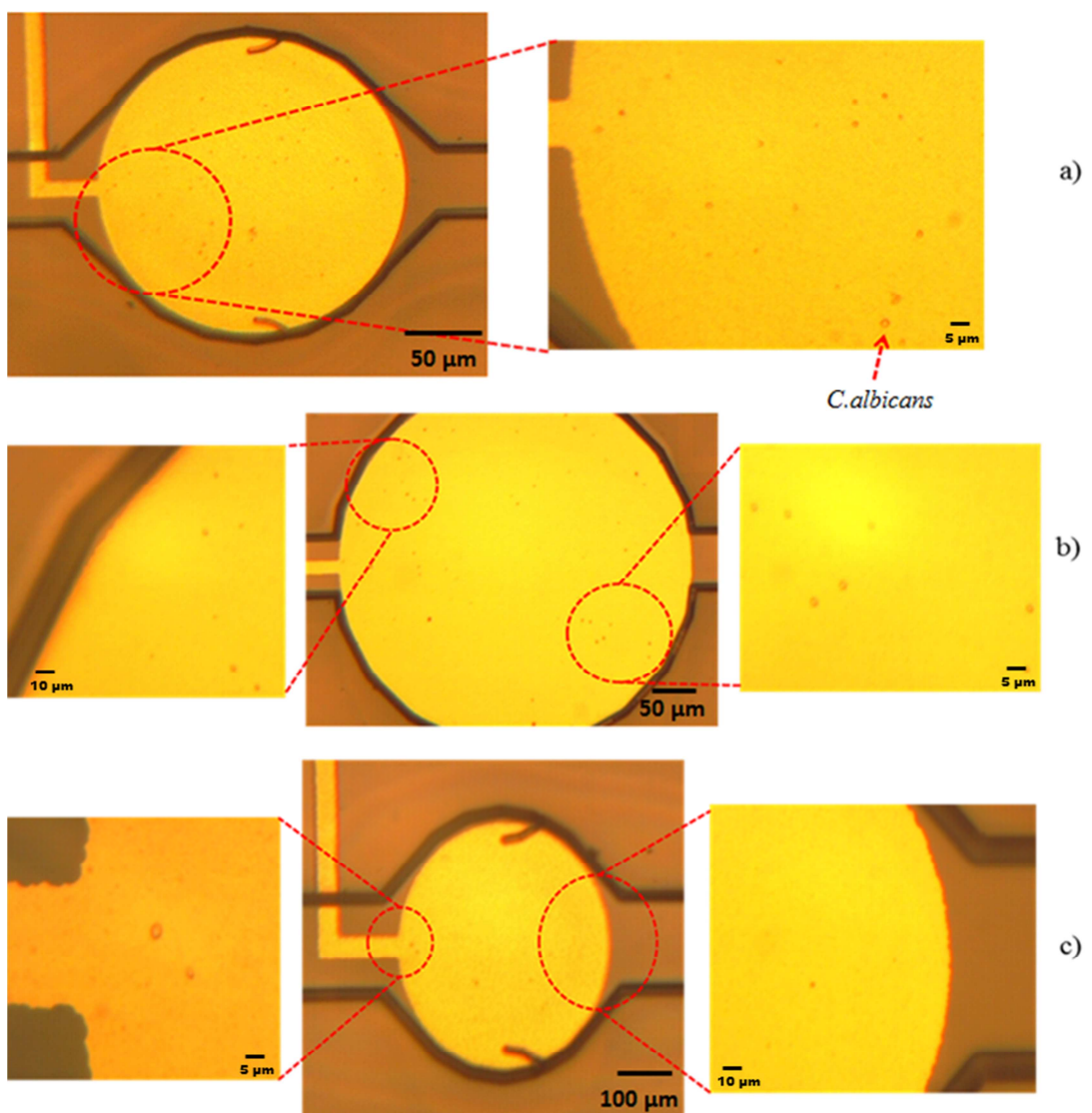


Figure 5.16 Immobilization of a) 500 µg/ml b) 1 ng/ml and c) 250 pg/ml *C. albicans* inside the biosensor channel.

As can be seen in **Figure 5.17**, *C. albicans* were not immobilized on the other parts of the biosensor (e.g. reservoir) which were made of parylene.

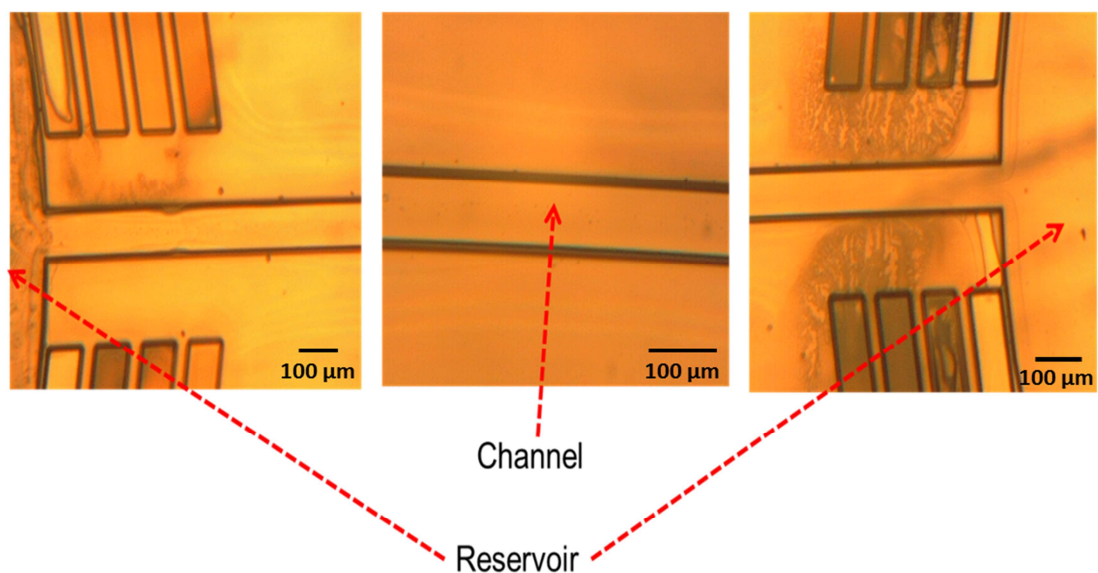


Figure 5.17 Immobilization of are 250 pg/ml *C. albicans* inside the biosensor channel.

The storage capacity of these biosensors was tested by keeping them again at -20 °C for one week. It was found that there is no difference in the amount of detected *C. albicans* same as it was on the gold biosensor surface without a channel (**Figure 5.18**).

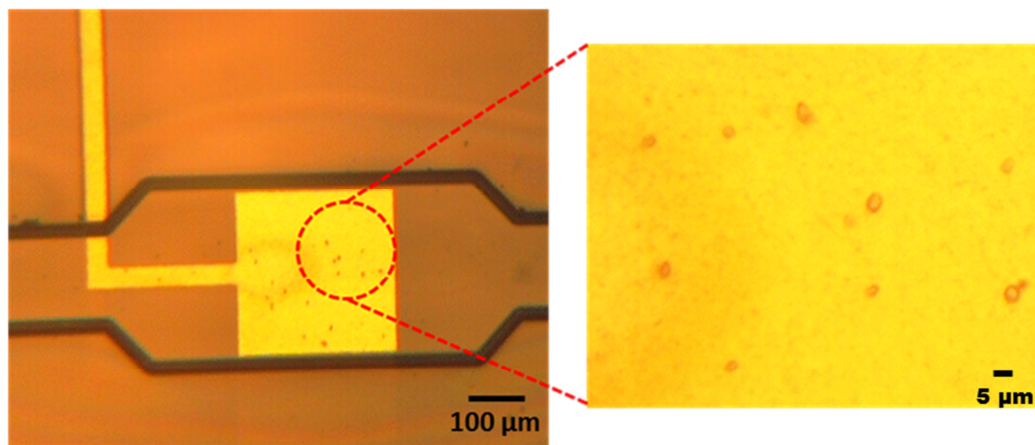


Figure 5.18 Immobilization of 1 µg/ml *C. albicans* on gold surface of biosensor in the channel stored at -20 °C for one week.

5.2 Results with Method II

The main difference between Method I and II as given in Chapter 3 is the immobilization of the antibody on SAM for Method II.

5.2.1 Toxin Modified Gold Surface Characterization with AFM

The arithmetic average roughness values (R_a) of bare gold surface before immunoassay, after immobilization of antibody and with gold nanorods are given in **Table 5.2**. It can be seen from **Figure 5.19 A**, the bare gold surface is clean enough because the arithmetic average (R_a) and root mean square roughness (R_q) values for bare gold surface are 0.94 and 1.20 nm, respectively (**Table 5.2**). After antibody immobilization on SAM prepared by 11-MUA, the R_a and R_q values slightly increased to 1.07 and 1.56, respectively. Antibody is an organic material. Thus there is a phase difference after immobilization of antibody on gold surface as presented in **Figure 5.19 B**. After immobilization of gold nanorods, the R_a and R_q values rise to 2.53 and 3.55, respectively proving that immobilization of gold nanorods was successful (**Figure 5.19 C**). In **Figure 5.19**, 2-D (a) and phase images (b) of AFM are given for bare gold surface (A) with SAM + antibody (B) and with SAM + antibody+gold nanorods (C).

Table 5.2 AFM roughness values for gold surface after each step of the sandwich immunoassay.

	Gold surface	Antibody	Gold Nanorod
R_a (nm)	0.94	1.07	2.53
R_q (nm)	1.20	1.56	3.55

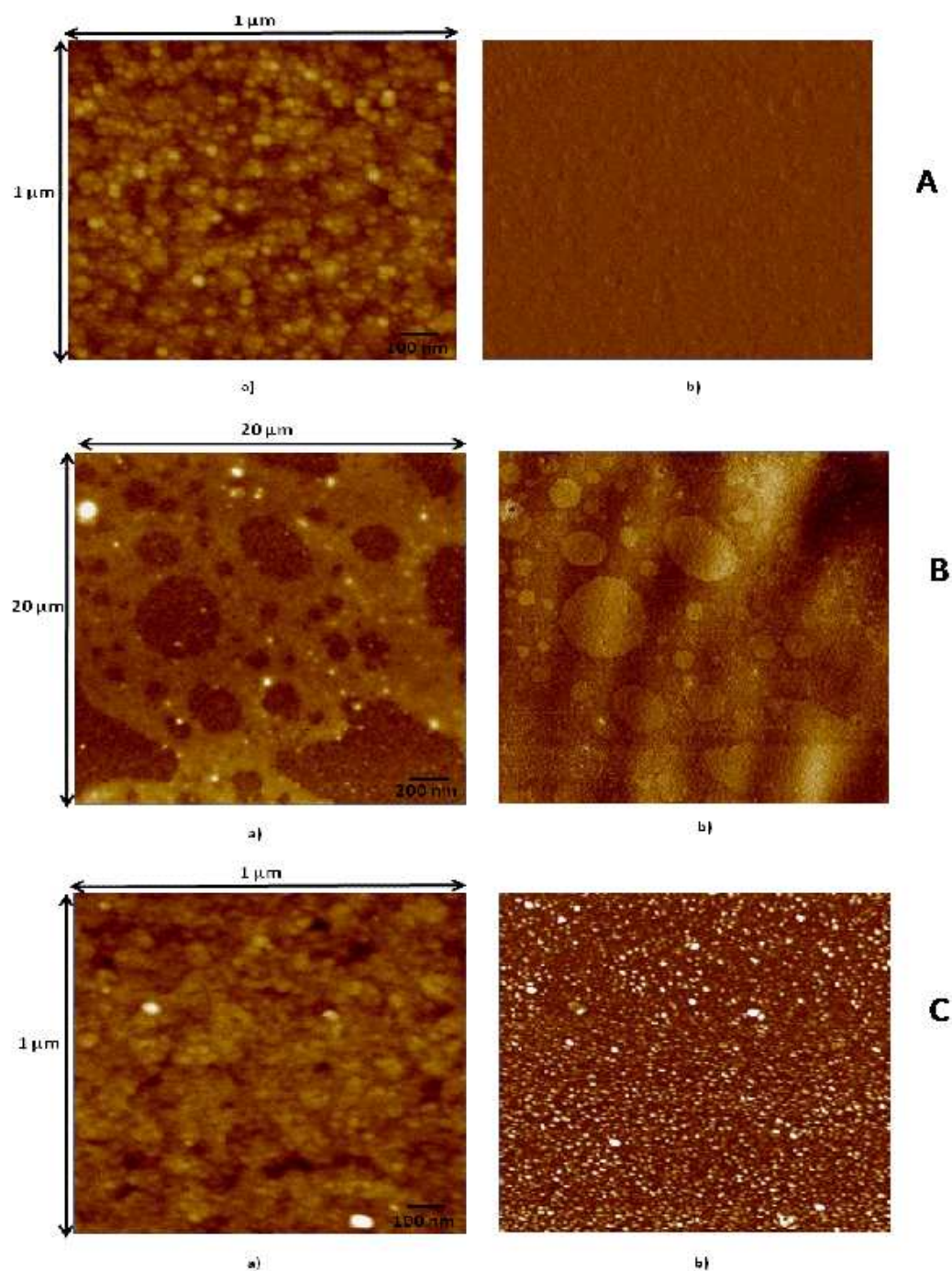


Figure 5.19 2D (a) and phase images (b) of AFM topography of A) bare gold surface; B) SAM+ antibody; C) SAM + antibody+SEB+ antibody + gold nanorods.

5.2.2 Toxin Modified Gold Surface Characterization with SERS

In this experiment, 11-MUA and 3-MPA were used for the formation of SAM. Then, antibodies were immobilized on the gold surface. SEB with different concentrations bound to the antibodies. Then, antibody conjugated gold particles were used as SERS tag. Finally, SEB with different concentrations (10^{-1} - 10^{-11} mg/ml) was detected by SERS. In this experiment, the minimum concentration of SEB detected by SERS was 10^{-11} mg/ml as shown in **Figure 5.20**.

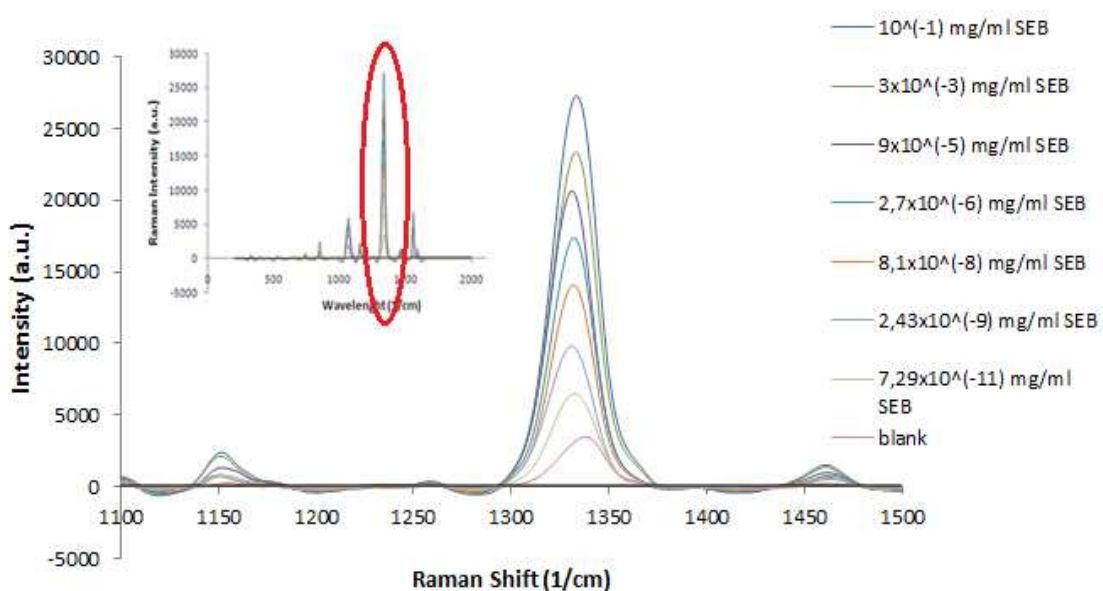


Figure 5.20 Raman intensity for different concentrations of toxin immobilization using SAM.

In **Figure 5.21**, calibration curve for toxin immobilization using SAM is given. R^2 of calibration curve is equal to 0.9967. Thus, the logarithm of concentration of toxin is proportional to Raman intensity.

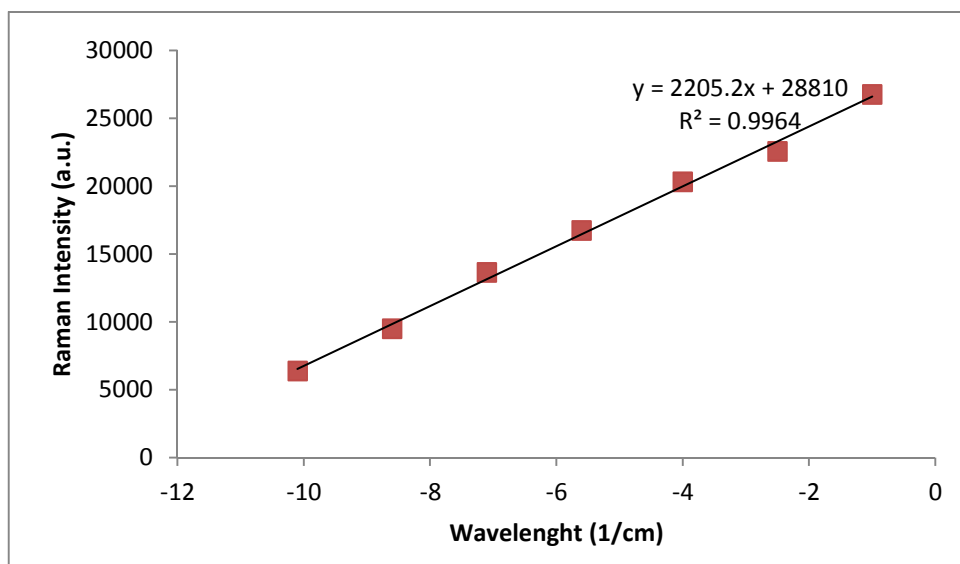


Figure 5.21 Calibration curve for toxin immobilization using SAM.

Also, the Raman intensities for 10^{-1} and 10^{-3} mg/ml of SEB and BSA were compared as seen in **Figure 5.22** with blank one. The intensities of BSA were very low. However, it was greater than that of blank surface. This was the result of nonspecific interaction between SEB antibody and BSA similar to Method I.

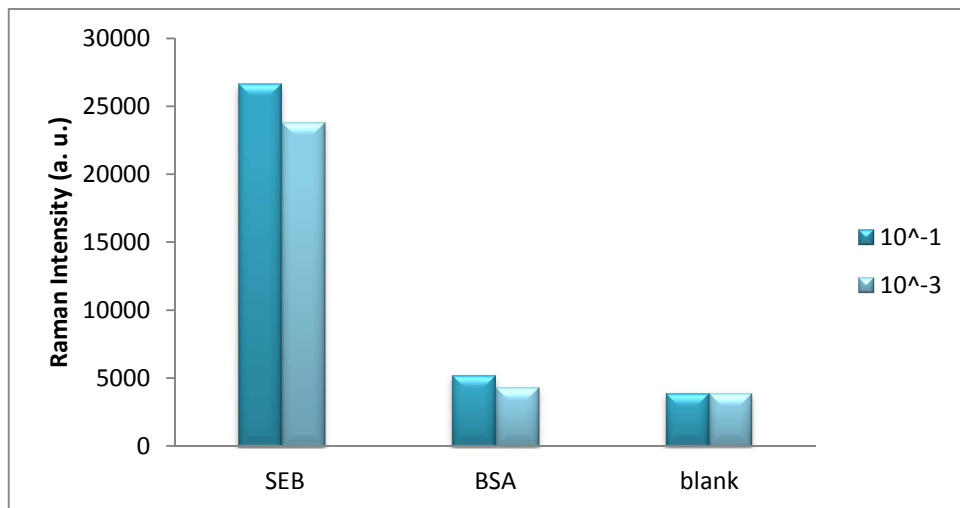


Figure 5.22 Comparison of Raman intensity between 10^{-1} mg/ml and 10^{-3} mg/ml of SEB and BSA using SAM.

CHAPTER 6

CONCLUSIONS AND RECOMMENDATIONS

- In this work, a sensitive homogeneous immunoassay procedure for the determination of pathogens based on AFM and SERS detection was developed. The developed procedure was compared with a procedure used in the literature. First, thiolated antibody was obtained in a method named as Method I whereas SAM was formed in Method II.
- The surface roughness was obtained by AFM before and after formation of sandwich structure using both procedures. SEB immobilized on the gold biosensor surface was detected by AFM. In addition, SEB immobilization was detected by SERS using Method I and II. To get SERS signal, DTNB was used as SERS tag. After formation of sandwich structure using DTNB-coated gold nanoparticles, vibrational peaks at 1326, 1149, 1060, 848, and 740 cm^{-1} were obtained.
- It was found that when the concentration of SEB decreased the Raman signals decreased.
- The minimum concentrations detected by using Method I and II were 1.00×10^{-13} and 7.29×10^{-11} mg/ml, respectively. These concentrations for pathogens can not be detected by conventional techniques.
- In addition, to prove nonspecific interaction between protein and SEB antibody, 10^{-1} and 10^{-3} mg/ml of SEB and BSA were compared. Results show that the intensity was not proportional to concentration of BSA. It was shown that there was no specific interaction between antibody of SEB and BSA.

- The theory of immobilization of pathogens on the biosensor surface, interaction between antibody and antigen were studied. In addition, the reaction rate constant between SEB and its antibody was reported as $1.6 \cdot 10^7 \text{ M}^{-1}$ which was similar to the rate constant which was determined in the literature.
- A biosensor was fabricated in the METU MEMS Research and Applications Center for detection of *C. albicans*. The minimum concentration of *C. albicans* detected by biosensor was 250 pg/ml.
- After storage of biosensor at -20 °C for one week, different concentrations of *C.albicans* were detected. 1 µg/ml was the minimum concentration of *C.albicans*.
- It is seen that different pathogens can be detected using developed procedure for sensitive and highly selective biosensor applications.
- In addition, different detection methods (optical, mechanical or electrochemical methods) can be used for detection of pathogens using the developed procedure.

REFERENCES

- Alouf, J. E. and M. R. Popoff, "The Comprehensive Sourcebook of Bacterial Protein Toxins", *Academic Press* (2006).
- Alvarez, M. and L. M. Lechuga, "Microcantilever-based platforms as biosensing tools." *Analyst* 135(5): 827-836, (2010).
- Baldrich, E., O. Laczka, F. Javier Del Campo and F. Xavier Munoz, "Gold immuno-functionalisation via self-assembled monolayers: Study of critical parameters and comparative performance for protein and bacteria detection." *Journal of Immunological Methods* 336(2): 203-212, (2008).
- Banada, P. P. and A. K. Bhunia, "Antibodies and Immunoassays for Detection of Bacterial Pathogens Principles of Bacterial Detection: Biosensors, Recognition Receptors and Microsystems". M. Zourob, S. Elwary and A. Turner, *Springer New York*: 567-602, (2008).
- Barreiros dos Santos, M., C. Sporer, N. Sanvicens, N. Pascual, A. Errachid, E. Martinez, M. P. Marco, V. Teixeira and J. Samiter, "Detection of pathogenic Bacteria by Electrochemical Impedance Spectroscopy: Influence of the immobilization strategies on the sensor performance". Proceedings of the Eurosensors Xxiii Conference. J. B. D. Brugger. 1: 1291-1294, (2009).
- Bhattacharya, S., J. Jang, L. Yang, D. Akin and R. Bashir, "Biomems and nanotechnology-based approaches for rapid detection of biological entities." *Journal of Rapid Methods and Automation in Microbiology* 15(1): 1-32, (2007).
- Biswas, B. B., P. S. Basu and M. K. Pal, "Gram Staining and Its Molecular Mechanism". International Review of Cytology. J. F. D. G.H. Bourne and K. W. Jeon, *Academic Press*. Volume 29: 1-27, (1970).

Books, H., Gram-positive Bacteria, including: *Bacillus*, *Streptococcus*, *Clostridium Botulinum*, *Streptococcus Pyogenes*, *Staphylococcus Aureus*, *Enterococcus*, *Perfringens*, *Streptococcus Pneumoniae*., *Hephaestus Books* (2011).

Borck, B., H. Stryhn, A. K. Ersboll and K. Pedersen, "Thermophilic *Campylobacter* spp. in turkey samples: evaluation of two automated enzyme immunoassays and conventional microbiological techniques." *Journal of Applied Microbiology* 92(3): 574-582, (2002).

Boujday, S., R. Briandet, M. Salmain, J.-M. Herry, P.-G. Marnet, M. Gautier and C.-M. Pradier, "Detection of pathogenic *Staphylococcus aureus* bacteria by gold based immunosensors." *Microchimica Acta* 163(3-4): 203-209, (2008).

Braga, P. C. and D. Ricci, "Atomic force microscopy: Application to investigation of *Escherichia coli* morphology before and after exposure to cefodizime." *Antimicrobial Agents and Chemotherapy* 42(1): 18-22, (1998).

Byrne, B., E. Stack, N. Gilmartin and R. O'Kennedy, "Antibody-Based Sensors: Principles, Problems and Potential for Detection of Pathogens and Associated Toxins." *Sensors* 9(6): 4407-4445, (2009).

Carlsson, J., H. Drevin and R. Axen, "Protein thiolation and reversible protein-protein conjugation. N-Succinimidyl 3-(2-pyridyldithio)propionate, a new heterobifunctional reagent." *Biochemical Journal* 173(3): 723-737, (1978).

Carrascosa, L. G., M. Moreno, M. Alvarez and L. M. Lechuga, "Nanomechanical biosensors: a new sensing tool." *Trends in Analytical Chemistry* 25(3): 196-206, (2006).

Chevallier, F. G., O. V. Klymenko, J. Li, T. G. J. Jones and R. G. Compton, "Mathematical modelling and numerical simulation of adsorption processes at

microdisk electrodes." *Journal of Electroanalytical Chemistry* 574(2): 217-237, (2005).

Choi, S., J. Chae and Ieee, "Thyroglobulin detection using competitive protein adsorption". Mems 2010: 23rd Ieee International Conference on Micro Electro Mechanical Systems, Technical Digest: 887-890, (2010).

Choi, S., W. Xu, X. Zhang, J. Chae and Ieee, "Characterization of a high-Q in-liquid longitudinal-mode film bulk acoustic resonator for real-time in-situ monitoring of competitive protein adsorption". Mems 2010: 23rd Ieee International Conference on Micro Electro Mechanical Systems, Technical Digest: 739-742, (2010).

Cochran, W. D., "Rayleigh, Raman and particulate scattering". *Vibrational-Rotational Spectry. for Planetary Atmospheres*, (1982).

Darain, F., K. L. Gan and S. C. Tjin, "Antibody immobilization on to polystyrene substrate-on-chip immunoassay for horse IgG based on fluorescence." *Biomedical Microdevices* 11(3): 653-661, (2009).

Dauksaite, V., M. Lorentzen, F. Besenbacher and J. Kjems, "Antibody-based protein detection using piezoresistive cantilever arrays." *Nanotechnology* 18(12), (2007).

de Freitas, C. G., A. P. Santana, P. H. Caldeira da Silva, V. S. Picao Goncalves, M. d. A. Ferreira Barros, F. A. Goncalves Torres, L. S. Murata and S. Perecmanis, "PCR multiplex for detection of *Salmonella Enteritidis*, *Typhi* and *Typhimurium* and occurrence in poultry meat." *International Journal of Food Microbiology* 139(1-2): 15-22, (2010).

Duong, D. D., Adsorption analysis: equilibria and kinetics, *Imperial College Press* (1998).

El-Boubou, K., C. Gruden and X. Huang, "Magnetic glyco-nanoparticles: A unique tool for rapid pathogen detection, decontamination, and strain differentiation." *Journal of the American Chemical Society* 129(44): 13392-+, (2007).

Emmeluth, D., L. Freeman-Cook and K. D. Freeman-Cook, *Staphylococcus Aureus Infections*, Chelsea House Pub (L) (2011).

Forrest, G. N., A. M. Kopack and E. N. Perencevich, "Statins in Candidemia: clinical outcomes from a matched cohort study." *Bmc Infectious Diseases* 10, (2010).

Fritz, J., M. K. Baller, H. P. Lang, H. Rothuizen, P. Vettiger, E. Meyer, H. J. Guntherodt, C. Gerber and J. K. Gimzewski, "Translating biomolecular recognition into nanomechanics." *Science* 288(5464): 316-318, (2000).

Glauert, A. M., "Fine structure of bacteria." *British Medical Bulletin* 18(3): 245-&, (1962).

Gudlaugsson, O., S. Gillespie, K. Lee, J. V. Berg, J. F. Hu, S. Messer, L. Herwaldt, M. Pfaller and D. Diekema, "Attributable mortality of nosocomial candidemia, revisited." *Clinical Infectious Diseases* 37(9): 1172-1177, (2003).

Gutierrez-Escribano, P., A. Gonzalez-Novo, M. Belen Suarez, C.-R. Li, Y. Wang, C. R. Vazquez de Aldana and J. Correa-Bordes, "CDK-dependent phosphorylation of Mob2 is essential for hyphal development in *Candida albicans*." *Molecular Biology of the Cell* 22(14): 2458-2469, (2011).

Hall, R. A., L. De Sordi, D. M. MacCallum, H. Topal, R. Eaton, J. W. Bloor, G. K. Robinson, L. R. Levin, J. Buck, Y. Wang, N. A. R. Gow, C. Steegborn and F. A. Muehlschlegel, "CO(2) Acts as a Signalling Molecule in Populations of the Fungal Pathogen *Candida albicans*." *Plos Pathogens* 6(11), (2010).

Han, T.-L., R. D. Cannon and S. G. Villas-Boas, "The metabolic basis of *Candida albicans* morphogenesis and quorum sensing." *Fungal Genetics and Biology* 48(8): 747-763, (2011).

Han, T.-L., R. D. Cannon and S. G. Villas-Bôas, "The metabolic basis of *Candida albicans* morphogenesis and quorum sensing." *Fungal Genetics and Biology: FG & B*, (2011).

Hasebe, Y., M. Fukuzawa and H. Matsuhisa, "Quantitative determination of *Escherichia coli* based on the electrochemical measurement of bacterial catalase activity using H₂O₂-selective organic/inorganic-hybrid sol-gel film-modified Pt electrode." *Journal of Environmental Sciences* 21, Supplement 1(0): S44-S47, (2009).

Hiramatsu, K. and D. A. Aldeen, *Staphylococcus Aureus: Molecular and Clinical Aspects*, Woodhead Publishing (2004).

Hogg, D. S., *Essential Microbiology*, Wiley (2005).

Huff, J. L., M. P. Lynch, S. Nettikadan, J. C. Johnson, S. Vengasandra and E. Henderson, "Label-free protein and pathogen detection using the atomic force microscope." *Journal of Biomolecular Screening* 9(6): 491-497, (2004).

Jenkinson, H. F. and L. J. Douglas, "Interactions between *Candida* Species and Bacteria in Mixed Infections". Polymicrobial Diseases. K. Brogden and J. Guthmiller, *ASM Press*, (2002).

Koch, A. L., *The Bacteria: Their Origin, Structure, Function and Antibiosis*, Springer (2006).

Koydemir, H. C., H. Külah and C. Özgen, "A Micro Electrochemical Sensor for the Detection of Methicillin Resistance in *Staphylococcus aureus*". *Biosensors*, Cancun, Mexico, (2012).

Kumar, C. P. G., T. Menon, P. S. Rohini, S. Rajasekaran, T. Sundararajan and W. Venkatadesikalu, "Anti-Candida antibodies and candidemia in ninety patients with HIV/AIDS and cancer." *Journal De Mycologie Medicale* 17(1): 50-53, (2007).

Labib, M., M. Hedström, M. Amin and B. Mattiasson, "A capacitive biosensor for detection of staphylococcal enterotoxin B." *Analytical and Bioanalytical Chemistry* 393(5): 1539-1544, (2009).

Lazcka, O., F. J. D. Campo and F. X. Muñoz, "Pathogen detection: A perspective of traditional methods and biosensors." *Biosensors and Bioelectronics* 22(7): 1205-1217, (2007).

Le Brun, A. P., S. A. Holt, D. S. Shah, C. F. Majkrzak and J. H. Lakey, "Monitoring the assembly of antibody-binding membrane protein arrays using polarised neutron reflection." *European Biophysics Journal with Biophysics Letters* 37(5): 639-645, (2008).

Lee, H. J., D. Nedelkov and R. M. Corn, "Surface plasmon resonance imaging measurements of antibody arrays for the multiplexed detection of low molecular weight protein biomarkers." *Analytical Chemistry* 78(18): 6504-6510, (2006).

Liao, W., F. Wei, D. Liu, M. X. Qian, G. Yuan and X. S. Zhao, "FTIR-ATR detection of proteins and small molecules through DNA conjugation." *Sensors and Actuators B-Chemical* 114(1): 445-450, (2006).

Lin, H.-Y., W.-H. Tsai, Y.-C. Tsao and B.-C. Sheu, "Side-polished multimode fiber biosensor based on surface plasmon resonance with halogen light." *Applied Optics* 46(5): 800-806, (2007).

Liu, D. and W. Shu, "Microcantilever Biosensors: Probing Biomolecular Interactions at the Nanoscale." *Current Organic Chemistry* 15(4): 477-485, (2011).

Liu, T.-T., Y.-H. Lin, C.-S. Hung, T.-J. Liu, Y. Chen, Y.-C. Huang, T.-H. Tsai, H.-H. Wang, D.-W. Wang, J.-K. Wang, Y.-L. Wang and C.-H. Lin, "A High Speed Detection Platform Based on Surface-Enhanced Raman Scattering for Monitoring Antibiotic-Induced Chemical Changes in Bacteria Cell Wall." *Plos One* 4(5), (2009).

Mattingly, J. A., B. T. Butman, M. C. Plank, R. J. Durham and B. J. Robison, "Rapid monoclonal antibody-based enzyme-linked immunosorbent assay for detection of Listeria in food products." *Journal of the Association of Official Analytical Chemists* 71(3): 679-681, (1988).

Moises, S. S., Development of a competitive Immunoassay Microarray for the detection of the *Staphylococcus Aureus* enterotoxins A-D and H in dairy products, Universität Regensburg, (2010).

Molero, G., R. Diez-Orejas, F. Navarro-Garcia, L. Monteoliva, J. Pla, C. Gil, M. Sanchez-Perez and C. Nombela, "Candida albicans: genetics, dimorphism and pathogenicity." *International microbiology: the official journal of the Spanish Society for Microbiology* 1(2): 95-106, (1998).

Montville, T. J. and K. R. Matthews, Food Microbiology: An Introduction, *ASM Press* (2008).

Nakanishi, K., T. Sakiyama, Y. Kumada, K. Imamura and H. Imanaka, "Recent Advances in Controlled Immobilization of Proteins onto the Surface of the Solid

Substrate and Its Possible Application to Proteomics." *Current Proteomics* 5(3): 161-175, (2008).

Natesan, M., M. A. Cooper, J. P. Tran, V. R. Rivera and M. A. Poli, "Quantitative Detection of Staphylococcal Enterotoxin B by Resonant Acoustic Profiling." *Analytical Chemistry* 81(10): 3896-3902, (2009).

Nedelkov, D. and R. W. Nelson, "Detection of staphylococcal enterotoxin B via Biomolecular interaction analysis mass spectrometry." *Applied and Environmental Microbiology* 69(9): 5212-5215, (2003).

Nelson, B. P., T. E. Grimsrud, M. R. Liles, R. M. Goodman and R. M. Corn, "Surface plasmon resonance imaging measurements of DNA and RNA hybridization adsorption onto DNA microarrays." *Analytical Chemistry* 73(1): 1-7, (2001).

Nelson, D. L. and M. M. Cox, *Lehninger Principles of Biochemistry*, *W. H. Freeman & Company* (2004).

Palecek, E. and M. Fojta, "Magnetic beads as versatile tools for electrochemical DNA and protein biosensing." *Talanta* 74(3): 276-290, (2007).

Papageorgiou, A. C., H. S. Tranter and K. R. Acharya, "Crystal structure of microbial superantigen staphylococcal enterotoxin B at 1.5 angstrom resolution: Implications for superantigen recognition by MHC class II molecules and T-cell receptors." *Journal of Molecular Biology* 277(1): 61-79, (1998).

Pei, J. H., F. Tian and T. Thundat, "Glucose biosensor based on the microcantilever." *Analytical Chemistry* 76(2): 292-297, (2004).

Pfaller, M. A. and D. J. Diekema, "Epidemiology of invasive candidiasis: a persistent public health problem." *Clinical Microbiology Reviews* 20(1): 133-+, (2007).

Quiel, A., B. Juergen, G. Piechotta, A.-P. Le Foll, A.-K. Ziebandt, C. Kohler, D. Koester, S. Engelmann, C. Erck, R. Hintsche, J. Wehland, M. Hecker and T. Schweder, "Electrical protein array chips for the detection of staphylococcal virulence factors." *Applied Microbiology and Biotechnology* 85(5): 1619-1627, (2010).

Riebeseel, K., B. Enderle, G. Jobst, G. A. Urban, I. Moser and Ieee, "BioMEMS for the electrochemical detection of troponin I". 2006 Ieee Sensors, Vols 1-3: 160-161, (2006).

Saerens, D., L. Huang, K. Bonroy and S. Muyldermans, "Antibody fragments as probe in biosensor development." *Sensors* 8(8): 4669-4686, (2008).

Sapsford, K. E., J. Francis, S. Sun, Y. Kostov and A. Rasooly, "Miniaturized 96-well ELISA chips for staphylococcal enterotoxin B detection using portable colorimetric detector." *Analytical and Bioanalytical Chemistry* 394(2): 499-505, (2009).

Schreiber, F., "Structure and growth of self-assembling monolayers." *Progress in Surface Science* 65(5-8): 151-256, (2000).

Selvaganapathy, P. R., E. T. Carlen and C. H. Mastrangelo, "Recent progress in microfluidic devices for nucleic acid and antibody assays." *Proceedings of the Ieee* 91(6): 954-975, (2003).

Seokheun Choi, Wencheng Xu, Xu Zhang, ve Junseok Chae, "Characterization of a high-Q in-liquid longitudinal-mode film bulk acoustic resonator for real-time in-situ monitoring of competitive protein adsorption", ss. 739-742, (2010).

Su, X. L. and Y. B. Li, "A QCM immunosensor for Salmonella detection with simultaneous measurements of resonant frequency and motional resistance." *Biosensors & Bioelectronics* 21(6): 840-848, (2005).

Subramanian, A., J. Irudayaraj and T. Ryan, "A mixed self-assembled monolayer-based surface plasmon immunosensor for detection of E-coli O157 : H7." *Biosensors & Bioelectronics* 21(7): 998-1006, (2006).

Swaminathan, S., W. Furey, J. Fletcher and M. Sax, "Crystal-structure of Staphylococcal Enterotoxin-B, a Superantigen." *Nature* 359(6398): 801-806, (1992).

Takaki, K., N. Shimoно, T. Ishimaru, K. Okada, Y. Sawae and Y. Niho, "Detection of Candida antigen and antibody in serum from patients with invasive candidiasis." *International Journal of Infectious Diseases* 1(2): 78-82, (1996).

Temur, E., I. H. Boyaci, U. Tamer, H. Unsal and N. Aydogan, "A highly sensitive detection platform based on surface-enhanced Raman scattering for Escherichia coli enumeration." *Analytical and Bioanalytical Chemistry* 397(4): 1595-1604, (2010).

Tortora, G. J., B. R. Funke and C. L. Case, *Microbiology: An Introduction with MasteringMicrobiology*, Benjamin Cummings (2010).

Tsai, W.-C. and P.-J. R. Pai, "Surface plasmon resonance-based immunosensor with oriented immobilized antibody fragments on a mixed self-assembled monolayer for the determination of staphylococcal enterotoxin B." *Microchimica Acta* 166(1-2): 115-122, (2009).

USCSW, G., "United States Cancer Statistics: 1999–2007 Incidence and Mortality Web-based Report." from www.cdc.gov/uscs, (2010).

Vandeventer, A. J. M., W. H. F. Goessens, A. Vanbelkum, H. J. A. Vanvliet, E. W. M. Vanetten and H. A. Verbrugh, "Improved Detection Of Candida-Albians By Pcr In Blood Of Neutropenic Mice With Systemic Candidiasis." *Journal of Clinical Microbiology* 33(3): 625-628, (1995).

Velusamy, V., K. Arshak, O. Korostynska, K. Oliwa and C. Adley, "An overview of foodborne pathogen detection: In the perspective of biosensors." *Biotechnology Advances* 28(2): 232-254, (2010).

Vericat, C., G. A. Benitez, D. E. Grumelli, M. E. Vela and R. C. Salvarezza, "Thiol-capped gold: from planar to irregular surfaces." *Journal of Physics-Condensed Matter* 20(18), (2008).

Villamizar, R. A., A. Maroto and F. X. Rius, "Improved detection of *Candida albicans* with carbon nanotube field-effect transistors." *Sensors and Actuators B: Chemical* 136(2): 451-457, (2009).

Wee, K. W., G. Y. Kang, J. Park, J. Y. Kang, D. S. Yoon, J. H. Park and T. S. Kim, "Novel electrical detection of label-free disease marker proteins using piezoresistive self-sensing micro-cantilevers." *Biosensors and Bioelectronics* 20(10): 1932-1938, (2005).

Whitman WB, Coleman DC, Wiebe WJ "Prokaryotes: the unseen majority". Proceedings of the National Academy of Sciences of the United States of America 95 (12): 6578–83, (1998).

Wu, G., R. H. Datar, K. M. Hansen, T. Thundat, R. J. Cote and A. Majumdar, "Bioassay of prostate-specific antigen (PSA) using microcantilevers." *Nature biotechnology* 19(9): 856-860, (2001).

Xu, Y., S. Xia, C. Bian, S. Chen and Ieee, A micro amperometric immunosensor based on protein A/Gold nanoparticles/Self-assembled monolayer-modified gold electrode. *1st IEEE International Conference on Nano/Micro Engineered and Molecular Systems.* 1-3: 38-41, (2006).

Yang, S.-Y., K.-Y. Lien, K.-J. Huang, H.-Y. Lei and G.-B. Lee, "Micro flow cytometry utilizing a magnetic bead-based immunoassay for rapid virus detection." *Biosensors & Bioelectronics* 24(4): 855-862, (2008).

Yıldırım, E., A. Koyuncuoğlu and H. Külah, An electrostatic parylene microvalve for lab-on-a-chip applications. *15th National Biomedical Engineering Meeting*. Antalya: 1-4, (2010).

Yu, C. X., A. Ganjoo, H. Jain, C. G. Pantano and J. Irudayaraj, "Mid-IR biosensor: Detection and fingerprinting of pathogens on gold island functionalized chalcogenide films." *Analytical Chemistry* 78(8): 2500-2506, (2006).

Zourob, M., Recognition Receptors in Biosensors, *Springer* (2010).

Zourob, M., S. Elwary and A. P. F. Turner, Principles of Bacterial Detection: Biosensors, Recognition Receptors and Microsystems, *Springer* (2008).

APPENDIX A

DATA FOR METHOD I FOR THE DETECTION OF *C. albicans* BY MICROSCOPE

Different concentrations of *C. albicans* (500 µg/ml, 100 µg/ml, 50 µg/ml, 10 µg/ml, 1 µg/ml, 1 ng/ml, 50 ng/ml, 800 pg/ml and 500 pg/ml) immobilized on gold biosensor surface were detected by microscope. The number of *C. albicans* which is immobilized on the gold biosensor surface decreased with decreasing concentration as shown in **Figure A.1- A.9**.

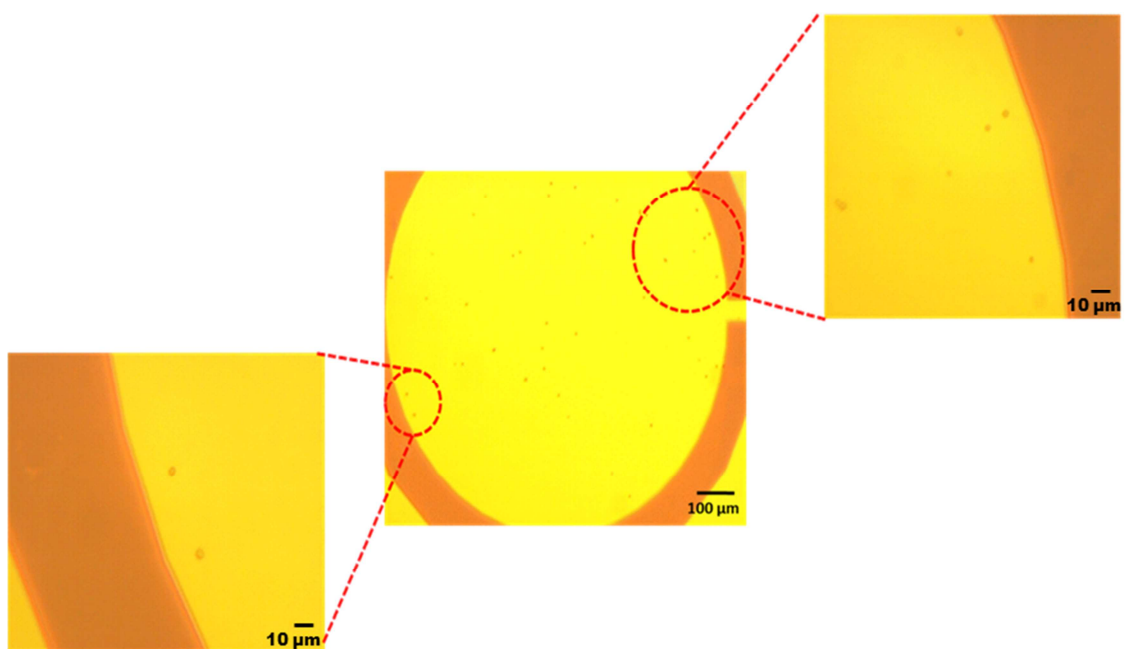


Figure A.1 Characterization of 500 µg/ml *C. albicans* on gold biosensor surface.

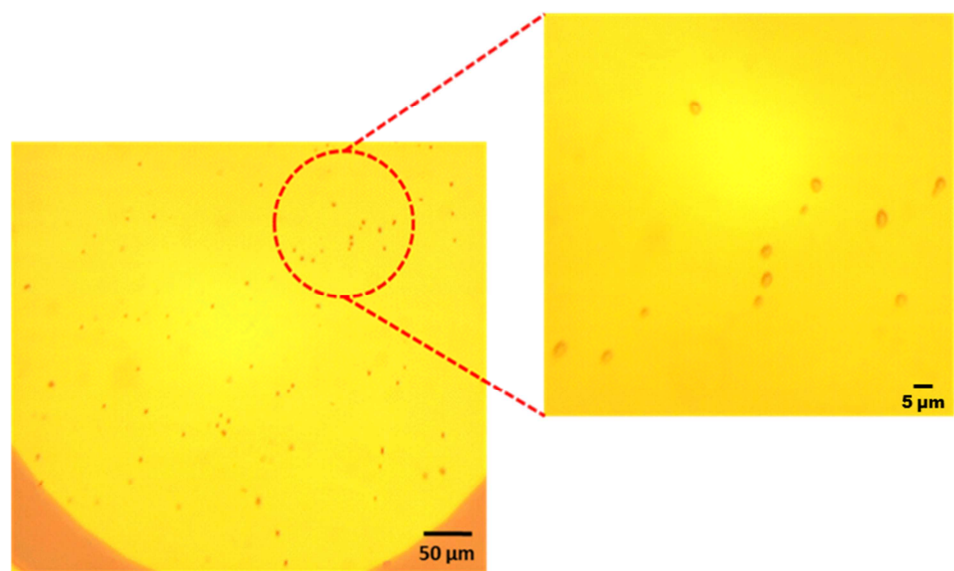


Figure A.2 Characterization of 100 µg/ml *C. albicans* on gold surface.

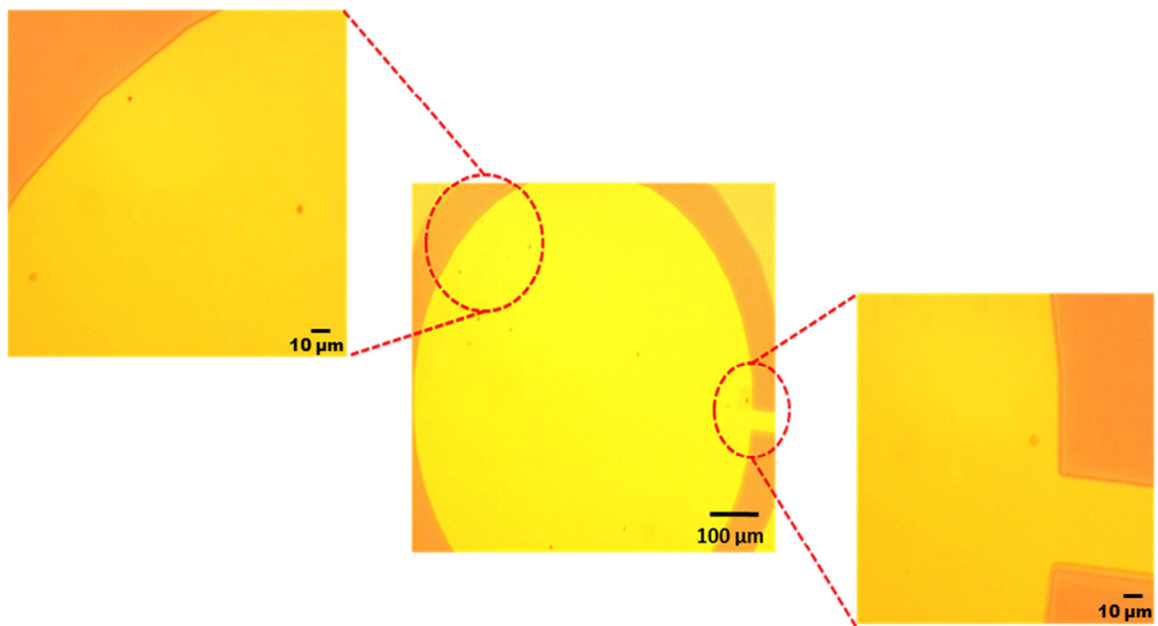


Figure A.3 Characterization of 50 µg/ml *C. albicans* on gold surface.

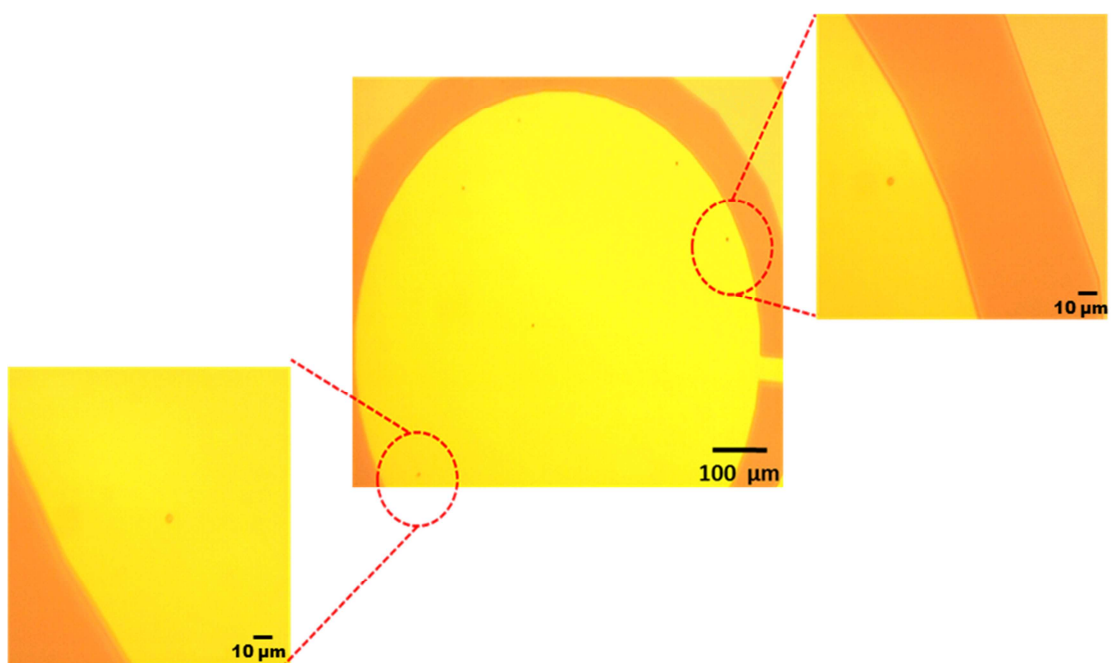


Figure A.4 Characterization of 10 $\mu\text{g}/\text{ml}$ *C. albicans* on gold surface.

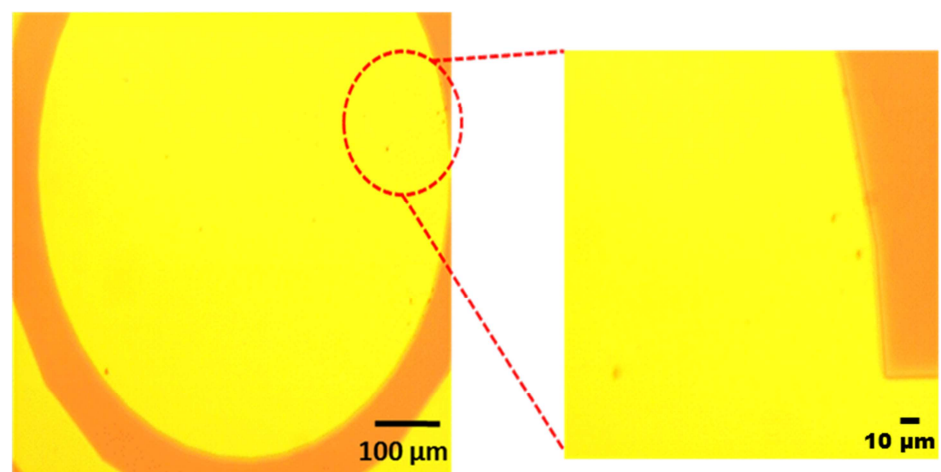


Figure A.5 Characterization of 1 $\mu\text{g}/\text{ml}$ *C. albicans* on gold surface.

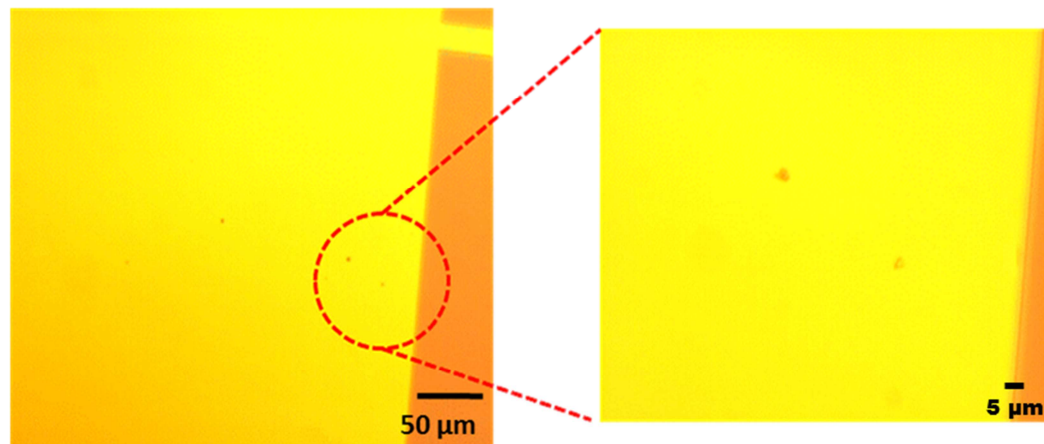


Figure A.6 Characterization of 50 ng/ml *C. albicans* on gold surface.

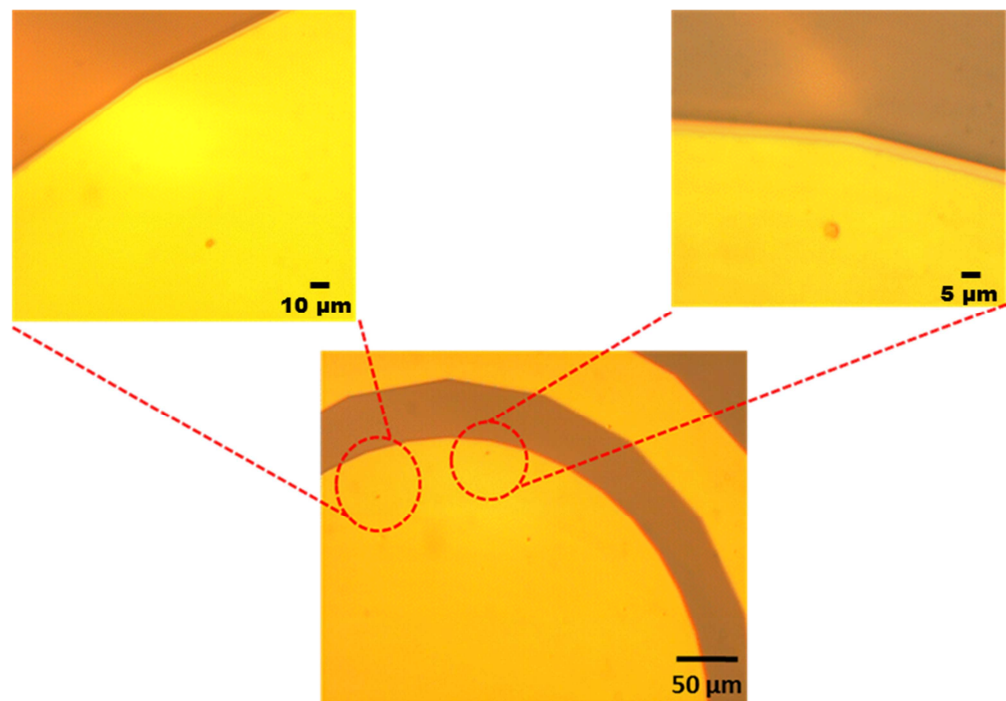


Figure A.7 Characterization of 1 ng/ml *C. albicans* on gold surface.

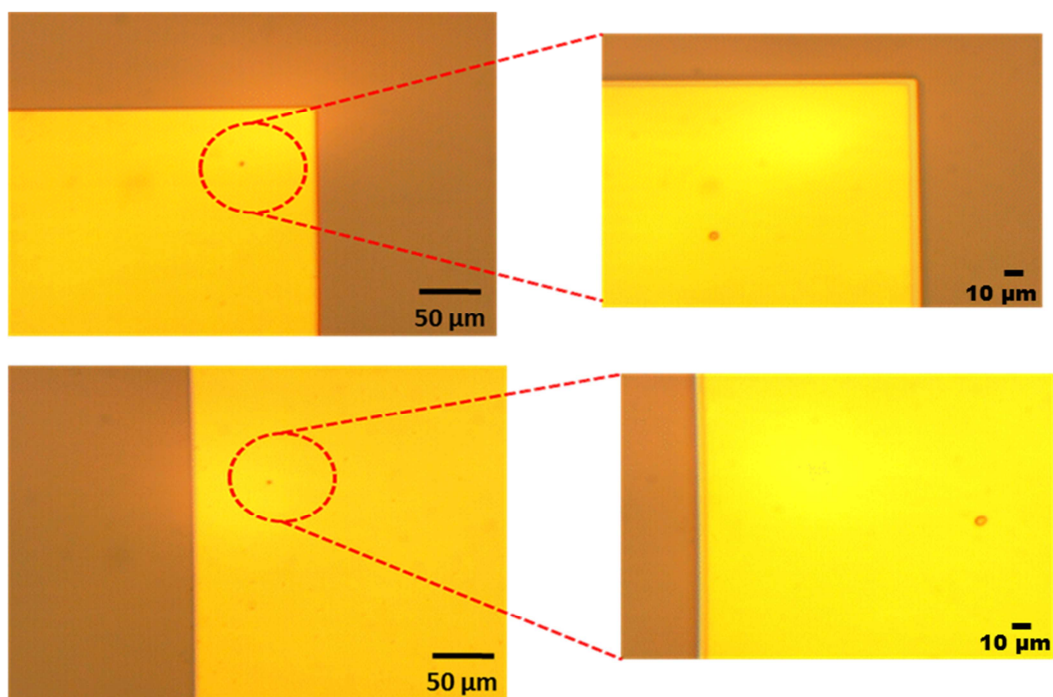


Figure A.8 Characterization of 800 pg/ml *C. albicans* on gold surface.

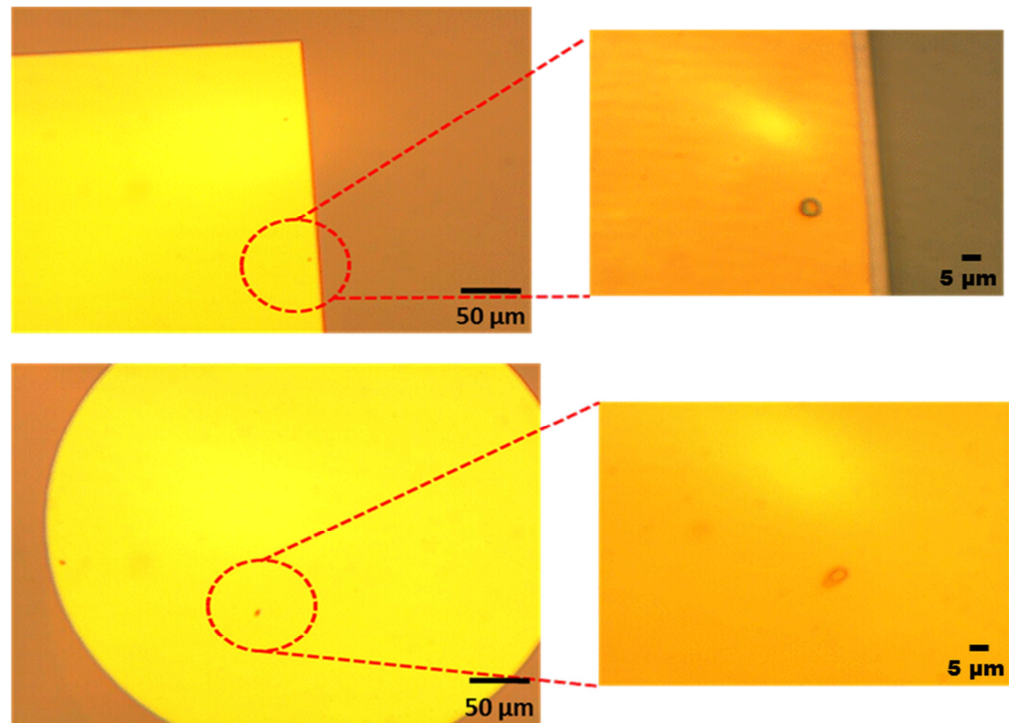


Figure A.9 Characterization of 500 pg/ml *C. albicans* on gold surface.

Primary antibodies (with different concentrations ($10 \mu\text{g/ml}$, $1 \mu\text{g/ml}$ and 1ng/ml) conjugated to gold surface was stored at -20°C for 1 week. Then, *C. albicans* were detected by microscope as seen in **Figure A.10-12**.

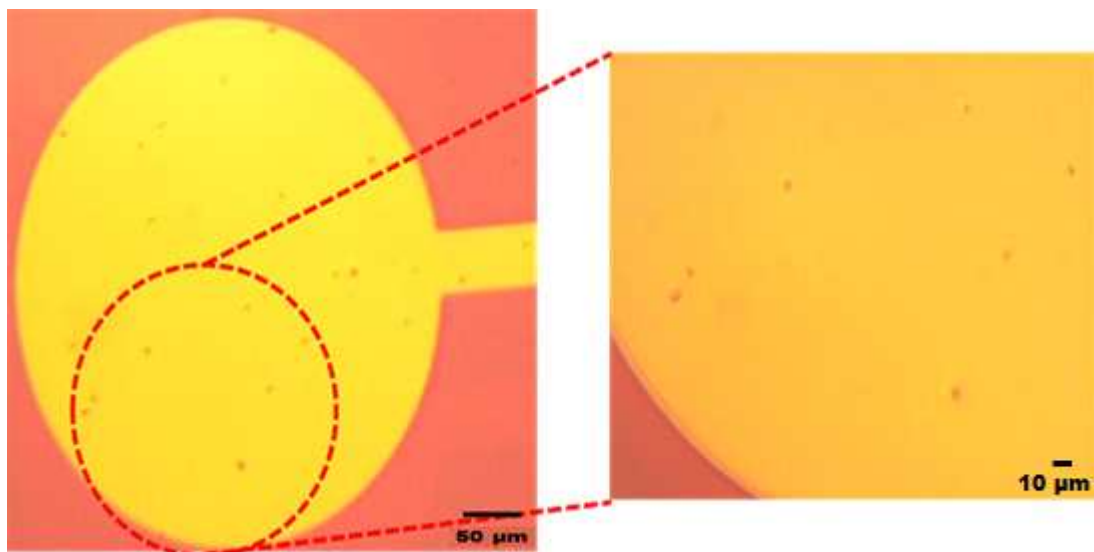


Figure A.10 Characterization of $10 \mu\text{g/ml}$ *C. albicans* on gold surface stored at -20°C for one week.

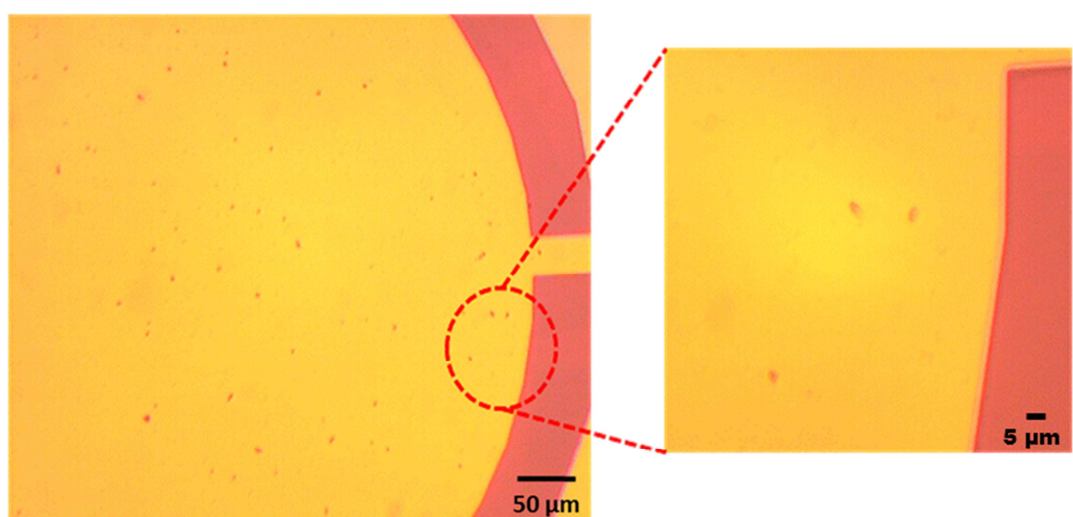


Figure A.11 Characterization of $1 \mu\text{g/ml}$ *C. albicans* on gold surface stored at -20°C for one week.

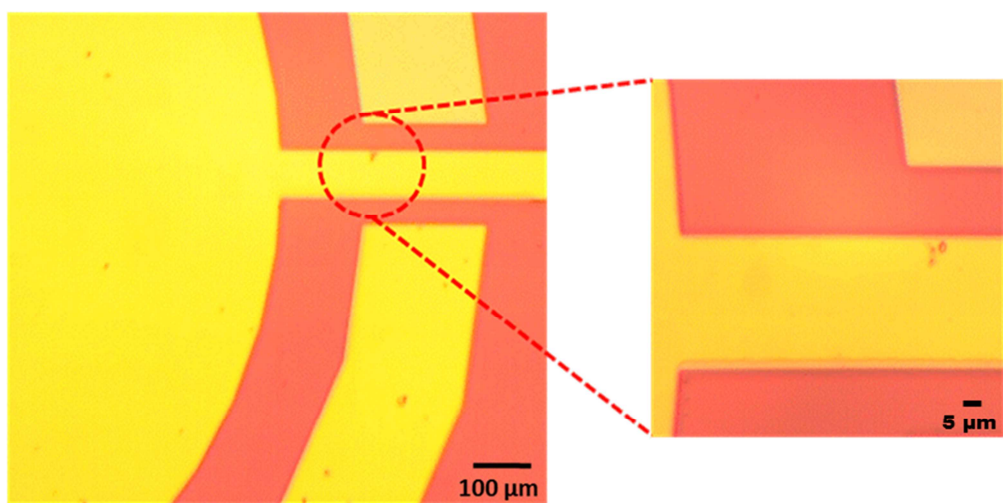


Figure A.12 Characterization of 1 ng/ml *C. albicans* on gold surface stored at -20 °C for one week.